Surface meteorology and Solar Energy (SSE) Release 6.0 Methodology
Version 3.2.0 June 2, 2016

Paul W. Stackhouse, Jr[1], William S. Chandler[2], Taiping Zhang[2]
David Westberg[2], Andy J. Barnett[3], James M. Hoell[2],
[1]NASA Langley Research Center [2]SSAI/NASA Langley Research Center,
[3]Booz Allen Hamilton Inc, Norfolk, VA

1. Introduction

NASA, through its' Earth science research program has long supported satellite systems and research providing data important to the study of climate and climate processes. These data include long-term estimates of meteorological quantities and surface solar energy fluxes. These satellite and model-based products have also been shown to be accurate enough to provide reliable solar and meteorological resource data over regions where surface measurements are sparse or nonexistent, and offer two unique features – the data is global and, in general, contiguous in time. These two important characteristics, however, tend to generate very large data archives which can be intimidating for commercial users, particularly new users with little experience or resources to explore these large data sets. Moreover the data products contained in the various NASA archives are often in formats that present challenges to new users. Accordingly, NASA's Earth Science Division Applied Sciences Program has provided the means to make these data available for government and public sector usage. To foster the usage of the global solar and meteorological data, NASA supported, and continues to support, the development of the Surface meteorology and Solar Energy (SSE) data sets and web portal which has been formulated specifically for photovoltaic and renewable energy system design needs. Of equal importance is the access to these data; to this end the SSE parameters are available via a user-friendly web-based portal designed based on user needs.

The original SSE data-delivery web site, intended to provide easy access to parameters needed in the renewable energy industry (e.g. solar and wind energy), was made available to the public in 1997. The solar and meteorological data contained in this first release was based on the 1993 NASA/World Climate Research Program Version 1.1 Surface Radiation Budget (SRB) science data and TOVS data from the International Satellite Cloud Climatology Project (ISCCP). This initial design approach proved to be of limited value because of the use of "traditional" scientific terminology that was not compatible with terminology/parameters used in the energy industry to design renewable energy power systems. After consultation with industry, Release 2 SSE was made public in 1999 with parameters specifically tailored to the needs of the renewable energy community. Subsequent releases of SSE - SSE-Release 3.0 in 2000, SSE-Release 4.0 in 2003, SSE-Release 5.0 in 2005, and SSE-Release 6.0 in 2008 – have continued to build upon an interactive dialog with potential customers resulting in updated parameters using the most recent NASA data as well as inclusion of new parameters that have been requested by the user community.

The Prediction Of Worldwide Energy Resource (POWER) project was initiated in 2003 both to improve subsequent releases of SSE, and to create new datasets applicable to other industries from new satellite observations and the accompanying results from forecast modeling. The POWER web interface (http://power.larc.nasa.gov) currently provides a portal to the SSE data archive, tailored for the renewable energy industry, as well as to the Sustainable Buildings Archive with parameters tailored for the sustainable buildings community, and the Agro-climatology Archive with parameters for the agricultural industry. In general, the underlying data behind the parameters used by each of these industries is the same – solar radiation, or Irradiance, and meteorology, including surface and air temperatures, moisture, and winds. Differences are based upon the various application area within the respective industries.

The purpose of this document is to describe the underlying data contained in SSE Release 6.0, and to provide additional information relative to the various industry specific parameters, their limitations, and estimated accuracies based on information available to NASA at the time of this document. The intent is to provide information that will enable new and/or long time users to make decisions concerning the suitability of the SSE data for his or her project in a particular region of the globe. And finally, it is noted this document is focused primarily on SSE Release 6.0 and parameters of interest to the renewable energy industry although the underlying solar and meteorological data for all three POWER archives are derived from common data sources.

A companion document describes the data and parameters in the POWER/Sustainable Buildings and POWER/Agroclimatology sections of the POWER archive.

SSE Release 6.0 provides (1) solar and meteorological data now spanning 22 years from July 1, 1983 through June 30, 2005, (2) the solar radiation data taken from the Surface Radiation Budget project release 3.0 which provides an overall improvement in the estimation of the surface solar radiation of about 2.8%; (3) the temperature data and related parameters are based upon the Goddard Earth Observing System model version 4 (GEOS-4), and (4) approximately 200 parameters based upon the base solar and meteorological parameters that are of interest to the renewable energy community.

(Return to Content)

2.0. Summary of Parameter Accuracy. The remainder of this section provides a summary of the estimated uncertainty associated with solar and meteorological parameters available through SSE 6.0. The uncertainty estimates were derived through comparisons with ground measurements. A more detailed description of the parameters is given in the subsequent sections of this document and the methodology for assessing the accuracy of the respective parameter is discussed in Appendix A
.
(Return to Content)

2.1 Solar Irradiance Quality ground-measured data are generally considered more accurate than satellite-derived values. However, measurement uncertainties from calibration drift, operational uncertainties, or data gaps are often unknown or unreported for many ground site data sets. In 1989, the World Climate Research Program estimated that most routine-operation solar-radiation ground sites had "end-to-end" uncertainties from 6 to 12%. Specialized high quality research sites such as those in the Baseline Surface Radiation Network (BSRN) are estimated to be more accurate by a factor of two.

Table 2.1a summarizes the results of comparing the total or global SSE solar Irradiance on a horizontal surface to observations from the BSRN for the time period January 1, 1992, the beginning of the BSRN observations, through June 30, 2005. Table 2.1b summarizes the results of comparing diffuse and direct solar Irradiance derived from the SRB horizontal Irradiance to BSRN observations of the corresponding solar components. Table 2.1c summarizes the results of comparing solar Irradiance on a south facing tilted surface derived from the SRB horizontal Irradiance to the corresponding Irradiance derived from BSRN observations.

Table 2.1a: Regression analysis of SSE versus BSRN 3-hourly, monthly and daily mean Irradiance on a horizontal surface for the time period January 1, 1992 - June 30, 2005

Parameter	Region	Bias (%)	RMSE (%)
Monthly Mean 3-Hrly All Sky Irradiance (Figure 5.3.1.1)	All Sites 60° Poleward 60° Equatorward	-2.24 -9.29 -1.57	15.37 38.77 12.85
Daily Mean All Sky Irradiance (Figure 5.3.2.1)	All Sites 60° Poleward 60° Equatorward	-1.58 -7.69 -0.83	20.57 41.16 17.87
Monthly Mean All Sky Irradiance (Figure 5.3.3.1)	All Sites 60° Poleward 60° Equatorward	-2.22 -8.43 -1.25	13.94 32.20 10.62
Monthly Mean Clear Sky Irradiance (Figure 5.3.4.2)	All Sites 60° Poleward 60° Equatorward	-2.77 n/a n/a	4.11 n/a n/a

Table 2.1b: Statistical parameters associated with a regression analysis of SSE VS BSRN: Diffuse Horizontal Irradiance (DHI) and Direct Normal Irradiance (DHI) (January 1, 1992 - June 30, 2005).

Daily Mean DNI All Sky (Figure 6.2.1.1)	All Sites 60° Poleward 60° Equatorward	3.70 18.59 2.13	48.90 126.95 39.17
Monthly Mean DNI All sky (Figure 6.2.2.1)	All Sites 60° Poleward 60° Equatorward	3.17 14.98 1.72	26.55 68.59 20.03
Daily Mean DHI All Sky (Figure 6.2.3.1)	All Sites 60° Poleward 60° Equatorward	-0.01 -25.31 3.03	44.03 68.07 38.80
Monthly Mean DHI All sky (Figure 6.2.4.1)	All Sites 60° Poleward 60° Equatorward	-1.44 -25.10 2.84	26.08 48.40 20.14

Table 2.1c: Regression analysis of SSE versus BSRN monthly mean Irradiance on a tilted surface for the time period January 1, 1992 - June 30, 2005.

Monthly Mean All Sky Irradiance (Figure VI.2)	All Sites 60° Poleward 60° Equatorward	2.92 n/a n/a	13.70 n/a n/a

(Return to Content)

2.2 Meteorology Table 2.2.1 summarizes the results of comparing GEOS-4 meteorological parameters to ground observations from the National Center for Environmental Information (NCEI – formally National Climatic Data Center). Table 2.2.2 summarizes the comparison statistics for wind speeds. The SSE Release 6.0 wind speeds are based upon GEOS-1 because newer data sets do not provide enough information about vegetation/surface types to permit an updated validation of the resulting wind data. The RETScreen Weather Database (RETScreen 2005) was used to test uncertainties in the SSE wind speeds.

Table 2.2.1. Linear least squares regression analysis of SSE GEOS-4 meteorological values versus NCEI monthly averaged values for the time period January 1983 through December 31, 2006

Parameter	Slope	Intercept	R^2	RMSE	Bias
Tmax (°C)	0.99	-1.58	0.95	3.12	-1.83
Tmin (°C)	1.02	0.10	0.95	2.46	0.24
Tave (°C)	1.02	-0.78	0.96	2.13	-0.58
Tdew (°C)	0.96	-0.80	0.95	2.46	-1.07
RH (%)	0.79	12.72	0.56	9.40	-1.92
Heating Degree Days (degree days)	1.02	12.47	0.93	77.20	17.28
Cooling Degree Days (degree days)	0.86	2.36	0.92	28.90	-5.65
Atmospheric Pressure (hPa)	0.89	102.16	0.74	27.33	-10.20

Table 2.2.2: Estimated uncertainty for monthly averaged GEOS-1 wind speeds for the time period July 1983 through June 1993

Parameter	Method	Bias	RMSE
Wind Speed at 10 meters for terrain similar to airports (m/s)	RETScreen Weather Database (documented 10-m height airport sites)	-0.2	1.3
	RETScreen Weather Database (unknown-height airport sites)	-0.0	1.3

(Return to Content)

3. Overview of Underlying NASA Data Used to Derive Parameters in SSE Release 6.0

SSE Release 6.0 (SSE 6.0) contains more than 200 primary and derived solar, meteorology and cloud related parameters from data spanning the 22 year period from July 1, 1983 through June 31, 2005. Table III.1 gives an overview of the various NASA programs from which the underlying solar and meteorological data are obtained and Table 3.1 gives a more explicit list of the underlying data used to derive the parameters currently available through SSE 6.0. Table 3.1a and 3.1b gives an overview list of most of the parameters available through SSE 6.0. The listed parameters are available globally on a 1-degree latitude, longitude grid which is selectable by the user.

The underlying solar and cloud related data (Table 3.1) are obtained from the Surface Radiation Budget (SRB) portion of NASA's Global Energy and Water Cycle Experiment (GEWEX). The current SRB archive is Release 3.0 (https://eosweb.larc.nasa.gov/project/srb/srb_table).

Table 3.1. SSE Release 6.0 Data Flow/Sources

Programs Contributing to SSE Release 6.0		**SSE Release 6.0**
NASA/ISCCP & CERES/MODIS: TOA Radiance, Clouds, and Surface Parameters **NCAR MATCH:** Aerosols **TOMS/TOVS:** Ozone **NASA/GMAO GEOS-4:** Atmospheric temperature and humidity profiles and surface parameters.	**NASA GEWEX/SRB Release 3.0:** Global estimates of the short and long wavelength solar radiation at earth's surface	(See Table 3.2 for explicit list of data from underlying projects)
NASA/GMAO GEOS-1: Winds at 1st layer above the earth's surface **NOAA/GPCP:** Surface precipitation		

The underlying meteorological data were obtained from NASA's Global Model and Assimilation Office (GMAO), Goddard Earth Observing System model version 4 (GEOS-4), and precipitation parameters were obtained from the Global Precipitation Climate Project (GPCP). The wind data is based upon the NASA/GMAO GEOS version 1 (GEOS-1).

The right most column of Table 3.2 enumerates the basic parameters that are extracted from the SRB 3.0 archive, the GMAO programs (GEOS-1 & 4), and the NOAA/GPCP programs.

Table 3.2. Basic solar and meteorological data used in SSE Release 6.0

Contributing Programs (see Table 3.1)	**SSE Archive.**
NASA GEWEX/SRB Release 3.0: Global estimates of the solar and thermal infrared wavelength radiation at earth's surface and top of atmosphere	**Daily Averaged time series parameters (July 1, 1983 - June 30, 2005):** 1. Top of atmosphere Irradiance 2. Shortwave (solar, 0.2 - 4.0 µm) Irradiance on a horizontal surface at the Earth's surface 3. Irradiance Clearness Index 4. Longwave (thermal infrared, 4.0 - 100 µm) on a horizontal surface at the Earth's surface 5. Clear sky Irradiance on a horizontal surface at the Earth's surface 6. Clear Sky Diffuse Irradiance on a horizontal surface at the Earth's surface 7. Surface Air Pressure 8. Earth Skin Temperature 9. Average Air Temperature at 10 m 10. Daily minimum Air Temperature at 10 m 11. Daily maximum Air Temperature at 10 m 12. Specific Humidity at 10 m **Monthly averaged parameters (July 1, 1983 - June 30, 2005):** 1. Cloud amount at available (0, 3, 6, 9, 12, 15, 18, 21) UT times 2. Frequency of cloud amount at 0, 3, 6, 9, 12, 15, 18, and 21 UT 3. Average Irradiance at available (0, 3, 6, 9, 12, 15, 18, 21) UT times 4. Average Irradiance at available (0, 3, 6, 9, 12, 15, 18, 21) UT times (Number of clear sky days (cloud amount < 10%). 5. Surface Albedo 6. Total column perceptible water 7. Minimum available Irradiance over consecutive-day period (1, 3, 7, 14, and 21 days) 8. Maximum available Irradiance over consecutive-day period (1, 3, 7, 14, and 21 days) 9. Surface precipitation (2.5°x2.5° latitude-longitude)
NASA GMAO GEOS-4: Air temperatures and moisture near the surface and through the atmosphere	
NASA GMAO GEOS-1: Winds at 50m above earth's surface	
NOAA/GPCP: Monthly averaged surface precipitation	

Table 3.2a. Overview of climatologically averaged parameters in SSE Release 6.0 :All solar related parameters are derived from Irradiance taken from the NASA GEWEX/SRB release 3.0 archive (http://gewex-srb.larc.nasa.gov) and averaged over the time period July 1, 1983 - June 30, 2005. Temperature and moisture related parameters are derived from data taken from the NASA GMAO (http://gmao.gsfc.nasa.gov) GEOS-4 assimilation model and averaged over the time period July 1, 1983 - June 30, 2005. The wind related parameters are derived from winds taken from the GMAO GEOS-1 assimilation model and averaged over the time period July 1, 1983 - June 30, 1993. Precipitation data has been obtained from the GPCP (http://precip.gsfc.nasa.gov) Version 2.1 data product.

1. Parameters for Solar Cooking:

- Average Irradiance
- Midday Irradiance
- Clear sky Irradiance
- Clear sky days

2. Parameters for Sizing and Pointing of Solar Panels and for Solar Thermal Applications:

- Irradiance on horizontal surface (Average, Min, Max)
- Diffuse radiation on horizontal surface (Average, Min, Max)
- Direct normal radiation (Average, Min, Max)
- Irradiance at 3-hourly intervals
- Irradiance clearness index, K (Average, Min, Max)
- Irradiance normalized clearness index
- Clear sky Irradiance
- Clear sky Irradiance clearness index
- Clear sky Irradiance normalized clearness index
- Downward Longwave Radiative Flux

3. Solar Geometry:

- Solar Noon
- Daylight Hours
- Daylight average of hourly cosine solar zenith angles
- Cosine solar zenith angle at mid-time between sunrise and solar noon
- Declination
- Sunset Hour Angle
- Maximum solar angle relative to the horizon
- Hourly solar angles relative to the horizon
- Hourly solar azimuth angles

4. Parameters for Tilted Solar Panels:

- Radiation on equator-pointed tilted surfaces
- Minimum radiation for equator-pointed tilted surfaces
- Maximum radiation for equator-pointed tilted surfaces

5. Parameters for Sizing Battery or other Energy-storage Systems:

- Minimum available Irradiance as % of average values over consecutive-day period
- Horizontal surface deficits below expected values over consecutive-day period
- Equivalent number of NO-SUN days over consecutive-day period

6. Parameters for Sizing Surplus-product Storage Systems:

- Available surplus as % of average values over consecutive-day period

7. Diurnal Cloud Information:

- Daylight cloud amount
- Cloud amount at 3-hourly intervals
- Frequency of cloud amount at 3-hourly intervals

8. Meteorology (Temperature):

- Air Temperature at 10 m
- Daily Temperature Range at 10 m
- Cooling Degree Days above 18 °C
- Heating Degree Days below 18 °C
- Arctic Heating Degree Days below 10 °C
- Arctic Heating Degree Days below 0 °C
- Earth Skin Temperature
- Daily Mean Earth Temperature (Min, Max, Amplitude)
- Frost Days
- Dew/Frost Point Temperature at 10 m
- Air Temperature at 3-hourly intervals
- Wind Speed at 50 m (Average, Min, Max)

Table 3.2a .(concl'd) Overview of climatologically averaged parameters in SSE Release 6.0

9. Meteorology (Wind):

- Percent of time for ranges of Wind Speed at 50 m
- Wind Speed at 50 m for 3-hourly intervals
- Wind Direction at 50 m
- Wind Direction at 50 m for 3-hourly intervals
- Wind Speed at 10 m for terrain similar to airports

10. Meteorology (Moisture, pressure):

- Relative Humidity
- Humidity Ratio (i.e. Specific Humidity)
- Surface Pressure
- Total Column Precipitable Water
- Precipitation

11. Supporting Information

- Top of Atmosphere Irradiance
- Surface Albedo

12.Global Radiation Data Files of Monthly and Annual Averages by Year

- Irradiance on Horizontal Surface
- Irradiance Clearness Index
- Clear Sky Irradiance
- Diffuse Radiation
- Minimum Diffuse Radiation
- Maximum Diffuse Radiation
- Direct Normal Radiation
- Minimum Direct Radiation
- Maximum Direct Radiation
- Clear Sky Irradiance Clearness Index
- Downward Longwave Radiative Flux
- Top-of-atmosphere Irradiance
- Maximum NO_SUN of BLACK Days

13, Global Metrological Data Files of Monthly and Annual Averages by Year

- Surface Air Pressure
- Earth Skin Temperature
- Average Air Temperature at 10 m
- Minimum Air Temperature at 10 m
- Maximum Air Temperature at 10 m
- Specific Humidity at 10 m
- Relative Humidity at 10 m
- Dew/Frost Point Temperature at 10 m
- Heating Degree-Days Below 18C^{o}
- Cooling Degree-Days above 18C^{o}
- Cooling Degree-Days above 10C^{o}

14, Global Solar Geometry Data for the "Monthly Average Day"

Table 3.2b. Overview of daily mean parameters in SSE Release 6.0.
All daily values are available for the time period July 1, 1983 - June 30, 2005. Irradiance related parameters are derived from data taken from the NASA GEWEX/SRB (http://gewex-srb.larc.nasa.gov/) release 3.0 archive. Meteorological related parameters are derived from data taken from the NASA GMAO (http://gmao.gsfc.nasa.gov/) GEOS-4 assimilation model.

1. DAILY IRRADIANCE and RELATED PARAMETERS:

- Shortwave Irradiance on Horizontal Surface
- Irradiance Clearness Index
- Clear Sky Irradiance
- Clear Sky Diffuse Irradiance
- Clear Sky Direct Normal Irradiance
- Clear Sky Irradiance Clearness Index
- Downward Longwave Radiative Flux
- Top-of-atmosphere Irradiance
- Top-of-Atmosphere Irradiance

2. DAILY METEOROLOGICAL:

- Surface Air Pressure
- Earth Skin Temperature
- Average Air Temperature at 10 m
- Minimum Air Temperature at 10 m
- Maximum Air Temperature at 10 m
- Specific Humidity at 10 m
- Relative Humidity at 10 m
- Dew/Frost Point Temperature at 10 m

While it is not the purpose of this document to discuss in detail the process by which the basic solar data (i.e. SRB Release 3.0), the meteorological data (i.e. GEOS-4), or precipitation data (GPCP) are derived, we provide herein an overview perspective on the process for each of these data sets with particular emphasis on how these data are used in SSE Release 6.0. More detailed descriptions of the SRB, GEOS-4, and GPCP data can be found in documentation and publications enumerated on their respective online web sites at http://gewex-srb.larc.nasa.gov , https://eosweb.larc.nasa.gov/project/srb/srb_table, http://gmao.gsfc.nasa.gov/index.php , http://precip.gsfc.nasa.gov , and http://disc.sci.gsfc.nasa.gov/precipitation/ .

(Return to Content)

4. Validation Methodology The validation of the solar and meteorological parameters is based upon comparisons of the primary parameter to surface observations of the corresponding parameters and, where possible, comparisons of the SSE parameters calculated using the primary data to the corresponding parameters calculated using surface observations. Examples of primary parameters comparisons include the solar and temperature values compared to surface observations; while comparisons of relative humidity and Dew point temperature typify comparisons of calculated parameters using the POWER primary data and the corresponding surface based observational data.

Statistics associated with the SSE vs. surface based values are reported to provide users with information necessary to assess the applicability of the SSE data to their particular project. Scatter plots of the SSE parameter vs. surface based values along with the correlation and accuracy parameters for each scatter plots are typically provided. The statistical parameters associated with a linear least squares fit to the respective scatter plots that are reported include:

Pearson's correlation coefficient; the Bias between the mean of the respective SSE parameter and the surface observations; the root mean square error (RMSE) calculated as the root mean square difference between the respective SSE and observational values. Additional parameters typically provided are the variance in the SSE and observational data and the number of SSE:observational data pairs.

Appendix A provides the explicit equations used to calculate the statistical validation parameters.

(Return to Content)

5. Global Irradiance on a Horizontal Surface

The solar radiation and cloud parameters contained in SSE 6.0 are obtained directly or derived from parameters available from the NASA/Global Energy and Water Cycle Experiment - Surface Radiation Budget (NASA/GEWEX SRB) Project Release 3.0 archive (https://eosweb.larc.nasa.gov/project/srb/srb_table). The NASA/GEWEX SRB Project focuses on providing estimates of the Earth's Top-of-atmosphere (TOA) and surface radiative energy flux components.

While it is not the intent or purpose of this document to provide a detailed description of the methodology for inferring solar data from satellite observations, a brief synopsis of the overall components of the process is provided in the following sections.

5.1. Earth's Radiation Budget: Figure 5.1 illustrates the major components/processes associated with the Earth's Energy Budget including the radiative flux components estimated from SRB Release 3.0 in the yellow boxes. These values are based on a 24 year (July 1983 – Dec. 2007) annual global averaged radiative fluxes with year-to-year annual average variability of +/- 4 W m^{-2} in the solar wavelengths and +/- 2 W m^{-2} in the thermal infrared (longwave) flux estimates. The absolute uncertainty of these components is still the subject of active research.

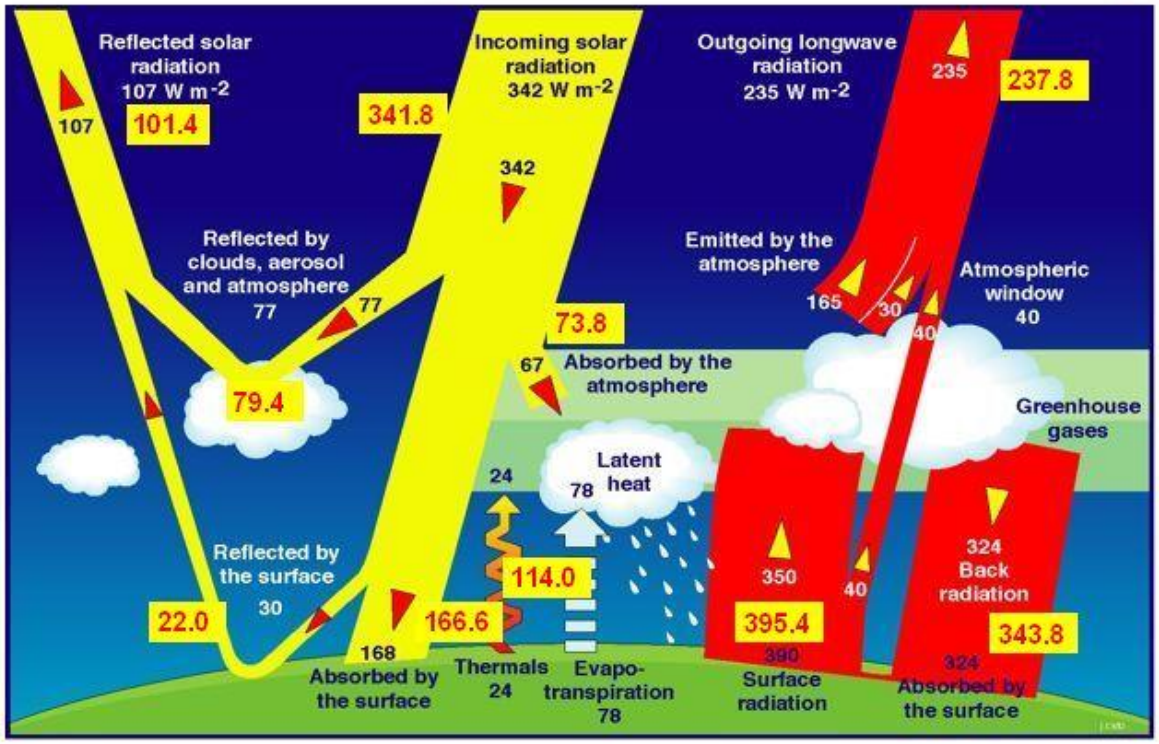

Figure 5.1. The major components/processes associated with the Earth's Energy Budget. The values in the yellow rectangles are based upon the updated solar and thermal infrared radiation estimates in SRB Release 3.0. (Note that all units are in W/m^2; multiplying W/m^2 by 0.024 yields $kWh/day/m^2$, and by 0.0864 yields $MJ/day/m^2$.)

For instance, the most recent satellite based measurements of the incoming solar radiation disagree with previous measurements and indicate this value should be closer 340.3 W m^{-2} providing another source of uncertainty. Other uncertainties involving the calibration of satellite radiances, atmospheric properties of clouds, aerosols and gaseous constituents, surface spectral albedos are all the subject of research within the SRB project.

(Return to Content)

5.2. SRB Radiative Transfer Model*:* The process of inferring the surface solar radiation, or Irradiance, from satellite observations employs the modified method of Pinker and Laszlo (1992). This method involves the use of a radiative transfer model, along with water vapor column amounts from the GEOS-4 product and ozone column amounts from satellite measurements. Three satellite visible radiances are used: the instantaneous clear sky radiance, the instantaneous cloudy sky radiance, and the clear sky composite radiance, which is a representation of a recent dark background value. The observed satellite radiances are converted into broadband shortwave TOA albedos, using Angular Distribution Models from the Earth Radiation Budget Experiment (Smith et al., 1986). The spectral shape of the surface albedo is

fixed by surface type. The radiative transfer model (through the use of lookup tables) is then used to find the absolute value of the surface albedo which produces a TOA upward flux which matches the TOA flux from the conversion of the clear-sky composite radiance. For this step, a first guess of the aerosol amount is used. The aerosol used for this purpose was derived from six years (2000-2005) of daily output from the MATCH chemical transport model (Rasch *et al.*, 1997). A climatology of aerosol optical depth was developed for each of the twelve months by collecting the daily data for each grid cell, and finding the mode of the frequency distribution. The mode was used rather than the average so as to provide a typical background value of the aerosol, rather than an average which includes much higher episodic outbreak values. The surface albedo now being fixed, the aerosol optical depth is chosen within the radiative transfer model to produce a TOA flux which matches the TOA Flux from the conversion of the instantaneous clear sky radiance. Similarly the cloud optical depth is chosen to match the TOA flux implied from the instantaneous cloudy sky radiance. With all parameters now fixed, the model outputs a range of parameters including surface and TOA fluxes. All NASA/GEWEX SRB parameters are output on a 1^0 by 1^0 global grid at 3-hourly temporal resolution for each day of the month.

Primary inputs to the model include: visible and infrared radiances, and cloud and surface properties inferred from International Satellite Cloud Climatology Project (ISCCP) pixel-level (DX) data (Rossow and Schiffer, 1999; data sets and additional information can be found at https://eosweb.larc.nasa.gov/project/isccp/isccp_table); temperature and moisture profiles from GEOS-4 reanalysis product obtained from the NASA Global Modeling and Assimilation Office (GMAO; Bloom et al., 2005); and column ozone amounts constituted from Total Ozone Mapping Spectrometer (TOMS) and TIROS Operational Vertical Sounder (TOVS) archives, and Stratospheric Monitoring-group's Ozone Blended Analysis (SMOBA), an assimilation product from NOAA's Climate Prediction Center.

To facilitate access to the SRB data products, the SSE project extracts the parameters listed in Table 3.2 from the SRB archive, as well as other parameters from the GEOS-4 and GPCP archives. The data products listed in Table III.2 are available through the respective archives although in some instances the product may be bundled with a number of other parameters and generally are large global spatial files (i.e. 1 per day) rather than temporal files.

(Return to Content)

5.3. **Validation of Solar Irradiance***:* As noted in previous sections, the SSE solar data have been taken from SRB Release 3.0. The accuracy of the SRB values over the time period from 1992 – 2007 is given at http://gewex-srb.larc.nasa.gov/common/php/SRB_validation.php . The SSE values cover the 22-year period from July 1, 1983 – June 30, 2005. Validation of the SSE solar data is based upon comparisons against research quality observation from the Baseline Surface Radiation Network (BSRN; Ohmura *et al*., 1999) as described in Section 4. Figure 5.3.1 shows the location of ground stations within the BSRN networks/archives used for the SSE solar validation. Appendix A describes the statistical parameters provided as an assessment of the fidelity of the SSE parameters.

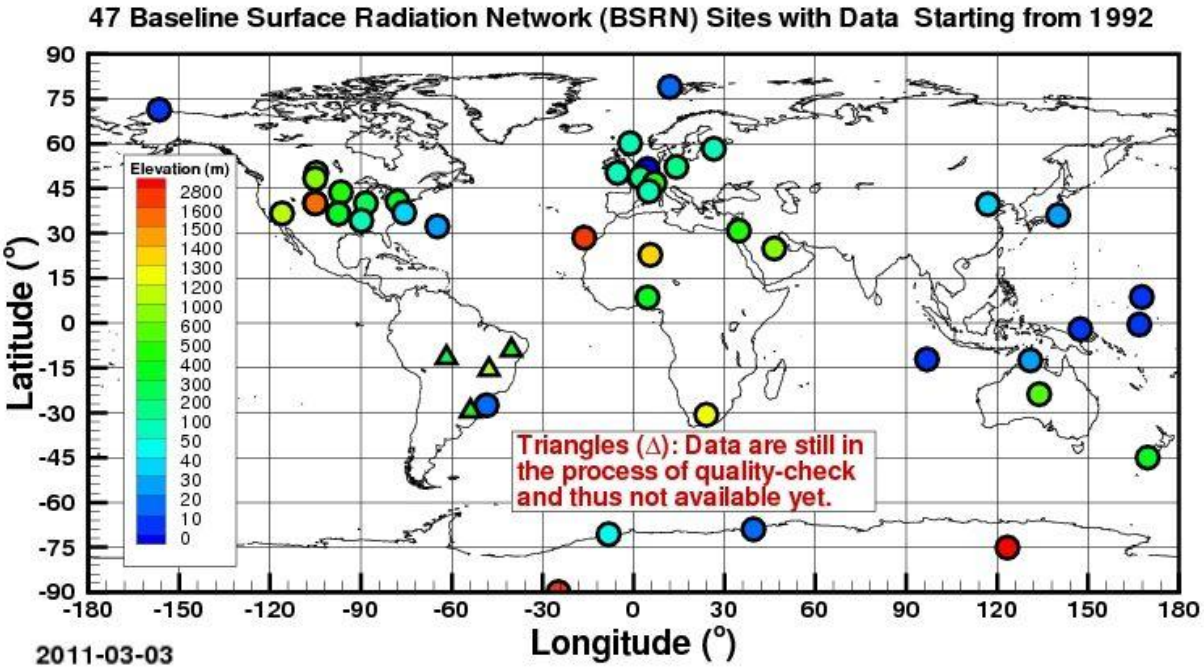

Figure 5.3.1. Location of ground stations in the Baseline Surface Radiation Network (BSRN).

The following section show the validation/scatter plots of the global irradiance (i.e. diffuse plus direct) data from measured at the BSRN ground sites shown in Figure 5.3.1versus the corresponding values from the SRB release 3.0 archive. **:** Figure 5.3.1.1 shows the scatter plot of the monthly averaged 3-hourly values; Figure 5.3.2.1 the daily mean values; and Figure 5.3.3.1 the monthly averaged values. Each plot covers the time period January 1, 1992, the earliest that data from BSRN sites are available, through June 30, 2005.

The statistical parameters associated with each of the scatter plots are given in the legend box in each figure. Note that the statistical parameters are given for all sites (e.g. Global), for the BSRN sites in regions above 60^o latitude, north and south (i.e. 60^0 poleward), and for BSRN sites between 60^o north and 60^o south (i.e. 60^o equatorward). The Bias is the difference between the mean (μ) of the respective solar radiation values for SRB and BSRN. The RMS is the root mean square difference between the respective SRB and BSRN values. The correlation coefficient between the SRB and BSRN values is given by ρ, the variance in the SRB values is given by σ, and N is number of SRB:BSRN pairs for each latitude region. The expressions used to calculate these parameters are given in Appendix A.

(Return to Content)

5.3.1 Monthly 3-Hourly Mean Irradiance: Figure 5.3.1.1 shows the scatter plot of the monthly averaged 3-hourly values vs the corresponding values based upon measurements at the BSRN sites shown in Figure 5.3.1. We note here that 3-hourly SRB values are the initial values estimated through the retrieval process described above and are used to calculate the daily total and the monthly Irradiance averages. The 3-hourly values are available through the

Atmospheric Science Data Center (ASDC/SRB – https://eosweb.larc.nasa.gov/project/srb/srb_table). Global spatial files of the daily and monthly Irradiance values are also available from ASDC/SRB. A more extensive listing of parameters based upon the daily and monthly SRB data for user defined latitude-longitude coordinates is listed at https://eosweb.larc.nasa.gov/project/sse/sse_table.

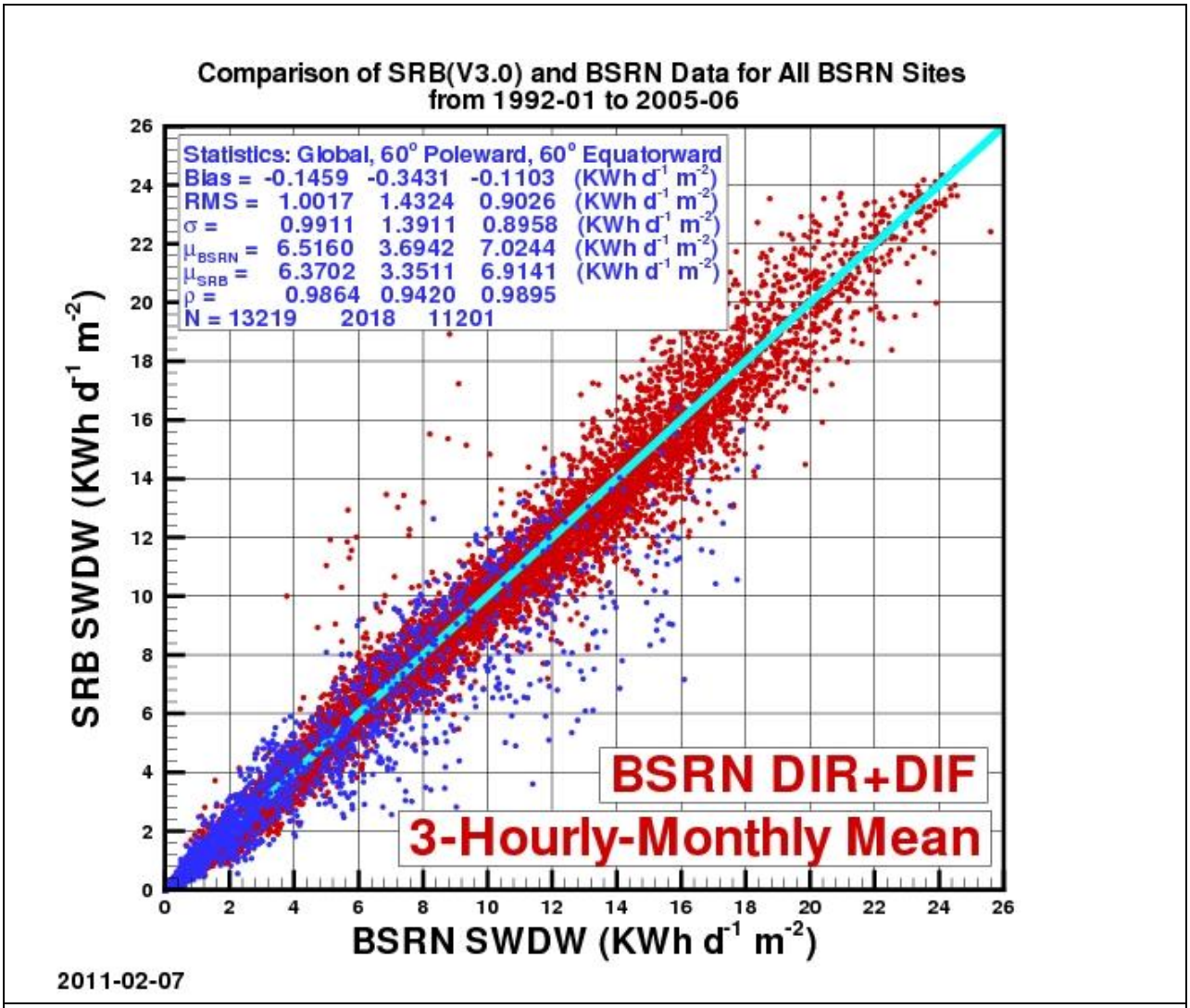

Figure 5.3.1.1. Scatter plot of 3-hourly total surface solar radiation observed at BSRN ground sites versus 3-hourly values from the SRB Release 3.0 archive. Note that solar radiation is in KWh/day/m^2; multiplying KWh/day/m^2 by 41.67 yields W/m^2, and by 3.6 yields MJ/day/m^2.)

The statistical parameters associated with the scatter plot are given in the legend box in each figure. Note that the statistical parameters are given for all sites (e.g. Global), for the BSRN sites in regions above 60^o latitude, north and south (i.e. 60^0 poleward), and for BSRN sites between 60^o north and 60^o south (i.e. 60^o equatorward). The Bias is the difference between the mean (μ) of the respective solar radiation values for SRB and BSRN. The RMS is the root mean square difference between the respective SRB and BSRN values. The correlation coefficient between the SRB and BSRN values is given by ρ, the variance in the SRB values is given by σ, and N is

number of SRB:BSRN pairs for each latitude region. The expressions used to calculate these parameters are given in Appendix A.

(Return to Content)

5.3.2. Daily Mean Irradiance: : Figure 5.3.2.1 shows the scatter plot of the SRB daily averaged values vs values measured at the BSRN site shown in Figure 5.3.1. The statistical parameters associated with the scatter plot are given in the legend box in each figure. Note that the statistical parameters are given for all sites (e.g. Global), for the BSRN sites in regions above 60^o latitude, north and south (i.e. 60^0 poleward), and for BSRN sites between 60^o north and 60^o south (i.e. 60^o equatorward). The Bias is the difference between the mean (μ) of the respective solar radiation values for SRB and BSRN. The RMS is the root mean square difference between the respective SRB and BSRN values. The correlation coefficient between the SRB and BSRN values is given by ρ, the variance in the SRB values is given by σ, and N is number of SRB:BSRN pairs for each latitude region. The expressions used to calculate these parameters are given in Appendix A.

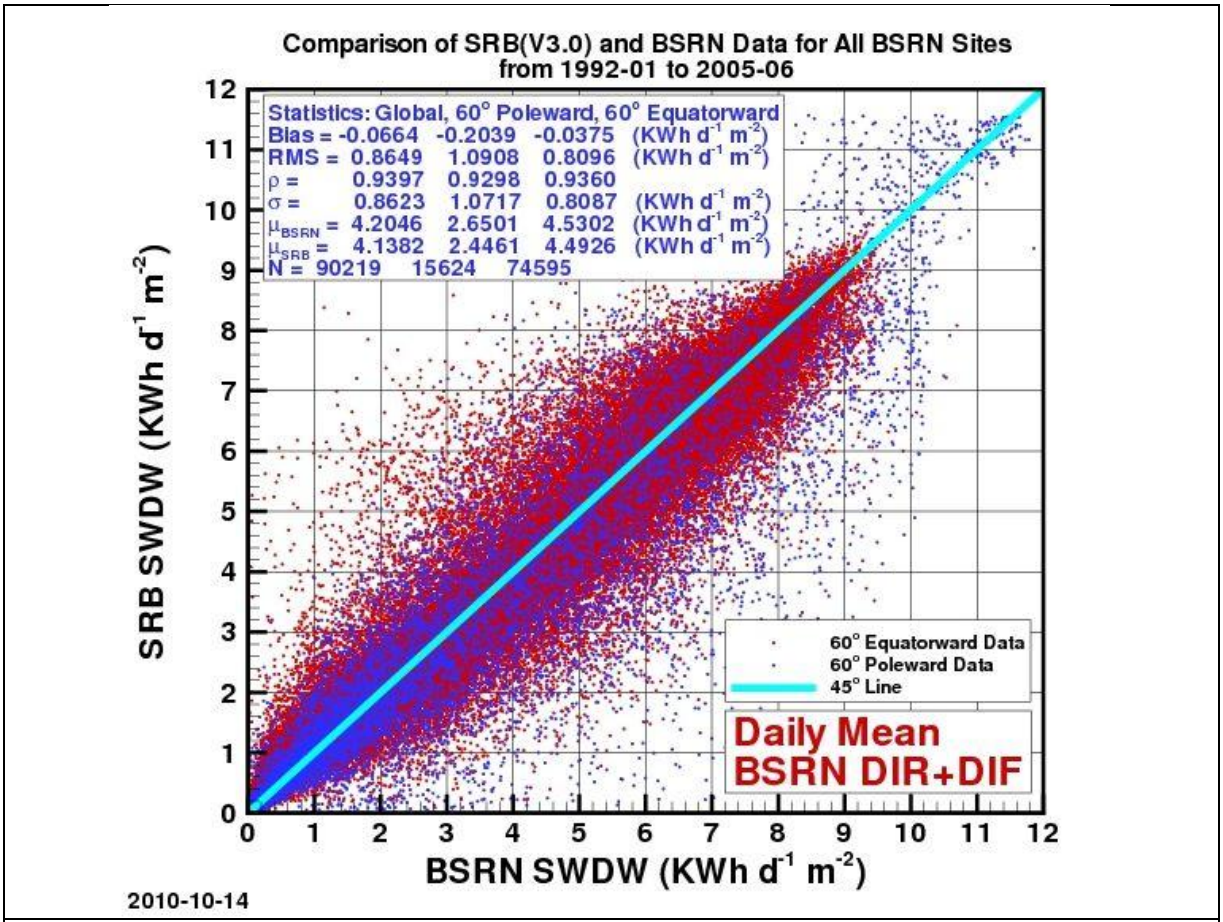

Figure 5.3.2.1. Scatter plot of daily total surface solar radiation observed at BSRN ground sites versus daily values from the SRB Release 3.0 archive. These daily are used to calculate the monthly averages that are provided in SSE Release 6.0. (Note that solar radiation is in KWh/day/m^2; multiplying KWh/day/m^2 by 41.67 yields W/m^2, and by 3.6 yields MJ/day/m^2.)

(Return to Content)

5.3.3 Monthly Mean Irradiance: Figure 5.3.3.1 shows the scatter plot of the monthly mean global irradiance based upon SRB data VS the corresponding values based upon observational data from the BSRN sites shown in Figure 5.3.1. The statistical parameters associated with the scatter plot are given in the legend box in each figure. Note that the statistical parameters are given for all sites (e.g. Global), for the BSRN sites in regions above 60^o latitude, north and south (i.e. 60^0 poleward), and for BSRN sites between 60^o north and 60^o south (i.e. 60^o equatorward). The Bias is the difference between the mean (μ) of the respective solar radiation values for SRB and BSRN. The RMS is the root mean square difference between the respective SRB and BSRN values. The correlation coefficient between the SRB and BSRN values is given by ρ, the variance in the SRB values is given by σ, and N is number of SRB:BSRN pairs for each latitude region. The expressions used to calculate these parameters are given in Appendix A.

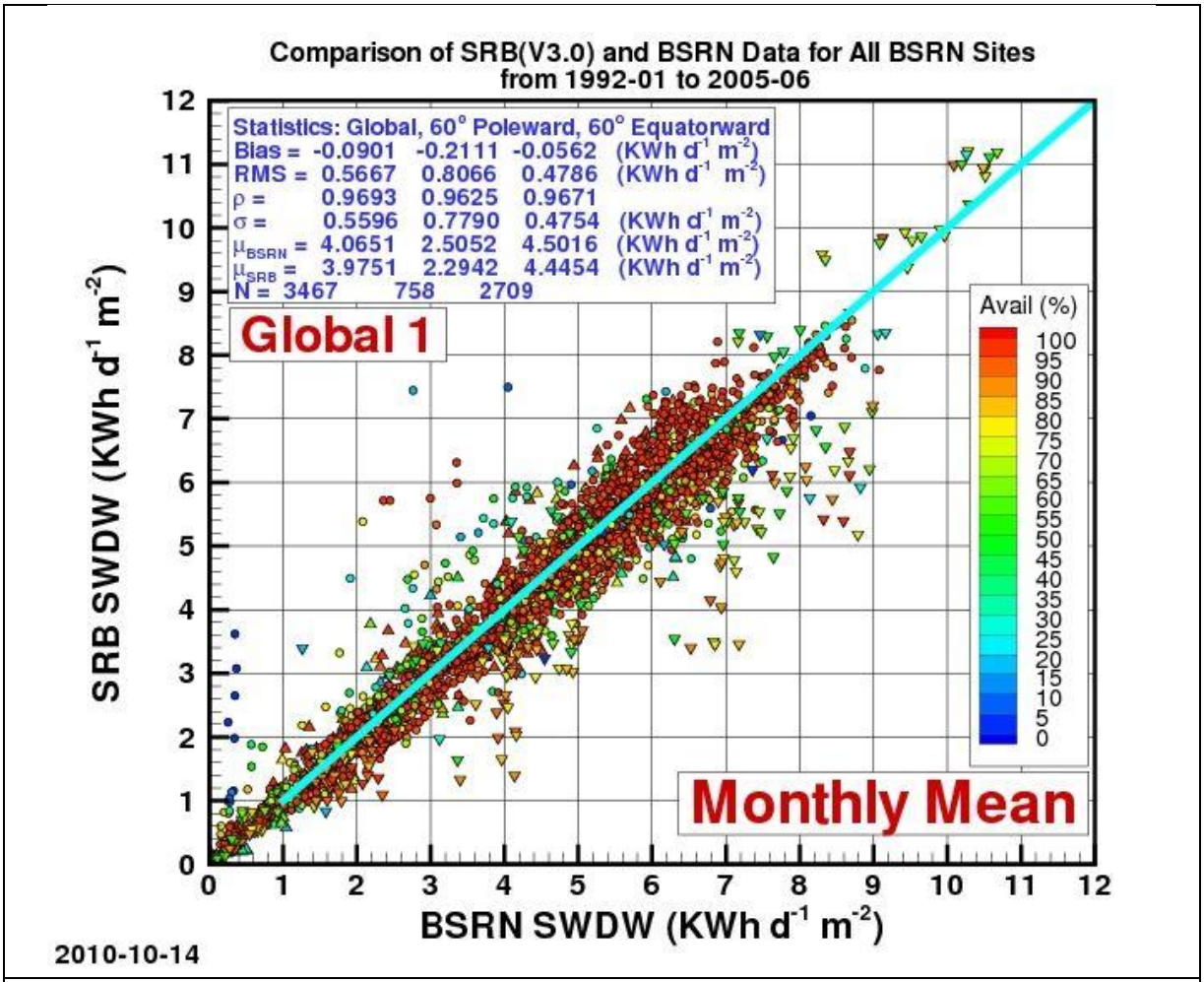

Figure 5.3.3.1. Scatter plot of monthly total surface solar radiation observed at BSRN ground sites versus monthly values from the SRB Release 3.0 archive. The daily values illustrated in figure V-5 are used to calculate the monthly averages. The bias differs from the daily value due to differences in sampling requirements. (Note that solar radiation is in KWh/day/m^2; multiplying KWh/day/m^2 by 41.67 yields W/m^2, and by 3.6 yields MJ/day/m^2.)

(Return to Content)

5.3.4. Monthly Mean Global Irradiance (Clear Sky): Global irradiance for clear sky conditions (i.e. cloud cover <10%) is obtained from the SRB Release 3.0 archive (https://eosweb.larc.nasa.gov/project/srb/srb_table). Corresponding observational data was obtained from the BSRN ground sites shown in Figure 5.3.4.1. Data from these sites and the satellite observational data provide information related to cloud cover for each observational period. Recall in Section 3 and in Table 3.2, it was noted that cloud parameters from the NASA ISCCP were used to infer the solar radiation in the SRB Release 3.0 archive. Parameters within the ISCCP data provide a measure of the clearness for each satellite observation use in the SRB-inversion algorithms. Similarly, observations from upward viewing cameras at the 27 BSRN sites shown in Figure 5.3.4.1 provided a measure of cloud cover for each ground observational period. The comparison data shown in Figures 5.3.4.2 used the ground cameras and the ISCCP data to matched clearness conditions. In particular, the comparison shown below use clearness criteria defined such that clouds in the field of view of the upward viewing camera and the field of view from the ISCCP satellites must both be less than 10%.

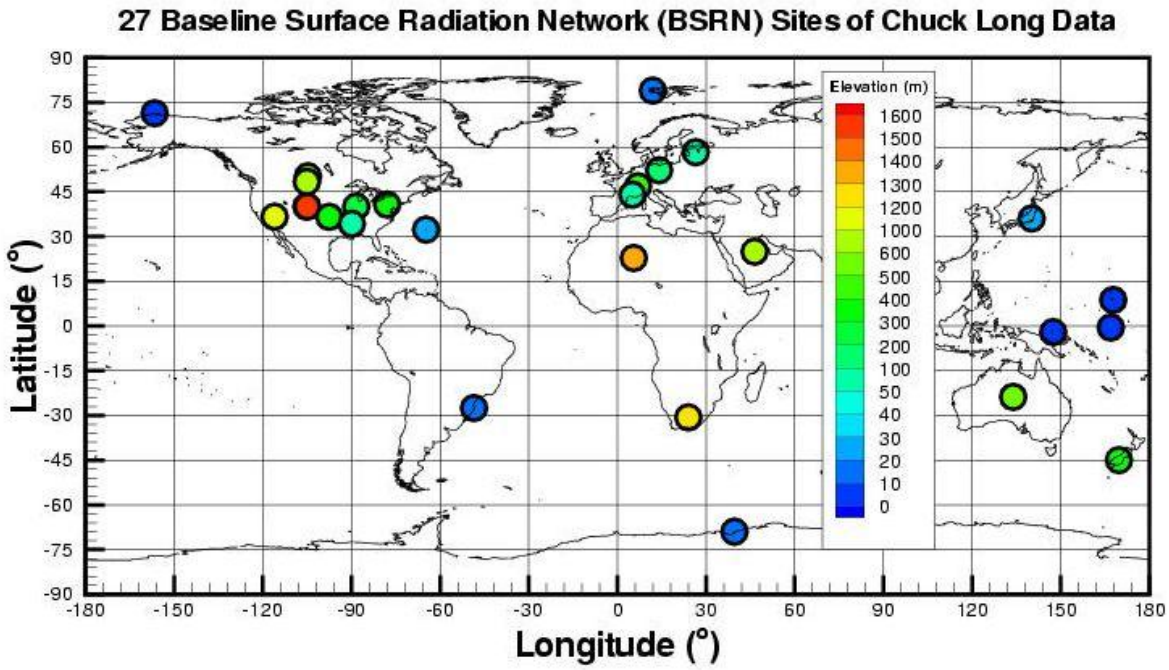

Figure 5.3.4.1. Location of ground stations in the Baseline Surface Radiation Network (BSRN) with upward viewing cameras.

In Figure 5.3.4.2 the monthly mean global irradiance on a horizontal surface is compared to ground observations from the BSRN network (Figure 5.3.4.1) for "clear" sky conditions. The statistical parameters associated with the scatter plots are given in the legend box. The Bias is the difference between the mean (μ) of the respective solar radiation values for SRB and BSRN. The RMS is the root mean square difference between the respective SRB and BSRN values. The correlation coefficient between the SRB and BSRN values is given by ρ, the variance in the SRB values is given by σ, and N is number of SRB:BSRN pairs for each latitude region. The expressions used to calculate these parameters are given in Appendix A.

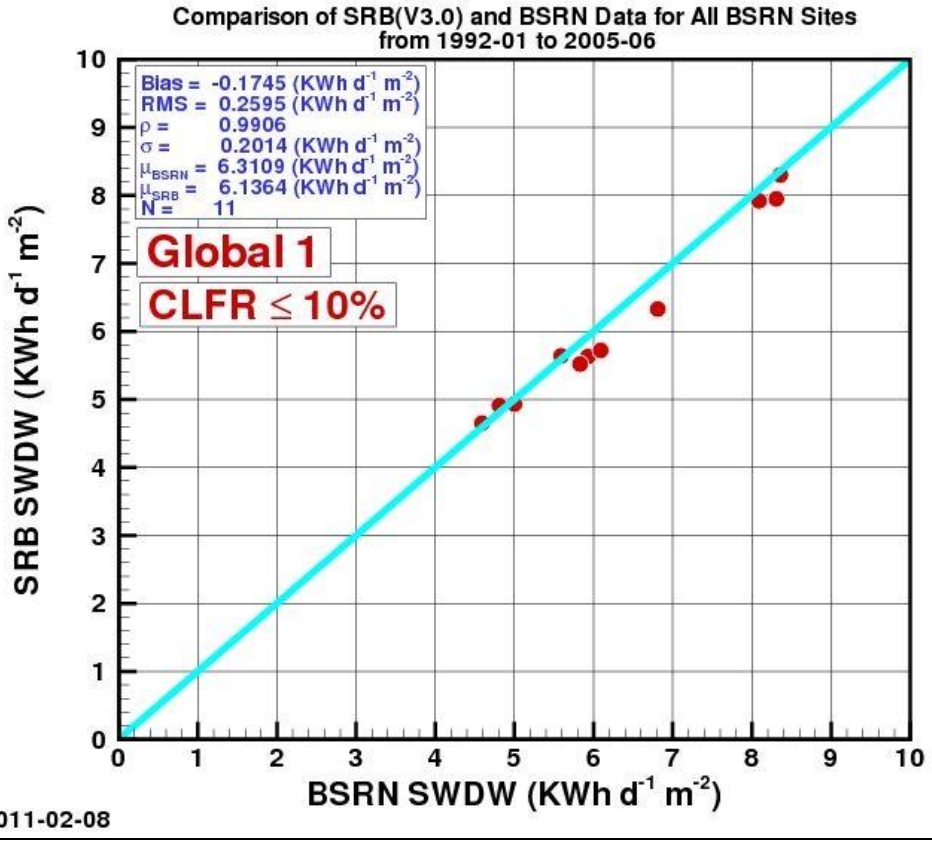

Figure 5.3.4.2 Scatter plots of the monthly averaged clear sky total radiation derived from observations at BSRN ground sites vs. monthly averaged values from SRB Release 6.0. Clear sky conditions are for less than 10% cloud cover in field-of-view of both the upward viewing ground and downward viewing satellite cameras. The comparison statistics are given for the entire globe (i.e. Global), for latitudes north and south of 60^0 (i.e. 60^0 Poleward), and for latitudes from 60^0 S to 60^0 N (i.e. 60^0 Equatorward). The Bias is the difference between the mean (μ) of the respective solar radiation values for SRB and BSRN. RMS is the root mean square difference between the respective SRB and BSRN values. The correlation coefficient between the SRB and BSRN values is given by ρ, the variance in the SRB values is given by σ, and N is number of SRB:BSRN month pairs for each latitude region. (Note that the solar radiation unit is kWh/day/m^2; multiplying kWh/day/m^2 by 3.6 yields MJ/day/m^2, and by 41.67 yields W/m^2.)

(Return to Content)

6.0. Diffuse Horizontal and Direct Normal Irradiance: The all sky (i.e. including the effect of clouds if present) total global solar radiation from the SRB archive discussed in Section VI is the sum of diffuse and direct radiation on the horizontal surface. However, estimates of all sky diffuse, $(H^{All})_{Diff}$, and direct normal radiation, $(H^{All})_{DNR}$, are often needed parameters for the design of hardware such as solar panels, solar concentrator size, day lighting, as well as agricultural and hydrology applications. From an observational perspective, $(H^{All})_{Diff}$ on a horizontal surface is that radiation remaining with $(H^{All})_{DNR}$ from the sun's beam blocked by a shadow band or tracking disk. $(H^{All})_{Diff}$ is typically measured using a sun tracking pyrheliometer with a shadow band or disk to block the direct radiation from the sun. Similarly, from an observational perspective, $(H^{All})_{DNR}$ is the amount of the beam radiation impinging on a surface perpendicular to the beam, and is typically measured using a pyrheliometer tracking the sun throughout the day.

(Return to Content)

6.1. SSE Method: Measurements of $(H^{All})_{Diff}$ and $(H^{All})_{DNR}$ are difficult to make and consequently are generally only available at high quality observational sites such as those in the BSRN network. In order to use the global estimates of the total surface solar radiation, H^{All}, from SRB Release 3.0 to provide estimates of $(H^{All})_{Diff}$ and $(H^{All})_{DNR}$, a set of polynomial equations have been developed relating the ratio of $[(H^{All})_{Diff}]/[H^{All}]$ to the clearness index $KT = [H^{All}]/[H^{TOA}]$ using ground based observations from the BSRN network. These relationships were developed by employing observations from the BSRN network to extend the methods employed by RETScreen (RETScreen, 2005) to estimate $(H^{All})_{DNR}$.

In this section we outline the techniques for estimating the $[(H^{All})_{Diff}]$ and $[(H^{All})_{DNR}]$ from the solar insolation values available in SRB Release 3.0. In the following section results of comparative studies with ground site observations are presented, which serve to validate the resulting $[(H^{All})_{Diff}]$ and $[(H^{All})_{DNR}]$ and provide a measure of the overall accuracy of our global results.

All Sky Monthly Averaged Diffuse Radiation **$[(H^{All})_{Diff}]$** ***on a Horizontal Surface:*** As just noted, measurements of $(H^{All})_{Diff}$, $(H^{All})_{DNR}$, and H^{All} are made at the ground stations in the BSRN network. These observational data were used to develop the set of polynomial equations given below relating the ratio $[(H^{All})_{Diff}]/[H^{All}]$ to the clearness index $KT = [H^{All}]/[H^{TOA}]$. We note that the top of atmosphere solar radiation, H^{TOA}, is known from satellite observations.

For latitude, ϕ, between 45°S and 45°N:

$$[(H^{All})_{Diff}]/[H^{All}] = 0.96268 - (1.45200*KT) + (0.27365*KT^2) + (0.04279*KT^3) + (0.000246*SSHA) + (0.001189*NHSA)$$

For latitude, ϕ, between 90°S and 45°S and between 45°N and 90°N:

If $0° \le SSHA \le 81.4°$:

$$[(H^{All})_{Diff}]/[H^{All}] = 1.441 - (3.6839*KT) + (6.4927*KT^2) - (4.147*KT^3) + (0.0008*SSHA) - (0.008175*NHSA)$$

If 81.4° < SSHA ≤ 100°:
$[(H^{All})_{Diff}]/[H^{All}] = 1.6821-(2.5866*KT)+(2.373*KT^2)-(0.5294*KT^3)-(0.00277*SSHA)-(0.004233*NHSA)$

If 100° < SSHA ≤ 125°:
$[(H^{All})_{Diff}]/[H^{All}] = 0.3498+(3.8035*KT)-(11.765*KT^2)+(9.1748*KT^3)+(0.001575*SSHA)-(0.002837*NHSA)$

If 125° < SSHA ≤ 150°:
$[(H^{All})_{Diff}]/[H^{All}] = 1.6586-(4.412*KT)+(5.8*KT^2)-(3.1223*KT^3)+(0.000144*SSHA)-(0.000829*NHSA)$

If 150° < SSHA ≤ 180°:
$[(H^{All})_{Diff}]/[H^{All}] = 0.6563-(2.893*KT)+(4.594*KT^2)-(3.23*KT^3)+(0.004*SSHA)-(0.0023*NHSA)$

where:

KT = $[H^{All}]/[H^{TOA}]$;
SSHA = sunset hour angle in degrees on the "monthly average day" (Klein 1977);
NHSA = noon solar angle from the horizon in degrees on the "monthly average day".

The above set of polynomial equations relate the ratio of monthly averaged horizontal diffuse radiation for all sky conditions to the monthly averaged total solar radiation for all sky conditions { $[(H^{All})_{Diff}]/[H^{All}]$ } to the clearness index KT = $[H^{All}]/[H^{TOA}]$.

All Sky Monthly Averaged Direct Normal Radiation:
$[(H^{All})_{DNR}] = ([H^{All}] - [(H^{All})_{Diff}])/ COS(THMT)$

where:

THMT is the solar zenith angle at the mid-time between sunrise and solar noon for the "monthly average day" (Klein 1977; also see Table VI.1 below).

$COS(THMT) = f + g\,[(g - f)/ 2g]^{1/2}$

H^{All} = Total of direct beam solar radiation and diffuse atmospheric radiation falling on a horizontal surface at the earth's surface

$(H^{All})_{Diff}$ = diffuse atmospheric radiation falling on a horizontal surface at the earth's surface

$f = \sin(\phi)\sin(\delta)$
$g = \cos(\phi)\cos(\delta)$

where:

ϕ is the latitude in radians;
δ is the solar declination in radians.

If SSHA = 180°, then COS(THMT) = f.
(Return to Content)

6.2 Validation: : Figures V-1 and V-2 show respectively scatter plots for the monthly mean diffuse and monthly mean direct normal radiation for all sky conditions computed from measured values at the BSRN sites (designated as BSRN SWDF and BSRN SWDN) versus the corresponding SSE values (designated as SRB SWDF and SRB SWDN) derived from the expression discussed above. Figures V-3 and V-4 show similar scatter plots for clear sky conditions.

Correlation and accuracy parameters are given in the legend boxes. Note that for the all sky condition the correlation and accuracy parameters are given for all sites (i.e. Global), for the BSRN sites regions above 60° latitude, north and south, (i.e. 60° poleward) and for BSRN sites below 60° latitude, north and south (60° equatorward).

6.2.1. Monthly Mean Diffuse (All Sky Conditions)

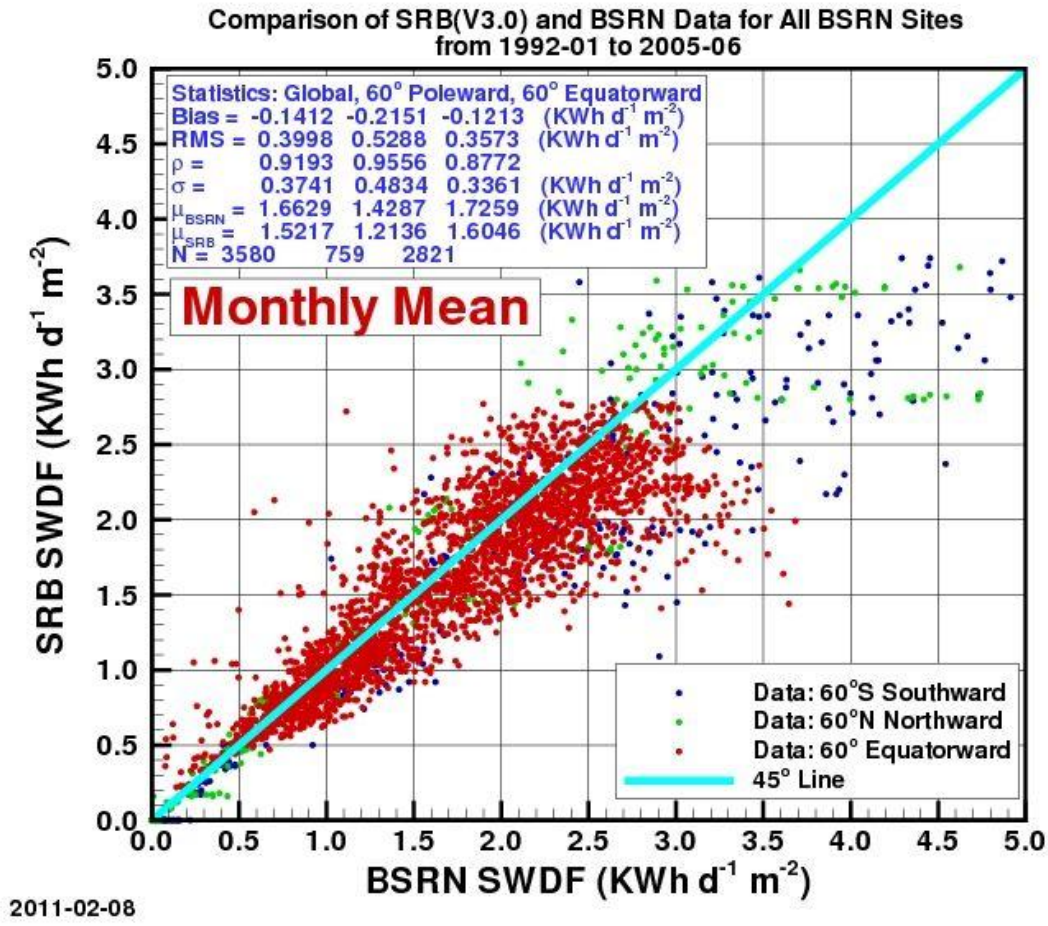

Figure 6.2.1. Scatter plot of the all sky monthly mean horizontal diffuse radiation calculated from BSRN observations and the corresponding radiation derived from SRB-Release 3.0 data. (1 KWh/day/m^2 = 41.67 W/m^2 = 3.6 MJ/day/m^2.)

However, because of the scarcity of clear sky values only the global region is used for the statistics in Figures V-3 and V-4. The Bias is the difference between the mean (μ) of the respective solar radiation values for SRB and BSRN. RMS is the root mean square difference between the respective SRB and BSRN values. The correlation coefficient between the SRB and BSRN values is given by ρ, the variance in the SRB-BSRN difference is given by σ, and N is the number of SRB-BSRN comparable pairs for each latitudinal region.
(Return to Content)

6.2.2. Monthly Mean Direct Normal (All Sly Conditions)

Figure 6.2.2.1 compares the monthly averaged direct normal radiation for all sky conditions computed from BSRN ground observations (designated as BSRN SWDN) to monthly averaged $(H^{All})_{DNR}$ calculated from SRB-R 3.0 (designated as SRB SWDN in Figure V-2) using the expressions discussed above.

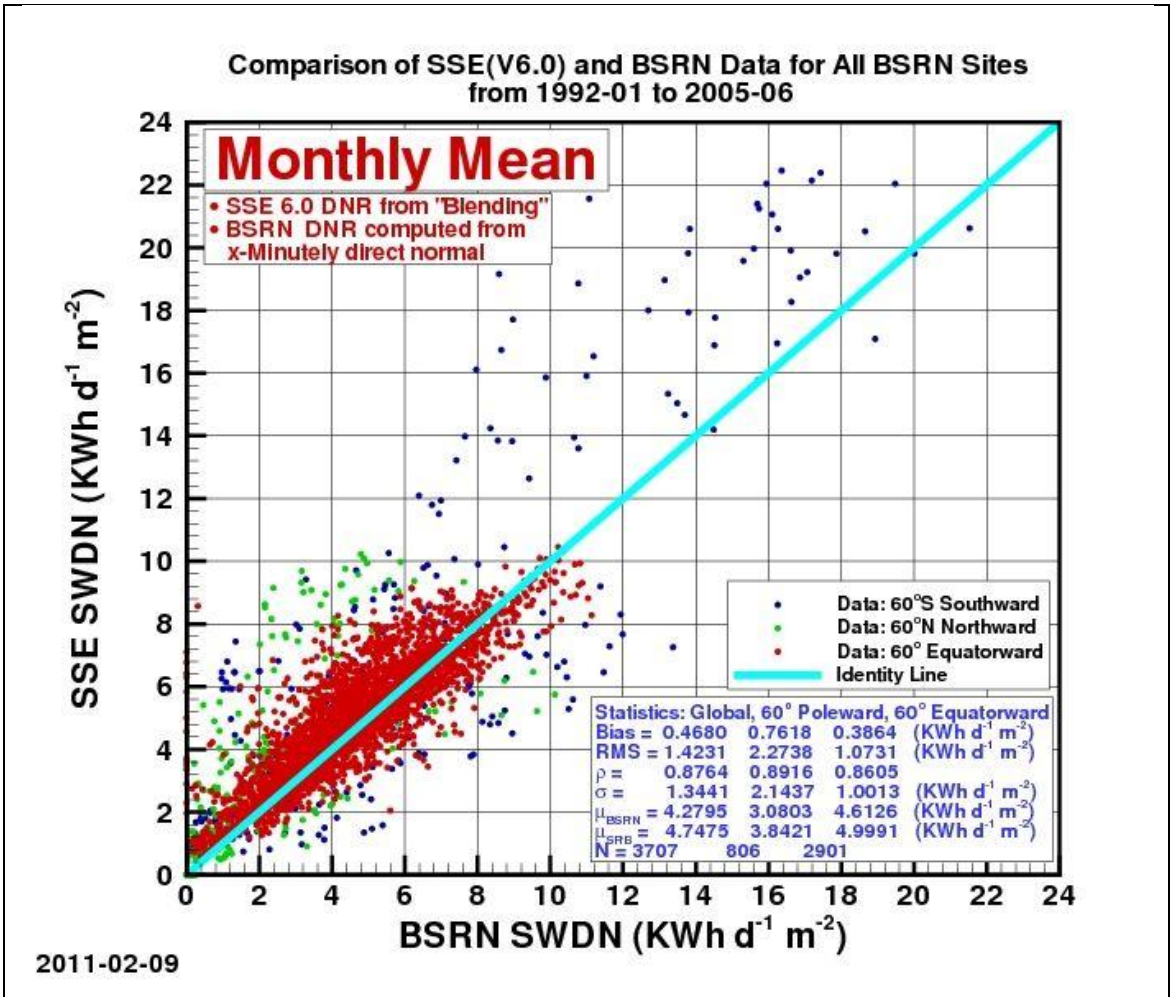

Figure 6.2.2.1. Scatter plot of the monthly mean all sky direct normal radiation determined from BSRN ground observations and the corresponding radiation derived from SRB-Release 3.0 data. (1 KWh/day/m^2 = 41.67 W/m^2 = 3.6 MJ/day/m^2.)

(Return to Content)

6.2.3. Monthly Mean Diffuse (Clear Sky Conditions)

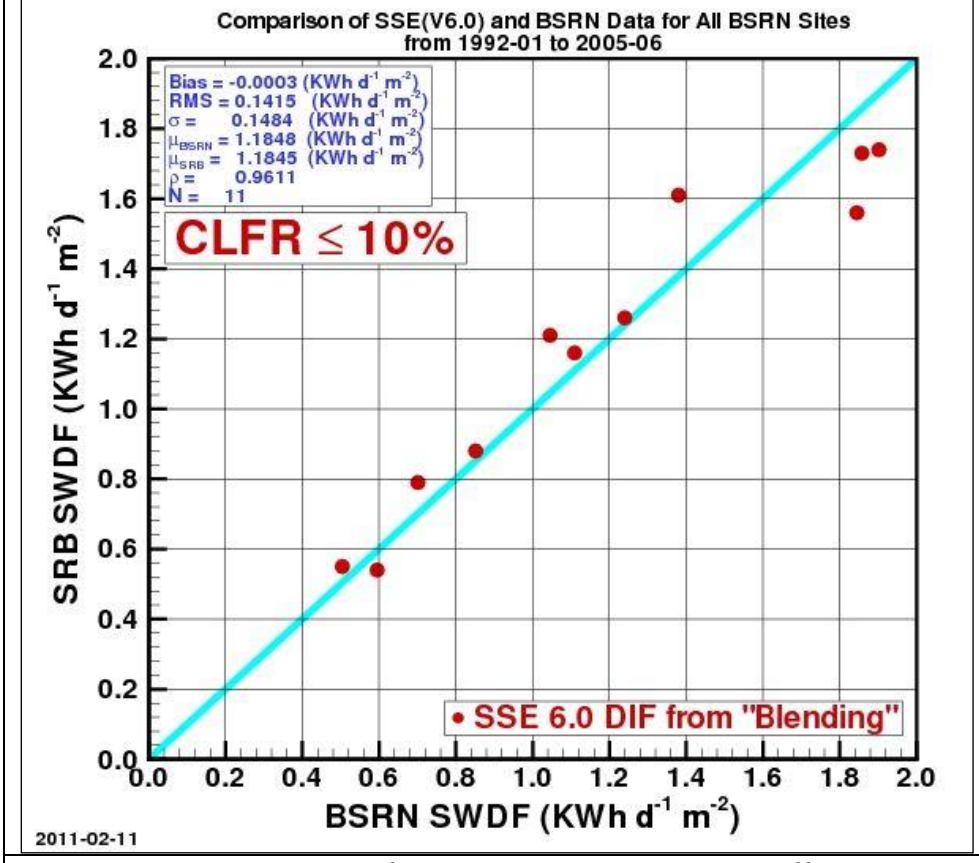

Figure 6.2.3.1. Scatter plot of the monthly mean clear sky diffuse radiation on a horizontal surface determined from BSRN ground observations and the corresponding radiation derived from SRB-Release 3.0 data. (1 KWh/day/m^2 = 41.67 W/m^2 = 3.6 MJ/day/m^2.)

6.2.4. Monthly Mean Direct Normal (Clear Sky Conditions)

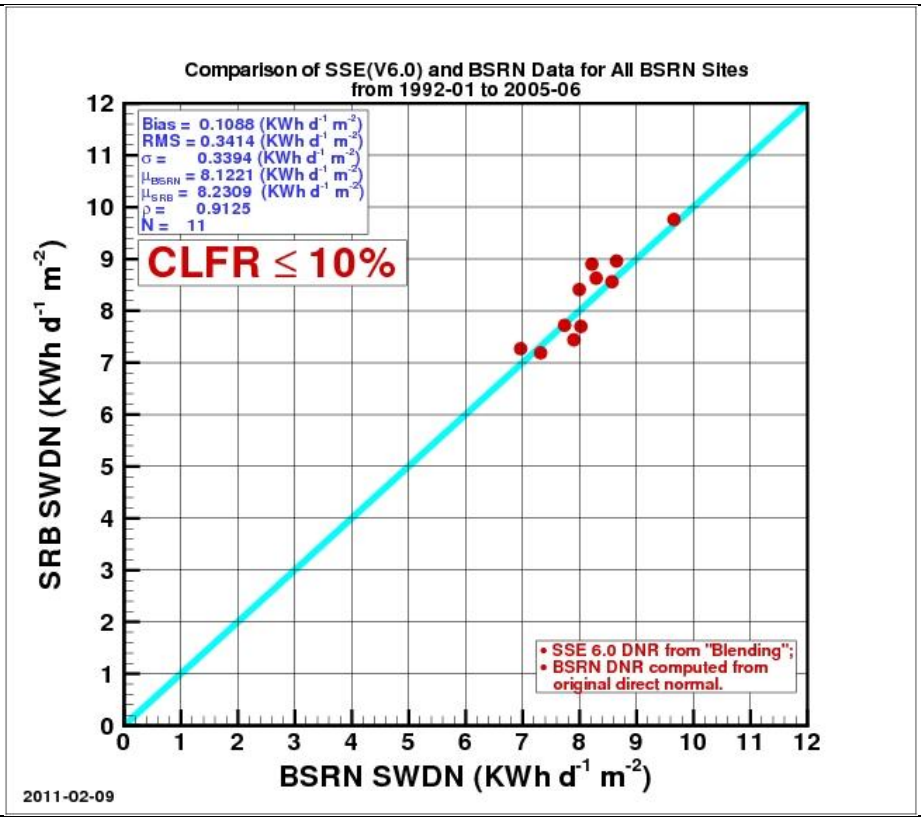

Figure 6.2.4.1. Scatter plot of the monthly mean clear sky direct normal radiation on a horizontal surface determined from BSRN ground observations and the corresponding monthly mean clear sky direct normal radiation derived from SRB-Release 3.0 data. (1 KWh/day/m^2 = 41.67 W/m^2 = 3.6 MJ/day/m^2.)

(Return to Content)

7.0 Irradiance On a Tilted Surface

The calculation of the Irradiance impinging on a tilted surface in SSE Release 6.0 basically follows the method employed by RETScreen (RETScreen 2005). The major difference is that the diffuse radiation is derived from the equations described in Section 6.
(Return to Content)

7.1. Overview of RETScreen Method: In this section we briefly outline the RETScreen method. The RETScreen method uses the "monthly average day" hourly calculation procedures where the equations developed by Collares-Pereira and Rabl (1979) and Liu and Jordan (1960) are used respectively for the "monthly average day" hourly Irradiance and the "monthly average day" hourly diffuse radiation.

Hourly Total and Diffuse Irradiance on a Horizontal Surface: We first describe the method of estimating the hourly horizontal surface Irradiance (H_h) and horizontal diffuse (H_{dh}) for daylight

hours between 30 minutes after sunrise to 30 minutes before sunset during the "monthly average day". The "monthly average day" is the day in the month whose solar declination is closest to the average declination for that month (Klein 1977). Table 7.1.1 lists the date and average declination, δ, for each month.

Table 7.1.1. List of the day in the month whose solar declination, δ, is closest to the average declination for that month

Month	Date in month	δ (°)	Month	Date in month	δ (°)
January	17	-20.9	July	17	21.2
February	16	-13.0	August	16	13.5
March	16	-2.4	September	15	2.2
April	15	9.4	October	15	-9.6
May	15	18.8	November	14	-18.9
June	11	23.1	December	10	-23.0

$H_h = r_t H$

$H_{dh} = r_d H_d$

where:

H is the monthly average Irradiance on a horizontal surface from the SRB 3.0 data set;
H_d is the monthly average diffuse radiation on a horizontal surface from the method described in section 6;
$r_t = (\pi/24)*(A + B\cos\omega)*[(\cos\omega - \cos\omega_s)/(\sin\omega_s - \omega_s \cos\omega_s)]$
(Collares-Pereira and Rabl; 1979)
$r_d = (\pi/24)*[(\cos\omega - \cos\omega_s)/(\sin\omega_s - \omega_s \cos\omega_s)]$ (Liu and Jordan; 1960)

where:

$A = 0.409 + 0.5016 \sin[\omega_s - (\pi/3)]$
$B = 0.6609 - 0.4767 \sin[\omega_s - (\pi/3)]$

where:

ω = solar hour angle for each daylight hour relative to solar noon between sunrise plus 30 minutes and sunset minus 30 minutes. The sun is displaced 15^o from the local meridian for each hour from local solar noon;
ω_s = sunset hour angle;
$\omega_s = \cos^{-1}[-\tan(\xi)*\tan(\phi)]$, (negative *before* solar noon)

where:

ϕ = Latitude
$\delta = 23.45*\sin[6.303*\{(284 + n)/365\}]$ = declination angle
n = day of year, 1 = January 1

Hourly total radiation on a tilted surface: Next, we describe the method of estimating hourly total radiation on a tilted surface (H_{th}) as outlined in the RETScreen tilted surface method. The equation, in general terms, is:

H_{th} = solar beam component + sky diffuse component + surface reflectance component

The solution is as follows:

$\cos\theta_{zh} = \cos\phi \cos\delta \cos\omega + \sin\phi \sin\delta$

$\cos\theta_h = \cos\theta_{zh} \cos\beta_h + (1 - \cos\theta_{zh}) (1 - \cos\beta_h) (\cos(\gamma_{sh} - \gamma_h))$

where:

β_h = hourly slope of the PV array relative to horizontal surface. β_h is constant for fixed panels or panels in a vertical- axis tracking system. $\beta_h = \theta_z$ for panels in a two-axis tracking system. Values for other types of tracking systems are given in Braun and Mitchell (1983).

$\gamma_{sh} = \sin^{-1} [(\sin\omega \cos(\text{solar declination}))/\sin\theta_{zh}]$

= hourly solar azimuth angle; angle between the line of sight of the Sun into the horizontal surface and the local meridian. Azimuth is zero facing the equator, positive west, and negative east.

γ_h = hourly surface azimuth of the tilted surface; angle between the projection of the normal to the surface into the horizontal surface and the local meridian. Azimuth is zero facing the equator, positive west, and negative east. γ_h is constant for fixed surfaces. $\gamma_h = \gamma_{sh}$ for both vertical- and two-axis tracking systems. See Braun and Mitchell (1983) for other types of tracking systems.

$H_{th} = (H_h - H_{dh})(\cos\theta_h/\cos\theta_{zh}) + H_{dh} [(1+\cos\beta_h)/2] + H_h*\rho_s[(1-\cos\beta_h)/2]$

where:

ρ_s = surface reflectance or albedo is assumed to be 0.2 if temperature is above 0^oC or 0.7 if temperature is below -5^oC. Linear interpolation is used for temperatures between these values.

Finally, the monthly average tilted surface Irradiance (H_t) is estimated by summing hourly values of H_{th} over the "monthly average day". It was recognized that such a procedure would be less accurate than using quality "day-by-day" site measurements, but RETScreen validation studies indicate that the "monthly average day" hourly calculation procedures give tilted surface results ranging within 3.9% to 8.9% of "day-by-day" hourly methods.

(Return to Content)

7.2. SSE Monthly Data Tables: The SSE data archive provides multi-year averaged monthly and annual values of solar Irradiance incident on a tilted surface for a user specified latitude and longitude. The irradiance incident on an equator facing panel is provide for a horizontal panel (tilt angle = 0°), and at angles equal to the latitude, and latitude ± 15 ° along with the optimum tilt angle for the given latitude/longitude. It should be emphasized that the optimum tilt angle of a solar panel at a given latitude and longitude is not simply based on solar geometry and the site latitude. The solar geometry relative to the Sun slowly changes over the period of a month because of the tilted axis of the Earth. There is also a small change in the distance from the Sun to Earth over the month because of the elliptical Earth orbit around the Sun. The distance variation may cause a change in the trend of the weather at the latitude/longitude location of the tilted solar panel. The weather trend over the month may be toward either clearer or more cloudy skies over that month for that particular year. Either cloudy- diffuse or clear-sky direct normal radiation may vary from year to year. As a result, the SSE project makes hourly calculations of tilted solar panel performance for a monthly-average day for all 1-degree cells over the globe for a 22-year period. Both the tilt angles and Irradiance values provided should be considered as average values over that 22-year period.

The expressions used for calculating the solar geometry are given in Appendix D.
(Return to Content)

7.3. Validation of Monthly Mean Irradiance on a Tilted Surface: In this section results from three approaches for validation of the SSE monthly mean irradiance on a tilted surface are presented. The first involves comparison of the tilted surface irradiance values from the SSE and RETScreen formulation. The remaining two approaches provide more definitive validation statistics in that the SSE tilted surface Irradiance values are compared to measured tilted surface Irradiance values and to values that were derived from measurements of the diffuse and direct normal components of radiation at BSRN sites.

7.3.1. SSE vs RETScreen. Table 7.3.1.1 summarizes the agreement between the SSE and RETScreen formulation in terms of the Bias and RMSE between the two methods, and the parameters (i.e. slope, intercept, and R^2) characterizing the linear least square fit to the RETScreen values (x-axis) to SSE Release 6.0 values (y-axis) when both the RETScreen and SSE methods have the same horizontal irradiance as inputs. Recall that the major difference between the two methods involves the determination of the diffuse radiation, and note that the results from the two methods are in good agreement.

Table 7.3.1.1

Table VI-2 Summary results from a comparison of the insolation on a tilted surface calculated by RETScreen and SSE Release 6.0 using the same monthly averaged insolation on a horizontal surface

Location	Lat x Long	Tilt Angle	Titled-Bias	Titled-RMSE	Titled-Slope	Titled-In'cept	Titled-R2
Ottawa Int'l Airport, Ontario. Canada	45.3N x 75.7W	45	0.47	0.56	1.17	-1.19	0.94
Berverlodge,Alberta,CN	55.2N x 119.4W	40	0.30	0.36	1.09	-0.65	0.99
Castlegar AP, British Cl, CN	49.3N x 117.6W	49	0.35	0.45	1.24	-1.43	0.99
Totonto Int'l AP, Ontario, CN	43.7N x 79.6W	43	0.06	0.09	1.02	-0.12	1.00
Burmingham,AL	33.6N x 86.8W	48	0.06	0.07	1.05	-0.29	1.00
Dodge City, KS	37.8N x 100.0W	37	0.04	0.07	1.01	-0.11	0.99
Covington, KY	39.1N x 84.7W	39	0.03	0.05	1.00	-0.03	1.00
San Francisco, CA	37.6N x 122.4W	37	0.03	0.05	1.00	-0.01	1.00
San Jose, Costa Rica	10.0N x 84.2W	25	-0.09	0.24	0.79	1.08	0.93
Boulogne Sur Seine, France	50.7N x 1.6E	35	0.15	0.18	1.06	-0.36	1.00
Riyadh (Saud-AFB), Saudi Arabia	24.7N x 46.7E	39	0.09	0.11	1.07	-0.51	0.99
Tabuk (Saud-AFB),Saudi Arabia	28.4N x 36.6E	43	0.07	0.09	1.09	-0.59	0.97
Bisha (Civ/Mil),Saudi Arabia	20.0N x 42.6E	35	-0.16	0.45	0.53	2.99	0.26
Beer-Sheva/Teyman,Israel	31.2N x 34.8E	46	0.05	0.09	0.98	0.07	0.99
Jerusalem/Atarot, Israel	31.5N x 35.2E	46	0.10	0.12	0.99	-0.05	0.99
Naha (Civ/JASDF), Japan	26.2N x 127.7E	41	0.07	0.08	1.00	-0.08	1.00
Brasila, Brasil	15.8S x 47.9W	30	-0.09	0.24	0.83	1.02	0.94
Antofagasta, Chile	23.4S x 70.5W	38	0.08	0.10	1.01	-0.13	1.00
Arica/Chacallute, Chile	18.4S x 70.5W	33	-0.20	0.49	1.14	-0.50	0.90
Windhoek/Eros (SAAF), Namibia	22.6S x 17.1E	37	-0.05	0.32	0.89	0.74	0.74
Pretoria (Met), S. Africa	25.7S x 28.2E	40	0.06	0.09	1.02	-0.19	0.98
Pietersburg (SAAF), S. Africa	23.9S x 29.5E	38	0.07	0.09	0.99	-0.03	0.98
Johannesburg, S. Africa	26.1S x 28.2E	41	0.04	0.07	1.06	-0.38	0.99
Canberra, Australlia	35.3S x 149.2E	35	0.04	0.06	0.99	0.00	1.00
		AVE =	**0.06**	**0.19**	**1.00**	**-0.03**	**0.94**
		STD =	**0.15**	**0.16**	**0.14**	**0.86**	**0.15**

(Return to Content)

7.3.2 SSE vs Direct Measurements of Tilted Surface Irradiance. Figure 7.3.2.1 show the time series of the monthly mean solar irradiance derived from measurements and the corresponding values from SSE. Figure 7.3.2.1a gives the measured and SSE solar irradiance on a horizontal surface and Figure 7.3.2.1b gives the measured and SSE values on a South facing surface tilted at 45^{o}. The measured values were taken from the University of Oregon Solar Radiation Monitoring Laboratory archive (http://solardat.uoregon.edu/index.html) for Chaney, WA. For comparison the RETScreen values have also been included.

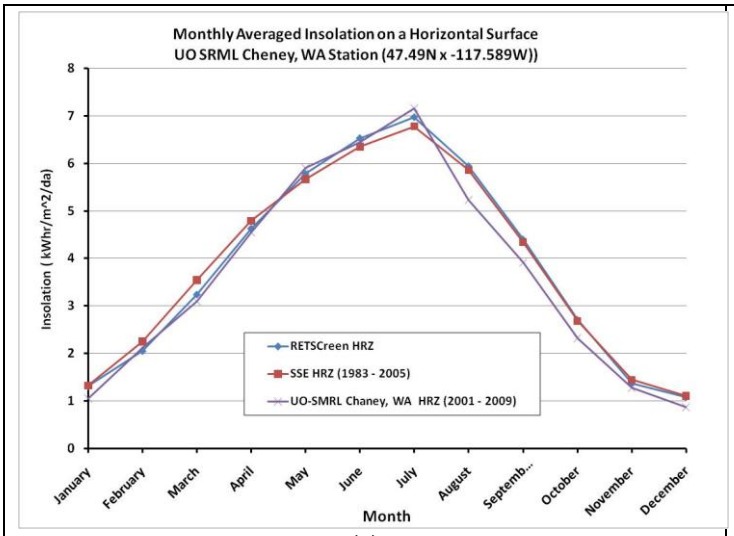

(a)

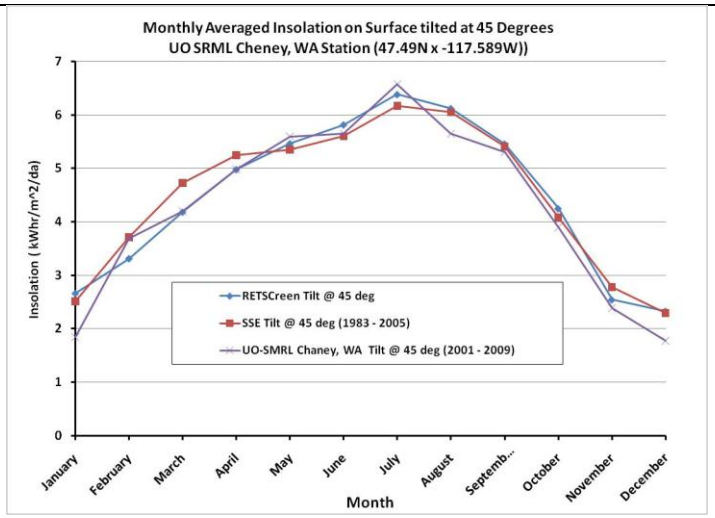

(b)

Figure 7.3.2.1 Monthly time series of solar irradiance measure on a horizontal (a) and tilted (b) surface at the University of Oregon Solar Radiation Monitoring Laboratory Chaney, WA station, and corresponding irradiance from RETScreen and SSE. *(1 KWh/day/m^2 = 41.67 W/m^2 = 3.6 MJ/day/m^2.)*

(Return to Content)

7.3.3 SSE vs BSRN Tilted Surface Irradiance. Solar irradiance measurements at the most of the ground sites in the Base Line Surface Network include the diffuse and direct normal components as well as a direct measurement of the global, or total, irradiance on a horizontal surface. These measurements are typically made with at 1-, 2-, 3- or 5-minute intervals throughout the day. The diffuse and direct normal measurements, coupled with the solar zenith angle, provide the necessary components to estimate solar irradiance on a tilted surface as outlined below.

For any given BSRN site, consider a 3-D coordinate system with the origin at the BSRN site, X-axis pointing eastward, Y-axis northward, and Z-axis upward. For any given instant corresponding to a BSRN record, the unit vector pointing to the Sun is {sin(Z)cos[(π/2)-A]***i***, sin(Z)sin[(π/2)-A]***j***, cos(Z)***k***}, and the unit vector along the normal of a surface tilted toward the equator is [0***i***, -sin(T)***j***, cos(T)***k***] for Northern Hemisphere, and [0***i***, sin(T)***j***, cos(T)***k***] for Southern Hemisphere, where Z is the solar zenith angle, A is the azimuth angle of the Sun, and T is the tilt angle of the tilted surface. And the direct flux on the tilted surface is the direct normal flux times the dot product of the aforementioned two unit vectors which is -sin(Z)cos(A)sin(T) + cos(Z)cos(T) for Northern Hemisphere and sin(Z)cos(A)sin(T) + cos(Z)cos(T) for Southern Hemisphere. If the dot product of the two unit vectors is less than zero, which means the Sun is behind the tilted surface, the direct flux on the tilted surface is set to zero. After this conversion, the 3-hourly, daily and monthly means of the direct component on the tilted surface can then be derived. The diffuse component on a tilted surface is partly from the ground reflectance. For the scarcity of surface albedo measurement at the BSRN sites, we assume that the diffuse component on the tilted surface is the same as on the horizontal surface for a first estimate. This is equivalent to treating the surface albedo as 0.4 on average based on the available comparable

SRB-BSRN pairs of data points. The sum of the direct and diffuse components is the total flux on the tilted surface.

Figure 7.3.3.1 is a scatter plot of the climatological monthly mean irradiance on a tilted surface derived from the BSRN measurements of the diffuse and direct normal components versus the corresponding SSE tilted surface radiation values.

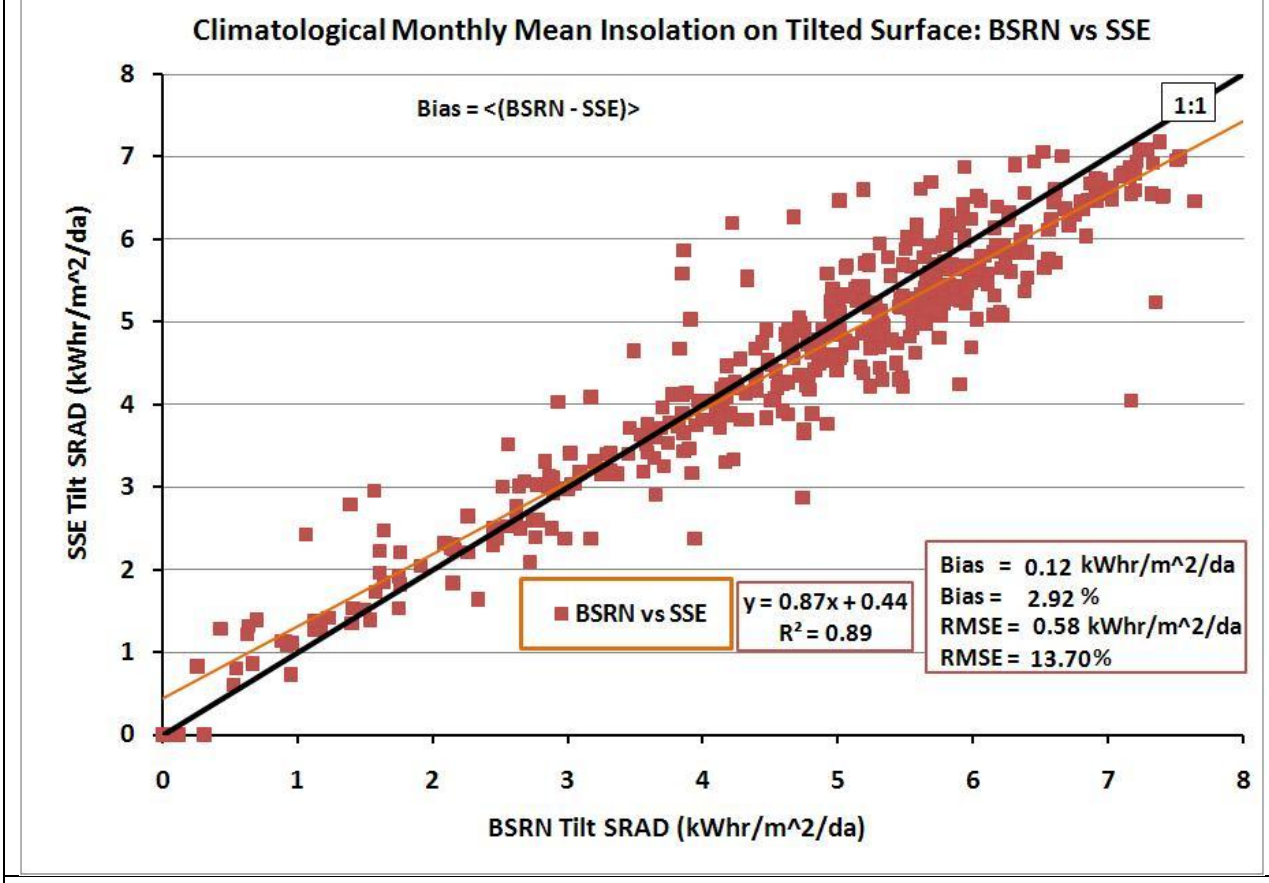

Figure 7.3.3.1 scatter plot of the climatological monthly mean irradiance on a tilted surface derived from the BSRN measurements of the diffuse and direct normal components versus the corresponding SSE tilted surface radiation values. (1 KWh/day/m^2 = 41.67 W/m^2 = 3.6 MJ/day/m^2.)

(Return to Content)

8. Parameters for Sizing Battery or Other Energy –Storage Systems

Solar energy systems that are not connected to an electrical grid system usually require back-up or storage equipment to provide energy during unusually cloudy days. Unusually cloudy conditions occurring over a number of consecutive days continually draw reserve power from batteries or other storage devices for solar systems not connected to an electrical grid. Storage devices must be designed to withstand continuous below-average conditions in various regions of the globe. Various industry organizations use different methods to size either battery or other types of backup systems. One international

organization has required that all stand-alone medical equipment that it purchases must operate for 6 BLACK or NO-SUN days in parts of the tropics. The methods used require different solar irradiance parameters. Three types of parameters are provided in the SSE data set. They are listed in Table 8.1 and described in the subsequent text and in Whitlock et al (2005).

Table 8.1. Parameters for Sizing Battery or other Energy-storage Systems:
• Minimum available irradiance as % of average values over consecutive-day period • Solar Insolation deficits below expected values over consecutive-day period • Equivalent number of NO-SUN days over consecutive-day period • Available Surplus Insolation Over Consecutive –day period (%)

(Return to Content)

8.1 Minimum percentage Irradiance over a consecutive-day period (1, 3, 7, 14, or 21 days) is the difference between the multi-year (Jul 1983 - Jun 2005) monthly averaged irradiance and the multi-year monthly averaged minimum irradiance over the indicated number of days (1, 3, … days) within each month. The average is computed over the indicated days is a running average within each month. The defining equations are given below.

For month j, and year k the running average of the daily irradiance over p days is given by

$$\langle SRAD \rangle^{p}_{jk} = [\sum^{p}_{i=i}(\langle SRAD \rangle_{ijk})]/p$$

Where:

$\langle SRAD \rangle_{ijk}$= Daily averaged surface irradiance for day i, in month j, and year k
i = day in month for j
j = month of year
k = year in n-year time multi-year span (Jul 1983 - Jun 2005)
p = averaging period =1, 3, 7, 14, or 21 days

The multi-year monthly average of the running sum of irradiance over the consecutive p-day average in month j is given by

$$\langle SRAD \rangle^{p}_{j} = \sum^{n}_{k=1}(\langle SRAD \rangle^{p}_{jk})/n$$

Where:

n = 22 the number years in time span from Jul. 1983 – Jun 2005

The parameter Min/p-day for month j is the % difference between multi-year monthly average value, $\langle SRAD \rangle^{p}_{j}$, and the minimum value of $\langle SRAD \rangle^{p}_{j}$ over the 1983 – 2005 time period and is given by

$$[\text{Min/p-day}]^{p}_{j} = 100 - (100*[\langle SRAD \rangle^{p}_{j} - \langle SRADmin \rangle^{p}_{j}]/ \langle SRAD \rangle^{p}_{j})$$

$$\langle SRADmin \rangle^{p}_{j} = MIN(\langle SRAD \rangle^{p}_{j})$$

(Return to Content)

8.2 Solar radiation deficits below expected values incident on a horizontal surface over a consecutive-day period is the multi-year monthly averaged deficit calculated as following

$$<SRADdef>^{p}_{j} = <SRADsum>^{p}_{j} - <SRADsummin>^{p}_{j}$$

where

$$<SRADsum>^{p}_{j} = \sum^{n}_{k=1}(<SRADsum>^{p}_{jk})/n$$

$$<SRADsum>^{p}_{j} = \sum^{n}_{k=1}(<SRADsum>^{p}_{jk})/n$$

$$(SRADsum)^{p}_{jk} = \sum^{p}_{i=1}(<SRAD>_{ijk})$$

$<SRAD>_{ijk}$= Daily averaged surface irradiance for day i, in month j, and year k

i = day in month for j

j = month of year

k = year in n-year time multi-year span (Jul 1983 - Jun 2005)

p = running average period =1, 3, 7, 14, or 21 days

And

$$<SRADsumMin>^{p}_{j} = MIN(<SRADsum>^{p}_{j})$$

(Return to Content)

8.3 Equivalent number of NO-SUN or BLACK days is based upon the deficit solar radiation below expected multi-year monthly averaged value and calculated as follows:

$$<NoSunDa>^{p}_{j} = <SRADdef>^{p}_{j} / <SRAD>^{p}_{j}$$

Where:

$$<SRADdef>^{p}_{j} = <SRADsum>^{p}_{j} - <SRADsumMin>^{p}_{j}$$

$$<SRADsum>^{p}_{j} = \sum^{n}_{k=1}(<SRADsum>^{p}_{jk})/n$$

$$<SRADsum>^{p}_{j} = \sum^{n}_{k=1}(<SRADsum>^{p}_{jk})/n$$

$$(SRADsum)^{p}_{jk} = \sum^{p}_{i=1}(<SRAD>_{ijk})$$

$$<SRADsumMin>^{p}_{j} = MIN\{(SRADsum)^{p}_{jk}\}$$

And

$<SRAD>_{j} = \sum^{n}_{k=1}(<SRAD>_{jk})/n$ = multi-year monthly averaged for month j

$<SRAD>_{jk} = \sum^{m}_{i=1}(<SRAD>_{ijk})/m$ = monthly average SRAD for month j in year k

$<SRAD>_{ijk}$ = daily averaged solar irradiance for day i, in month j, in year k.

i = day in month for j

j = month of year

k = 22 = number of years multi-year span (Jul 1983 - Jun 2005)

m = days in month j

(Return to Content)

8.4 Available Surplus Insolation Over Consecutive –day period (1, 3, 7, 14, or 21 days) is calculated for each month as the climatological average (i.e. multi-year monthly average) over the 22-year period (July 1983 – June 2005) as a percentage of the expected average insolation

over the same consecutive day period. The parameter Max/p-day for month j is the % difference between multi-year monthly average value, $<SRAD>^{p}_{j}$, and the maximum value of $<SRAD>^{p}_{j}$ over the 1983 – 2005 time period. The following summarizes the procedure for calculating the multi-year monthly average value of Max/p-day

$$[Max/p\text{-}day]^{p}_{j} = 100 - (100*[<SRAD>^{p}_{j} - <SRADmax>^{p}_{j}]/ <SRAD>^{p}_{j})$$

Where

$<SRAD>^{p}_{j} = \sum^{n}_{k=1}(<SRAD>^{p}_{jk})/n$

$=$ *The multi-year monthly average of* $<SRAD>^{p}_{jk}$ *for month j*

$<SRAD>^{p}_{jk} = [\sum^{p}_{i=i}(<SRAD>_{ijk})]/p$ = The running average of the daily insolation over p days for month j & year k

$<SRAD>_{ijk}$= Daily averaged surface insolation for day i, in month j, and year k

i = day in month for j

j = month of year

k = year in n-year time multi-year span (Jul 1983 - Jun 2005)

p = averaging period =1, 3, 7, 14, or 21 days

n = 22 the number years in time span from Jul. 1983 – Jun 2005

$<SRADmax>^{p}_{j} = MAX(<SRAD>^{p}_{j})$

(Return to Content)

9.0. Meteorological Parameters

The global distribution of meteorological parameters in the SSE archive (e.g dew/frost point minimum, maximum and daily averaged temperatures, relative humidity, and surface pressure) are taken directly from or calculated based upon parameters in NASA's Global Model and Assimilation Office (GMAO), Goddard Earth Observing System global assimilation model version 4 (GEOS-4) (http://gmao.gsfc.nasa.gov/systems/geos4/). Relative humidity is a calculated parameter based upon pressure, temperature and specific humidity, all parameters obtained from the assimilation model. Dew/frost point temperatures are calculated values based upon the relative humidity and air temperature which is obtained from the assimilation model. Precipitation data has been obtained from the Global Precipitation Climate Project (GPCP - http://precip.gsfc.nasa.gov/). The GPCP precipitation data product, Version 2.1, is a global 2.5° x 2.5° monthly accumulation based upon combination of observations from multiple platforms. The one degree SSE estimates of precipitation are based upon replicating GPCP values for SSE cells that overlap GPCP cells and averaging GPCP values when the SSE cell overlaps two or more GPCP cells. Monthly mean wind speed data is based upon the NASA/GMAO GEOS version 1 (GEOS-1) for the time period July 1983 –June 1993. In the following sections results associated with testing /validating each parameter against ground site observation is discussed.

(Return to Content)

9.1. Assessment of Assimilation Modeled Temperatures: As noted above all meteorological parameters, except precipitation, are based directly or indirectly (i.e. calculated) on the GMAO assimilation models. The meteorological parameters emerging from the GMAO assimilation models are estimated via "An atmospheric analysis performed within a data assimilation context [that] seeks to combine in some "optimal" fashion the information from irregularly distributed atmospheric observations with a model state obtained from a forecast initialized from a previous analysis." (Bloom, et al., 2005). The model seeks to assimilate and optimize observational data and model estimates of atmospheric variables. Types of observations used in the analysis include (1) land surface observations of surface pressure; (2) ocean surface observations of sea level pressure and winds; (3) sea level winds inferred from backscatter returns from space-borne radars; (4) conventional upper-air data from rawinsondes (e.g., height, temperature, wind and moisture); (5) additional sources of upper-air data include drop sondes, pilot balloons, and aircraft winds; and (6) remotely sensed information from satellites (e.g., height and moisture profiles, total perceptible water, and single level cloud motion vector winds obtained from geostationary satellite images). Emerging from the analysis are 3-hourly global estimates of the vertical distribution of a range of atmospheric parameters. The assimilation model products are bi-linearly interpolated to a 1^0 by 1^0 grid.

In addition to the analysis reported by the NASA's Global Model and Assimilation Office (GMAO) (Bloom, et al. 2005), the POWER project initiated a study focused on estimating the accuracy of the GEOS-4 meteorological parameters in terms of the applications within the POWER project. In particular, the GEOS-4 temperatures (minimum, maximum and daily averaged air and dew point), relative humidity, and surface pressure have been explicitly compared to global surface observational data from the National Center for Environmental Information (NCEI – formally National Climatic Data Center - http://www.ncdc.noaa.gov/oa/ncdc.html) global "Summary of the Day" (GSOD) files, and to observations from other high quality networks such as the Surface Radiation (SURFRAD - http://www.srrb.noaa.gov/surfrad/index.html), Atmospheric Radiation Measurement (ARM - http://www.arm.gov/), as well as observations from automated weather data networks such as the High Plains Regional Climate Center (HPRCC - http://www.hprcc.unl.edu/index.php).

In this section we will focus primarily on the analysis of the GEOS-4 daily maximum and minimum temperatures, and the daily mean temperature using observations reported in the NCEI - GSOD files, with only summary comments regarding results from the other observational networks noted above.

The GEOS-4 re-analysis model outputs meteorological parameters at 3-hourly increments (e.g. 0, 3, 6, 9, 12, 15, 18, and 21 Z) on a global 1- deg by 1.25-deg grid at 50 pressure levels. The 1-deg by 1.25-deg grid is bi-linearly interpolated to a 1-deg by 1-deg grid to match the GEWEX/SRB 3.0 solar radiation values. The local daily maximum (Tmax) and minimum (Tmin) temperature, and the local daily mean (Tave) temperature contained in the SSE archive are at 10 meters above the surface and are based upon the GEOS-4 3-hourly data. The GEOS-4 meteorological data spans the time period from July, 1983 - through June 2005; comparative analysis discussed here is based upon observational data from January 1, 1983 through December 31, 2006.

The observational data reported in the NCEI GSOD files are hourly observations from globally distributed ground stations with observations typically beginning at 0Z. For the analysis reported

herein, the daily Tmin, Tmax and Tave were derived from the hourly observations filtered by an "85%" selection criteria applied to the observations reported for each station. Namely, only data from NCEI stations reporting 85% or greater of the possible 1-hourly observations per day and 85% or greater of the possible days per month were used to determine the daily Tmin, Tmax, and Tave included in comparisons with the GEOS-4 derived data. Figure 9.1.1 illustrates the global distribution of the surface stations remaining in the NCEI data files for 1983 and 2004 after applying our 85% selection criteria. Note that the number of stations more than doubled from 1983 (e.g. 1104 stations) to 2004 (e.g. 2704 stations), and that majority of the stations are located in the northern hemisphere.

Unless specifically noted otherwise, all GEOS-4 air temperatures represent the average value on a 1^o x 1^o latitude, longitude grid cell at an elevation of 2 m above the earth's surface and NCEI values are ground observations at an elevation of 2 meters above the earth's surface. Scatter plots of Tave, Tmax, and Tmin derived from ground observations in the NCEI files versus GEOS-4 values for the years 1987 and 2004 are shown in Figure 9.1.2. These plots illustrate the agreement typically observed for all the years 1983 through 2006. In the upper left corner of each figure are the parameters for the linear least squares regression fit to theses data, along with the mean Bias and RMSE between the GEOS-4 and NCEI observations.

For the year 1987, 1139 stations passed our 85% selection criteria yielding 415,645 matching pairs on NCEI/GEOS-4 values; for 2004, 2697 stations passed yielding 987,451 matching pairs of NCEI/GEOS-4 temperature values. The color bar along the right side of the scatter plot provides a measure of the distribution of the NCEI/GEOS-4 temperature pairs. For example, in Figure 9.1.2, each data point shown in dark blue represents a 1-degree cell with 1 to 765 matching temperature pairs, and all of the 1-degree cells shown in dark blue contain 15.15% of the total number of ground site points. Likewise, the darkest orange color represent 1-degree cells for which there are from 6120 to 6885 matching temperature pairs, and taken as a group all of the 1-degree cells represented by orange contain 10.61% of the total number of matching ground site points. Thus, for the data shown in Figure 9.1.2a, approximately 85% of matching temperature pairs (i.e. excluding the data represented by the dark blue color) is "tightly" grouped along the 1:1 correlation line.

In general, the scatter plots shown in Figure 9.1.2, and indeed for all the years from 1983 through 2006, exhibit good agreements between the GEOS-4 data and ground observations. Notice however that for both the 1987 and 2004 data, on a global basis, the GEOS-4 Tmax values are cooler than the ground values (e.g. bias = -1.9 C in 1987 and -1.8 C in 2004); the GEOS-4 Tmin values are warmer (e.g. bias = 0.4^o C in 1987 and 0.2^o C in 2004); and that GEOS-4 Tave values are cooler (e.g. bias = -0.5^o C in 1987, and -0.6^o C in 2004. Similar trends in the respective yearly averaged biases between GEOS-4 and NCEI observations were noted for each year from 1983 – 2006 (see Table 9.1.1 below). The ensemble average for the years 1983 – 2006 yields a GEOS-4 Tmax which is 1.82^o C cooler than observed at NCEI ground Sites, a Tmin about 0.27^o C warmer, and a Tave about 0.55^o C cooler. Similar trends are also observed for measurements from other meteorological networks. For example, using the US National Weather Service Cooperative Observer Program (COOP) observations, White, et al (2008) found the mean values of GEOS-4 Tmax, Tmin, and Tave to be respectively 2.4^o C cooler, Tmin 1.1^o C warmer, and 0.7^o C cooler that the COOP values.

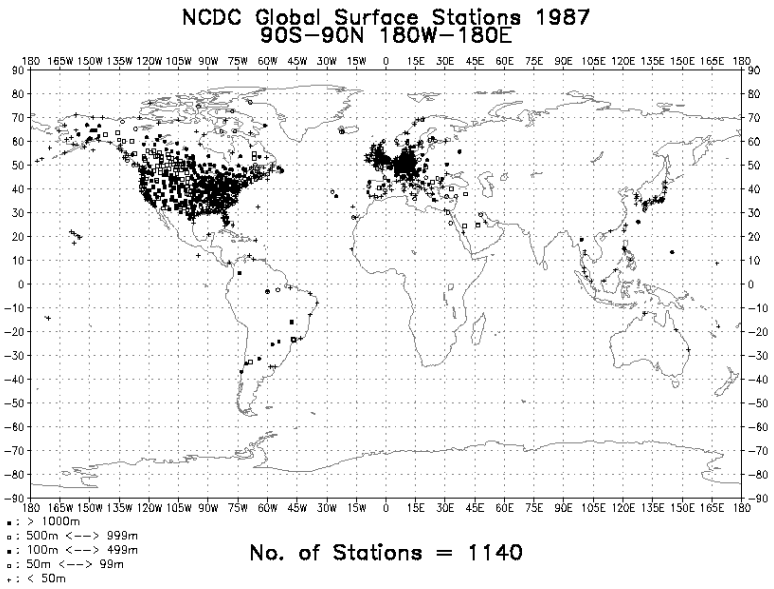

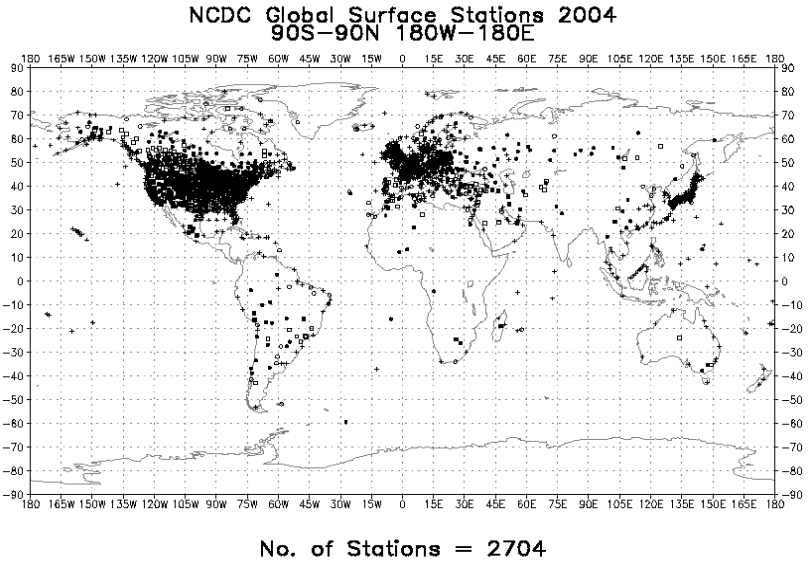

Figure 9.1.1: Top (a) and bottom (b) figures show distribution of NCEI stations meeting 85% selection criteria for 1987 and 2004, respectively.

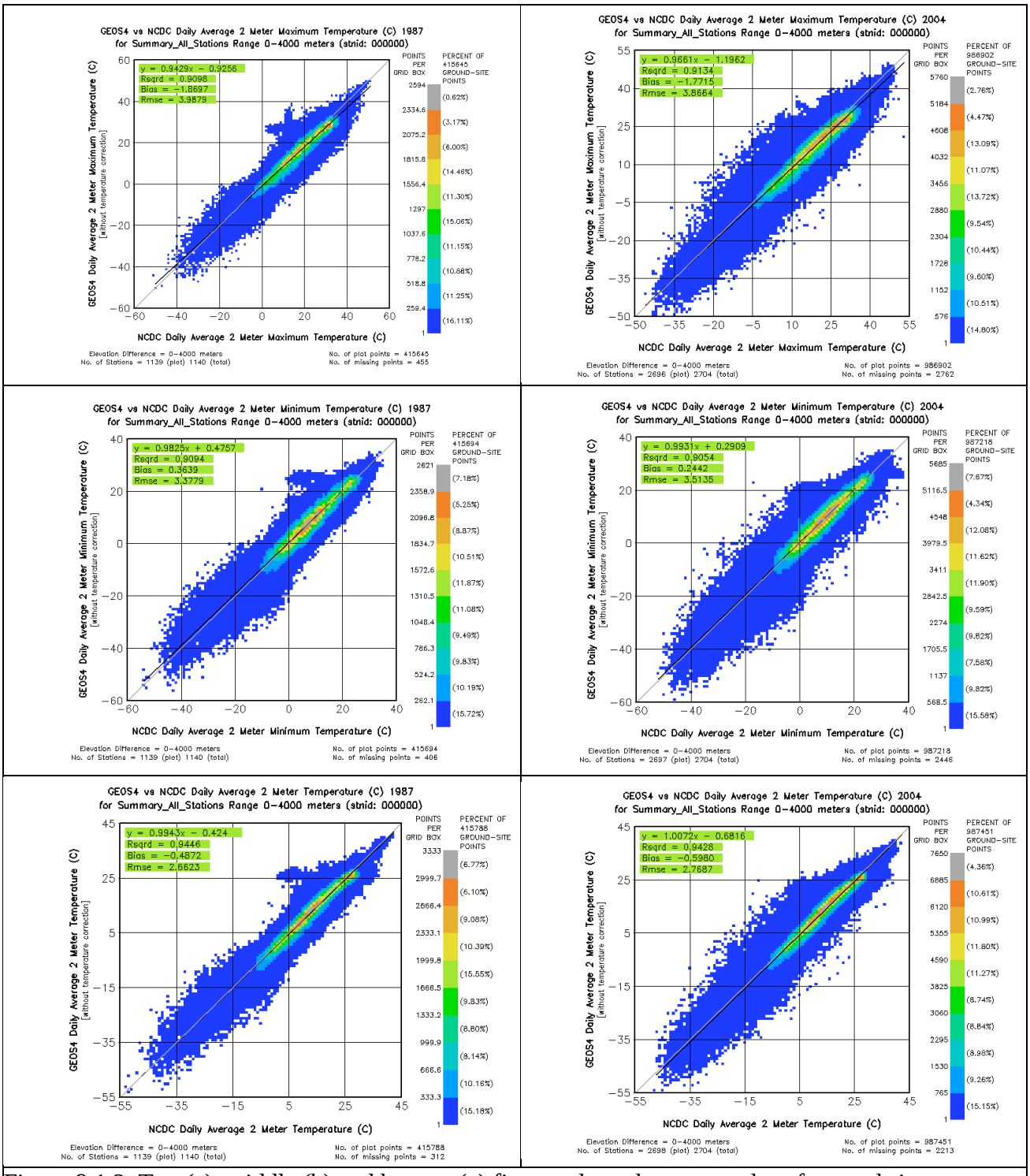

Figure 9.1.2. Top (a), middle (b) and bottom (c) figures show the scatter plot of ground site observations versus GEOS-4 values of Tmax, Tmin, and Tave for the years 1987 and 2004. The color bar in each figure indicates the number and percentage of ground stations that are included within each color range.

Table 9.1.1 Global year-by-year comparison of daily Tmax, Tmin, and Tave: NCEI GSOD values vs GEOS-4 temperatures

	Tmax					Tmin					Tave				
Year	Slope	Intercept (C)	R^2	RMSE (C)	Bias (C)	Slope	Intercept (C)	R^2	RMSE (C)	Bias (C)	Slope	Intercept (C)	R^2	RMSE (C)	Bias (C)
2006	0.97	-1.28	0.92	3.88	-1.72	1.00	0.09	0.90	3.59	0.11	1.02	-0.79	0.94	2.82	-0.59
2005	0.97	-1.40	0.92	4.00	-1.92	0.99	0.20	0.91	3.57	0.16	1.01	-0.81	0.95	2.81	-0.67
2004	0.97	-1.20	0.91	3.86	-1.78	0.99	0.28	0.91	3.50	0.24	1.01	-0.69	0.94	2.76	-0.60
2003	0.95	-0.91	0.91	3.96	-1.74	0.99	0.46	0.91	3.49	0.38	1.00	-0.47	0.94	2.82	-0.53
2002	0.94	-0.88	0.91	4.06	-1.94	0.98	0.47	0.90	3.55	0.30	0.98	-0.48	0.94	2.85	-0.66
2001	0.97	-1.69	0.92	4.00	-2.20	1.00	0.10	0.90	3.62	0.11	1.01	-0.97	0.95	2.78	-0.81
2000	0.97	-1.17	0.91	3.84	-1.67	1.00	0.25	0.91	3.50	0.27	1.01	-0.65	0.94	2.77	-0.52
1999	0.97	-1.25	0.91	3.80	-1.78	0.99	0.47	0.91	3.37	0.39	1.00	-0.60	0.95	2.63	-0.54
1998	0.98	-1.29	0.92	3.67	-1.71	0.99	0.11	0.91	3.27	0.07	1.01	-0.81	0.94	2.62	-0.68
1997	0.97	-1.20	0.92	3.64	-1.66	0.99	-0.01	0.91	3.30	-0.05	1.00	-0.72	0.95	2.67	-0.68
1996	0.95	-0.71	0.91	3.67	-1.56	0.98	0.27	0.91	3.31	0.15	0.99	-0.46	0.94	2.66	-0.55
1995	0.97	-1.44	0.92	3.93	-1.91	1.00	0.32	0.92	3.44	0.29	1.01	-0.69	0.95	2.69	-0.60
1994	0.98	-1.58	0.92	4.08	-1.93	1.00	-0.01	0.91	3.55	-0.04	1.01	-0.82	0.95	2.85	-0.71
1993	0.96	-1.22	0.92	3.93	-1.80	0.99	0.22	0.92	3.40	0.16	1.00	-0.51	0.95	2.68	-0.52
1992	0.95	-0.92	0.91	3.90	-1.70	0.98	0.43	0.90	3.46	0.33	1.00	-0.43	0.94	2.67	-0.43
1991	0.95	-1.05	0.91	4.14	-1.89	0.99	0.35	0.91	3.45	0.27	1.00	-0.45	0.94	2.80	-0.49
1990	0.95	-1.12	0.90	4.18	-1.94	0.99	0.40	0.91	3.49	0.35	1.00	-0.44	0.94	2.79	-0.49
1989	0.96	-1.18	0.91	4.15	-1.91	0.99	0.48	0.92	3.50	0.42	0.99	-0.40	0.95	2.79	-0.46
1988	0.95	-1.11	0.91	4.03	-1.90	0.99	0.55	0.91	3.38	0.47	1.00	-0.38	0.95	2.63	-0.42
1987	0.94	-0.93	0.91	3.99	-1.87	0.98	0.48	0.91	3.38	0.36	0.99	-0.42	0.94	2.66	-0.49
1986	0.95	-1.02	0.91	4.05	-1.88	0.98	0.52	0.91	3.37	0.39	0.99	-0.35	0.94	2.70	-0.45
1985	0.96	-1.11	0.92	4.03	-1.84	0.99	0.38	0.92	3.58	0.32	0.99	-0.44	0.95	2.83	-0.49
1984	0.96	-1.07	0.91	4.00	-1.79	1.00	0.44	0.91	3.46	0.41	1.00	-0.45	0.94	2.79	-0.47
1983	0.96	-1.19	0.91	4.02	-1.78	0.99	0.41	0.91	3.44	0.34	1.00	-0.49	0.94	2.82	-0.52
Average	**0.96**	**-1.16**	**0.91**	**3.95**	**-1.82**	**0.99**	**0.32**	**0.91**	**3.46**	**0.26**	**1.00**	**-0.57**	**0.94**	**2.75**	**-0.56**
STDEV	**0.01**	**0.22**	**0.01**	**0.15**	**0.13**	**0.01**	**0.17**	**0.01**	**0.10**	**0.14**	**0.01**	**0.17**	**0.00**	**0.08**	**0.10**

The average of the least square fit along with the average RMSE and Bias values given in Table 9.1.1 are taken as representative of the agreement expected between GEOS-4 temperatures and ground site measurements.

Further analysis, described in Appendix D, shows that one factor contributing to the temperature biases between the assimilation model estimates and ground site observations is the difference in the elevation of the reanalysis grid cell and the ground site. Appendix D describes a downscaling methodology based upon a statistical calibration of the assimilation temperatures relative to ground site observations. The resulting downscaling parameters (i.e. lapse rate and offset values) can be regionally and/or seasonally used to downscale the model temperatures yielding estimates of local temperatures with reduced biases relative to ground site observations.

Application of the downscaling procedure described in Appendix D is currently implemented in the SSE Archive to provide adjusted 22–year monthly mean Tmax, Tmin, and Tave temperatures based upon a user's input of the ground site elevation. As an example of downscaling, Table D.5 and Table D.6 in Appendix D give, respectively, the global monthly averaged Mean Bias Error (MBE) and Root Mean Square Error (RMSE) for unadjusted and downscaled 2007 GEOS-4 temperatures relative to NCEI temperatures.

(Return to Content)

9.2. Relative Humidity: Relative humidity, RH, is not explicitly calculated in NASA's assimilation models. The RH values in the POWER archives are calculated from pressure, air temperature and specific humidity, parameters that are available in the model. The following is a summary of the expressions used to calculate RH.

(9.2.1) $RH = [(Rho)_w / (Rho)^*_w] \times 100$

(9.2.2) $q = (Rho)_w / (Rho)_a$

Where
$(Rho)_w$ = Ambient water vapor density at P and T
$(Rho)^*_w$ = saturated water vapor density at P and T
$(Rho)_a$ = density of moist air
RH = Relative Humidity (%)
q = Specific Humidity from assimilation model

Combining (9.2.1) and (9.2.2) yields

(9.2.3) $RH = \{(q) \times (Rho)_a /(Rho)^*_w \} \times 100$

The ratio of the density of air at temperature Ta and Pa to air density at STP (Standard Temperature and Pressure: P_{STP} =1013.25mb; T_{STP} = +273.15 ^oK) is given by

(9.2.4) $(Rho)_a /(Rho)_{STP} = (P_a/R \times T_a) / (P_{STP} / R \times T_{STP})$
$= (P_a \times T_{STP}) / (P_{STP} \times T_a)$

Which gives,

(9.2.5) $(Rho)_a = [(Rho)_{STP}] \times [(Pa \times T_{STP})] / (P_{STP} * T_a)$

Where
$(Rho)_a$ = atmospheric density at P_a at T_a
$(Rho)_{STP}$ = atmospheric density at P_{STP} at T_{STP}
P_a = atmospheric pressure from assimilation model (mb)
T_a = atmospheric temperature from assimilation model (^oC)
$(Rho)_{STP}$ = atmospheric density at STP conditions = 1.225×10^3 Kg/m^3
T_{STP} = 273.15 ^oK
R = Universal gas constant

Which yields

(9.2.6) $(Rho)_a = \{ (1.225*10^3) *(P_a)*(273.15) \} / \{(1013.25)*(T_a)\}$

An empirical expression for saturated water vapor (Jupp, 2003) is given by.

(9.2.7) $(Rho)^*_w = A * E XP \{ (18.9766) - (14.9595)*(A) - (2.4388)*(A)^2 \}$

Where
$A = T_0 / (T_0 + T_a)$
T_o = ice point for pure water = 273.15 ^oK
T_a = air temperature in ^oC

Equations (9.2.3) , (9.2.6), and (9.2.7) are used to calculate RH for values of q >0.000001 and $q \leq 0.04$ and for $(Rho)^*_w > 0$, where q, T_a and P_a are taken from the assimilation model.

As an indication of the accuracy of the relative humidity, Table 9.2.1 Summarizes the comparison statistics for the relative humidity based upon GEOS-4 q, P, T values vs. ground observations reported in the 2007 NCEI GSOD files.

Table 9.2.1. Summary of statistics for a global comparison of the daily mean relative humidity based upon GEOS-4 q, P, T values to ground observations reported in the NCEI GSOD files during 2007.

Bias	RMSE	Slope	Intercept	R^2	Daily Values
-1.89	12.67	0.76	1.62	0.55	1,214,462

(Return to Content)

9.3. Dew/Frost Point Temperatures: The daily dew and frost point temperatures, DFpt, are calculated from the relative humidity, RH, and temperature, T_a. The following is a summary of the methodology used to calculate DFpt.

(9.3.1) $RH_1 = 1.0 - RH/100$

Where RH is calculated as described in Section 9.2, using the specific humidity, pressure, and temperature taken from the assimilation model.

The DFpt is calculated using the expression (Encyclopedia Edited by Dennis R. Heldman)

(9.3.2) $DFpt = T_a - (((14.55 + .114 \times T_a) \times RH_1 + ((2.5 + 0.007 \times T_a) \times (RH_1)^3 + ((15.9 + 117.0 \times T_a) \times (RH_1)^{14}$

Table 9.3.1 gives the statistics associated with comparing the dew/frost point temperatures based upon GEOS-4 RH (as described in Section 9.2) and T_a values to ground observations reported in the NCEI GSOD files for 2007.

Table 9.2.2. Summary of statistics for a global comparison of the GEOS-4 daily mean dew point to ground observations reported by 3410 station in the NCEI GSOD files during 2007.

Bias	RMSE	Slope	Intercept	R^2	Daily Values
-0.98	3.15	0.96	-0.74	0.92	1,214,462

(Return to Content)

9.4. Precipitation: The precipitation data in SSE Release 6.0 has been obtained from the Global Precipitation Climate Project (GPCP - http://precip.gsfc.nasa.gov). The GPCP precipitation data product, Version 2.1, is a global 2.5°x2.5° monthly accumulation based upon combination of observations from multiple platforms described at http://precip.gsfc.nasa.gov/gpcp_v2.1_comb_new.html . One degree SSE estimates of precipitation are based upon replicating GPCP values for SSE cells that overlap GPCP cells and averaging GPCP values when the SSE cell overlaps two or more GPCP cells. Validation and additional details relative to GPCP Version 2.1 precipitation values can be found in Adler, et. al. 2003.

(Return to Content)

9.5. Wind Speed The main focus of the wind parameters in SSE Release 6.0 continues to be applications related to power generation via wind. Accordingly, the primary emphasis was place on providing accurate winds at 50 m above the Earth's surface. Based upon analysis of the winds in GEOS-4 relative to winds provided in the previous release of SSE (i.e. Release 5.1), Release 6.0 winds continue to be based on the Version 1 GEOS (GEOS-1) reanalysis data set described in Takacs, Molod, and Wang (1994). In particular, the 50-meter velocities were derived from GEOS-1 surface values using equations provided by GEOS project personnel. Adjustments were made in a few regions based on surface type information from Dorman and Sellers (1989) and recent vegetation maps developed by the International Geosphere and Biosphere Project (IGBP) (Figure 9.5.1). GEOS-1 vegetation maps were compared with IGBP vegetation maps. Significant differences in the geographic distribution of crops, grasslands, and savannas were found in a few regions. In those regions, airport data were converted to new 50-m height velocities based on procedures in Gipe (1999). GEOS-1 50-m values were replaced with the Gipe-derived estimates in those regions.

Ten-year annual average maps of 50-m and 10-m "airport" wind speeds are shown in Figure 9.5.2. Velocity magnitude changes are now consistent with general vegetation heights that might be expected from the scene types in Figure 9.5.1. Note that SSE heights are above the soil, water, or ice surface and not above the "effective" surface in the upper portion of vegetation canopies.

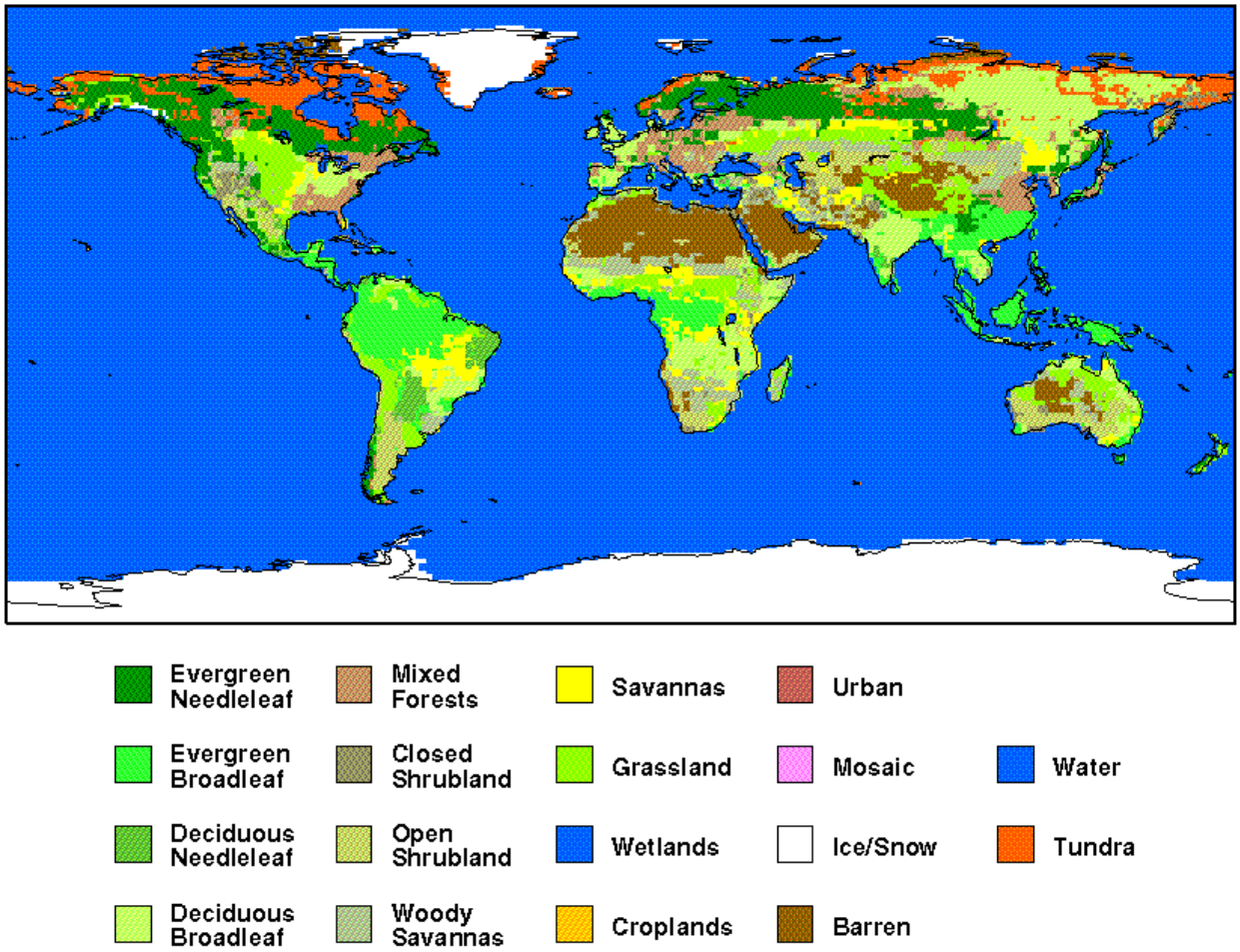

Figure 9.5.1. International Geosphere and Biosphere Project (IGBP) scene types.

Ten-year average SSE "airport" estimates were compared with 30-year average airport data sets over the globe furnished by the RETScreen project. In general, monthly bias values varied between ±0.2 m/s and RMS (including bias) values are approximately 1.3 m/s (Fig. IX-E.3). This represents a 20 to 25 percent level of uncertainty relative to mean monthly values and is about the same level of uncertainty quoted by Schwartz (1999). Gipe (1999) notes that operational wind measurements are sometimes inaccurate for a variety of reasons. Site-by-site comparisons at nearly 790 locations indicate SSE 10-m "airport" winds tend to be higher than airport measurements in remote desert regions in some foreign countries. SSE values are usually lower than measurements in mountain regions where localized accelerated flow may occur at passes, ridge lines or mountain peaks. One-degree resolution wind data is not an accurate predictor of local conditions in regions with significant topography variation or complex water/land boundaries.

Designers of "small-wind" power sites need to consider the effects of vegetation canopies affecting wind from either some or all directions. Trees and shrub-type vegetation with various heights and canopy-area ratios reduce near-surface velocities by different amounts. GEOS-1

calculates 10-m velocities for a number of different vegetation types. Values are calculated by parameterizations developed from a number of "within-vegetation" experiments in Canada, Scandinavia, Africa, and South America. The ratio of 10-m to 50-m velocities (V10/V50) for 17 vegetation types is provided in Table 9.5.1. All values were taken from GEOS-1 calculations except for the "airport" flat rough grass category that was taken from Gipe.

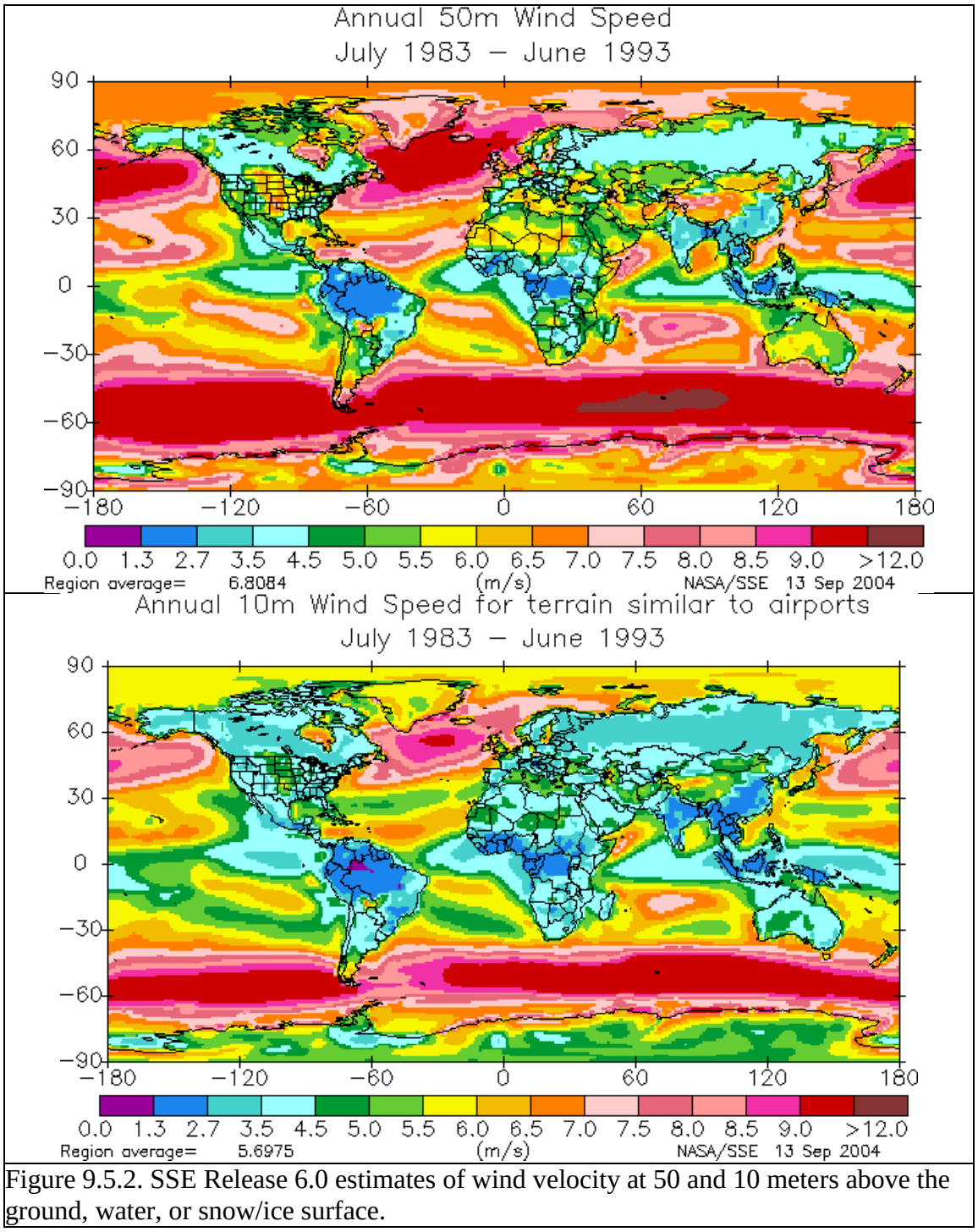

Figure 9.5.2. SSE Release 6.0 estimates of wind velocity at 50 and 10 meters above the ground, water, or snow/ice surface.

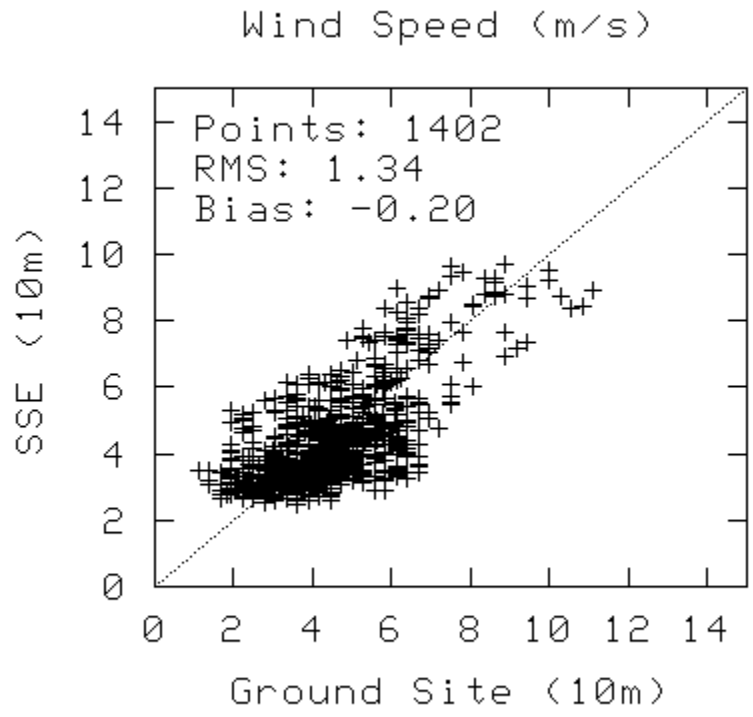

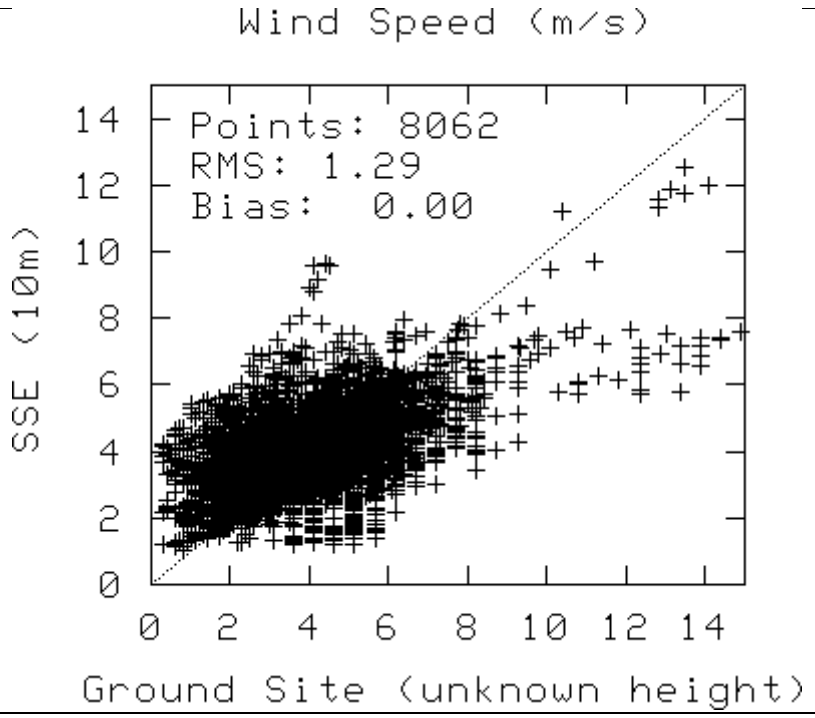

Figure 9.5.3. Comparison of monthly means based upon 10-year Release 6 SSE 10-m wind speed with monthly means based upon 30-year RETScreen site data.

Table 9.5.1. Wind Velocity V10/V50 Ratio for Various Vegetation Types.												
Northern hemisphere month	**1**	**2**	**3**	**4**	**5**	**6**	**7**	**8**	**9**	**10**	**11**	**12**
35-m broadleaf-evergreen trees (70%) small type	0.47	0.47	0.47	0.47	0.47	0.47	0.47	0.47	0.47	0.47	0.47	0.47
20-m broadleaf-deciduous trees (75%)	0.58	0.57	0.56	0.55	0.53	0.51	0.49	0.51	0.53	0.55	0.56	0.57
20-m broadleaf & needleleaf trees (75%)	0.44	0.47	0.50	0.52	0.53	0.54	0.54	0.52	0.50	0.48	0.46	0.45
17-m needleleaf-evergreen trees (75%)	0.50	0.53	0.56	0.58	0.57	0.56	0.55	0.55	0.55	0.54	0.53	0.52
14-m needleleaf-deciduous trees (50%)	0.52	0.53	0.55	0.57	0.57	0.58	0.58	0.54	0.51	0.49	0.49	0.50
18-m broadleaf trees (30%)/groundcover	0.52	0.52	0.52	0.52	0.52	0.52	0.52	0.52	0.52	0.52	0.52	0.52
0.6-m perennial groundcover (100%)	0.65	0.65	0.65	0.65	0.65	0.65	0.65	0.65	0.65	0.65	0.65	0.65
0.5-m broadleaf (variable %)/groundcover	0.65	0.65	0.65	0.65	0.65	0.65	0.65	0.65	0.65	0.65	0.65	0.65
0.5-m broadleaf shrubs (10%)/bare soil	0.65	0.65	0.65	0.65	0.65	0.65	0.65	0.65	0.65	0.65	0.65	0.65
0.6-m shrubs (variable %)/groundcover	0.65	0.65	0.65	0.65	0.65	0.65	0.65	0.65	0.65	0.65	0.65	0.65
Rough bare soil	0.70	0.70	0.70	0.70	0.70	0.70	0.70	0.70	0.70	0.70	0.70	0.70
Crop: 20-m broadleaf-deciduous trees (10%) & wheat	0.64	0.62	0.69	0.57	0.57	0.57	0.57	0.57	0.57	0.59	0.61	0.63
Rough glacial snow/ice	0.57	0.59	0.62	0.64	0.64	0.64	0.64	0.64	0.62	0.59	0.58	0.57
Smooth sea ice	0.75	0.78	0.83	0.86	0.86	0.86	0.86	0.82	0.78	0.74	0.74	0.74
Open water	0.85	0.85	0.85	0.85	0.85	0.85	0.85	0.85	0.85	0.85	0.85	0.85
"Airport": flat ice/snow	0.85	0.85	0.85	0.85	0.85	0.85	0.85	0.85	0.85	0.85	0.85	0.85
"Airport": flat rough grass	0.79	0.79	0.79	0.79	0.79	0.79	0.79	0.79	0.79	0.79	0.79	0.79
Note: 10-m and 50-m heights are above soil, water, or ice surfaces, not above the "effective" surface near the tops of vegetation.												

(Return to Content)

9.6. Heating/Cooling Degree Days: An important application of the historical temperature data is in the evaluation of heating degree days (HDD) and cooling degree days (CDD). The HDD and CDD are based upon the daily Tmin and Tmax with a base temperature, Tbase = 18^0C. The HDD and CDD were calculated using the following equations:

Heating Degree Days: For the days of a given time period (e.g. year, month, etc.) sum the quantity
[Tbase - (Tmin + Tmax) / 2] when (Tmin + Tmax) / 2 < Tbase

Cooling Degree Days: For the days of a given time period (e.g. year, month, etc.) sum the quantity
[((Tmin + Tmax) / 2) - Tbase] when (Tmin + Tmax) / 2 > Tbase.

The statistics associated with comparing the HDDs and CDDs based upon the GEOS-4 and observational temperatures are given in Table 9.6.1. The bottom row in Table 9.6.1 provides the mean estimates of the agreement between the HDDs and CDDs based assimilation and observational temperatures for the years 1983 – 2006. Values given in Table 9.6.1 used the uncorrected GEOS-4 temperatures. See Appendix D for a discussion of a methodology for

correcting/downscaling assimilation model temperatures and a comparison of the statistics associated with HDDs and CDDc based upon uncorrected vs corrected GEOS-4 temperatures. Application of the downscaling approach is only available for the SSE monthly mean temperatures over the time period July, 1983 – June, 2005,

Table 9.6.1

Comparison of yearly heating and cooling degree days: Uncorrected GEOS-4 vs ground site observations.															
Year	HDD using uncorrected GEOS-4 Temperatures vs ground site observations reported in NCDC GSOD files							CDD using uncorrected GEOS-4 Temperatures vs ground site observations reported in NCDC GSOD files							No. Stations
	Bias (HDD)	Bias (%)	RMSE (HDD)	RMSE (%)	Slope	Intercept (HDD)	Rsqd	Bias (CDD)	Bias (%)	RMSE (CDD)	RMSE (%)	Slope	Intercept (CDD)	Rsqd	
1983	16.30	6.44	68.59	27.11	1.03	9.85	0.95	-4.78	-8.93	28.53	53.34	0.86	2.68	0.92	1101
1984	16.37	6.34	64.45	24.97	1.03	8.46	0.95	-4.25	-8.35	27.01	53.07	0.86	2.86	0.92	1127
1985	16.13	6.01	64.31	23.97	1.03	9.19	0.96	-5.96	-11.21	27.82	52.33	0.85	1.80	0.92	1102
1986	14.07	5.55	85.41	33.72	0.98	18.25	0.91	-6.60	-12.50	27.73	52.56	0.84	1.91	0.93	1162
1987	14.92	5.91	69.30	27.42	1.02	10.71	0.94	-6.21	-12.01	27.17	52.52	0.85	1.76	0.93	1140
1988	15.20	6.20	65.39	26.68	1.03	6.79	0.95	-5.53	-10.10	27.39	50.05	0.86	2.22	0.93	1155
1989	14.71	5.85	66.75	26.54	1.03	7.55	0.95	-6.29	-11.91	29.02	54.96	0.84	2.35	0.91	1194
1990	16.84	7.09	66.45	27.97	1.04	7.67	0.95	-6.63	-11.92	28.70	51.60	0.83	2.66	0.93	1258
1991	14.69	6.03	78.74	32.33	1.01	11.89	0.92	-6.93	-11.60	30.28	50.71	0.84	2.59	0.92	1223
1992	12.94	5.19	79.58	31.91	1.00	12.11	0.92	-4.94	-10.62	25.52	54.79	0.86	1.80	0.92	1373
1993	17.79	6.94	71.34	27.83	1.03	10.14	0.94	-5.32	-9.97	26.29	49.30	0.88	1.10	0.93	1477
1994	22.88	9.24	72.22	29.17	1.05	11.59	0.95	-6.12	-10.75	27.96	49.09	0.87	1.36	0.93	1508
1995	17.54	7.10	70.60	28.60	1.03	9.83	0.95	-5.38	-9.13	28.04	47.55	0.87	2.28	0.93	1311
1996	10.15	4.64	99.68	45.60	0.93	25.32	0.84	-6.66	-10.70	30.31	48.68	0.86	2.09	0.92	1216
1997	19.61	8.56	62.21	27.16	1.05	7.08	0.95	-6.39	-11.33	28.24	50.06	0.85	2.02	0.92	1497
1998	24.65	11.56	68.35	32.06	1.09	5.74	0.94	-5.19	-8.91	27.48	47.17	0.87	2.30	0.93	1487
1999	18.58	8.53	61.38	28.18	1.06	6.22	0.95	-3.92	-6.53	28.87	48.11	0.88	3.01	0.92	1832
2000	17.61	7.32	66.54	27.67	1.05	6.15	0.95	-3.23	-6.06	27.74	52.00	0.88	3.06	0.92	2324
2001	24.33	9.94	64.77	26.46	1.06	8.60	0.96	-7.08	-12.74	30.00	53.97	0.84	1.75	0.92	1799
2002	16.62	6.92	67.75	28.22	1.03	9.73	0.94	-7.95	-13.80	29.96	52.00	0.83	1.58	0.92	2382
2003	14.75	6.24	66.15	27.96	1.04	6.33	0.94	-5.84	-9.97	30.91	52.77	0.85	3.23	0.91	2676
2004	16.52	6.87	90.29	37.56	1.00	17.33	0.90	-6.14	-11.66	27.97	53.10	0.84	2.19	0.92	2704
2005	20.40	8.32	66.41	27.07	1.05	7.56	0.95	-5.80	-9.96	29.13	49.99	0.86	2.39	0.93	3020
2006	16.56	6.76	126.66	51.69	0.91	39.49	0.81	-4.88	-8.89	29.25	53.28	0.87	2.44	0.92	3077
Mean of individual years	**17.09**	**7.07**	**73.47**	**30.33**	**1.02**	**11.40**	**0.93**	**-5.75**	**-10.40**	**28.39**	**51.37**	**0.86**	**2.23**	**0.92**	

(Return to Content)

9.7. Surface Pressure:

Recognizing that improvement in the GEOS-4 temperatures can be achieved through adjustments associated with differences in the average elevation of the GEOS-4 1-degree cell and that of the ground site of interest suggest that other altitude dependent parameters, such as pressure, might also benefit in similar altitude related adjustments. Figures 9.7.1(a-c) illustrate significant improvements in the GEOS-4 surface pressure values (p) by using the hypsometric equation (9.7.1), relating the thickness (h) between two isobaric surfaces to the mean temperature (T) of the layer.

$$(9.7.1) \quad h = z_1 - z_2 = (RT/g)\ln(p_1/p_2)$$

where:

z_1 and z_2 are the geometric heights at p_1 and p_2,

R = gas constant for dry air, and

g = gravitational constant.

Figure 9.7.1a shows the scatter plot of the GEOS-4 surface pressure versus the observations reported in the NCEI archive for 2004. Figure 9.7.1b shows the agreement with the application of equation 1, using the 2m daily mean temperature with no correction to the GEOS-4 temperatures (e.g. no lapse rate or offset correction). Figure 9.7.1c shows the scatter plot where the GEOS-4 surface pressure and temperature have been corrected for elevation differences. See Appendix D for a discussion of a methodology for correcting/downscaling assimilation model temperatures.

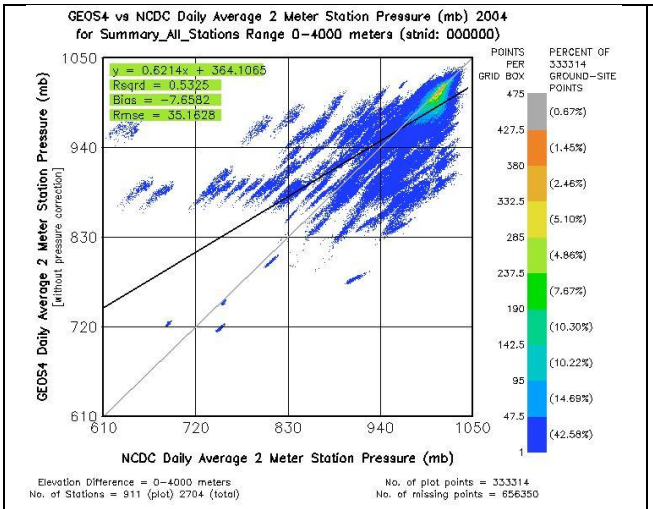

(a)

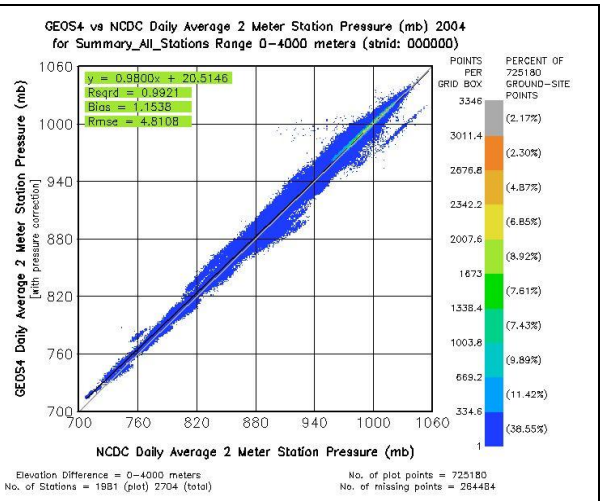

(b)

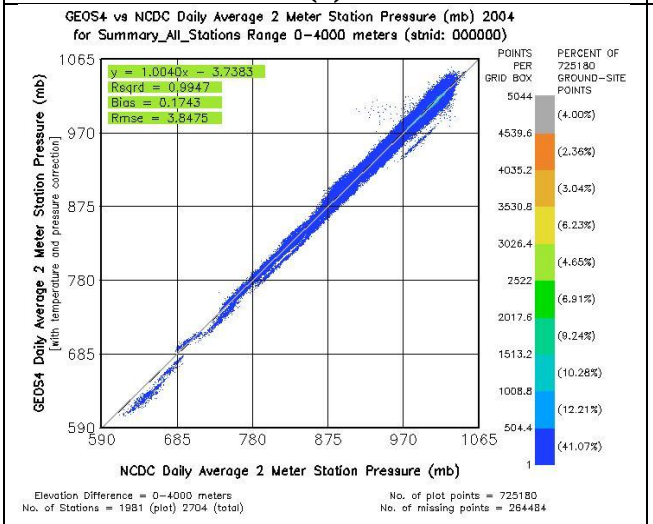

(c)

Figure 9.7.1. Panel (a) is a scatter plot of the uncorrected GEOS-4 pressures vs. ground observation in the NCEI GSOD files. Panel (b); Panel (b) is the scatter plot of the NCEI pressures vs the GEOS-4 pressure corrected according to Eq. 9.7.1 and the GEOS-4 2m temperature; Panel (c) is the scatter plot of the NCEI pressure and the GEOS-4 pressure according to Eq. 9.7.1 where now the GEOS-4 temperature is also corrected according to Eq. D.3.

(Return to Content)

10. Solar Geometry.

Multi-year monthly averaged solar geometry parameters are available for any user that provides the latitude/longitude via the SSE "Data Tables for a particular location" web application. Table 10.1 lists the SSE solar geometry parameters provided to assistance users in setting up solar panels. Appendix C provides the equations for calculating each of the parameters, while Appendix B describes the methodology for calculating the multi-year monthly averages. Note that each of the solar geometry parameters is calculated for the "monthly average day"; consequently each parameter is the monthly "averaged" value for the respective parameter for the given month. The monthly averaged day is described in section 7.1 with the monthly averaged day for each month listed in Table 7.1.1

Table 10.1. Multi-year monthly averaged solar geometry parameters for each User provided latitude/longitude that are calculated based upon the "monthly average day". These parameters provide guidance for solar panels.

Solar Geometry:

- Solar Noon
- Daylight Hours
- Daylight average of hourly cosine solar zenith angles
- Cosine solar zenith angle at mid-time between sunrise and solar noon (Eq)
- Declination
- Sunset Hour Angle
- Maximum solar angle relative to the horizon
- Hourly solar angles relative to the horizon
- Hourly solar azimuth angles

(Return to Content)

11. References

Adler, R.F., G.J. Huffman, A. Chang, R. Ferraro, P. Xie, J. Janowiak, B. Rudolf, U. Schneider, S. Curtis, D. Bolvin, A. Gruber, J. Susskind, P. Arkin, E. Nelkin 2003: The Version 2 Global Precipitation Climatology Project (GPCP) Monthly Precipitation Analysis (1979-Present). *J. Hydrometeor*., **4**, 1147-1167.

Barry, R. G. and R. J. Chorley, 1987: *Atmosphere, Weather, and Climate.* 5th ed. Methuen, 460 pp.

Blandford, Troy R., Karen S. Blandford, Bruan J. Harshburger, Brandon C. Moore, and Von P. Walden. Seasonal and Synoptic Variations in near-Surface Air Temperature Lapse Rates in a Mountainous Basin. J. Applied Meteorology and Climatology. 2008, Vol. 47, 249 – 261.

Bloom, S., A. da Silva, D. Dee, M. Bosilovich, J.-D. Chern, S. Pawson, S. Schubert, M. Sienkiewicz, I. Stajner, W.-W. Tan, M.-L. Wu, Documentation and Validation of the Goddard Earth Observing System (GEOS) Data Assimilation System - Version 4, Technical Report Series on Global Modeling and Data Assimilation, NASA/TM—2005–104606, Vol. 26, 2005

Braun, J. E. and J. C. Mitchell, 1983: Solar Geometry for Fixed and Tracking Surfaces. Solar Energy, Vol. 31, No. 5, pp. 439-444.

Briggs, Robert S., R. G. Lucas, Z. T. Taylor, 2003: Climate Classification for Building Energy Codes and Standards. Technical Paper, Pacific NW National Laboratory, March 26, 2002. Continue to use original climate zone definitions.

Collares-Pereira, M. and A. Rabl, 1979: The Average Distribution of Solar Radiation-Correlations Between Diffuse and Hemispherical and Between Daily and Hourly irradiance Values. Solar Energy, Vol. 22, No. 1, pp. 155-164.

Dorman, J. L. and P. J. Sellers, 1989: A Global Climatology of Albedo, Roughness Length and Stomatal Resistance for Atmospheric General Circulation Models as Represented by the Simple Biosphere Model (SiB). Journal of Atmospheric Science, Vol. 28, pp. 833-855.

Erbs, D. G., S. A. Klein, and J. A. Duffie, 1982: Estimation of the Diffuse Radiation Fraction for Hourly, Daily and Monthly average Global Radiation. Solar Energy, Vol. 28, No. 4, pp. 293-302.

Gipe, Paul, 1999: Wind Energy Basics, Chelsea Green Publishing, 122 pp.

Gupta, S. K., D. P. Kratz, P. W. Stackhouse, Jr., and A. C. Wilber, 2001: The Langley Parameterized Shortwave Algorithm (LPSA) for Surface Radiation Budget Studies. NASA/TP-2001-211272, 31 pp.

Harlow, R. C., E. J. Burke, R. L. Scott, W. J. Shuttleworth, C. M. Brown, and J. R. Petti. Derivation of temperature lapse rates in semi-arid southeastern Arizona, (2004) Hydrol. and Earth Systems Sci, 8(6) 1179-1185.

Klein, S.A., 1977: Calculation of monthly average irradiance on tilted surfaces. Solar Energy, Vol. 19, pp. 325-329.

Kinne, S., O'Donnel, D., Stier, P., Kloster, S., Zhang, K., Schmidt, H., Rast, S., Giorgetta, M., Eck, T.F., and Stevens, B., 2013. MAC-v1: A new global aerosol climatology for climate studies. *J Adv Model Earth Syst,* 5: 704-740, doi: 10.1002/jame.20035

Liu, B. Y. H. and R. C. Jordan, 1960: The Interrelationship and Characteristic Distribution of Direct, Diffuse, and Total Solar Radiation. Solar Energy, Vol. 4, No. 3, pp. 1-19.

Lookingbill, Todd R. and Dean L. Urban, Spatial estimation of air temperature differences for landscape-scale studies in mountain environments, (2003) Agri. and Forst. Meteor, 114(3-4) 141-151.

Ohmura, Atsumu, Ellsworth G. Dutton, Bruce Forgan Claus Fröhlich Hans Gilgen, Herman Hegner, Alain Heimo, Gert König-Langlo, Bruce McArthur, Guido Mueller, Rolf Philipona, Rachel Pinker, Charlie H. Whitlock, Klaus Dehne, and Martin Wild, 1998: Baseline Surface Radiation Network (BSRN/WCRP): New Precision Radiometry for Climate Research, Bull. Of American Meteor. Soc., **79**, 10, p 2115-2136.

RETScreen: Clean Energy Project Analysis: RETScreen® Engineering & Cases Textbook, Third Edition, Minister of Natural Resources Canada, September 2005. (http://www.retscreen.net/ang/12.php, Engineering e-Textbook, Version 4, RETScreen Photovoltaic Project Analysis Chapter, pp. PV.15-PV.21, ISBN: 0-662-35672-1, Catalogue no.: M39-99/2003E-PDF).

Pinker, R., and I. Laszlo, 1992: Modeling Surface Solar Irradiance for Satellite Applications on a Global Scale. *J. Appl. Meteor.*, 31, 194–211.

Rienecker, M.M., Suarez, M.J., Gelaro, R., Todling, R., Bacmeister, J., Liu, E., Bosilovich, M.G., Schubert, S.D., Takacs, L., Kim, G.-K., Bloom, S., Chen, J., Collins, D., Conaty, A., da Silva, et al., 2011. MERRA: NASA's Modern-**Era Retrospective Analysis for Research and Applications.** *J Climate*, **24**, 3624-3648, doi:10.1175/JCLI-D-11-00015.1

Schwartz, Marc, 1999: Wind Energy Resource Estimation and Mapping at the National Renewable Energy Laboratory. NREL Conf. Pub. NREL/CP-500-26245.

Smith, G.L., R. N. Green, E. Raschke, L. M. Avis, J. T. Suttles, B. A. Wielicki, and R. Davies, 1986: Inversion methods for satellite studies of the Earth's radiation budget: Development of algorithms for the ERBE mission. Rev. Geophys., 24, 407-421.

Surface Weather Observations and Reports, Federal Meteorological Handbook No. 1, FCM-H1-2005, Washington, D.C., 2005

Rasch, P. J., N. M. Mahowald, and B. E. Eaton (1997), Representations of transport, convection, and the hydrologic cycle in chemical transport models: Implications for the modeling of short-lived and soluble species, J. Geophys. Res., 102(D23), 28, 127-128, 138.

Takacs, L. L., A. Molod, and T. Wang, 1994: Volume 1: Documentation of the Goddard Earth Observing System (GEOS) general circulation model - version 1, NASA Technical Memorandum 104606, Vol. 1, 100 pp.

White, J.W. et al., Evaluation of NASA satellite- and assimilation model-derived long-term daily temperature data over the continental US, Agric. Forest Meteorol. (2008), doi:10.1016/j.agrformet.2008.05.017

Whitlock, Charles H., W.S. Chandler, J.M. Hoell, T. Zhang, P.W. Stackhouse, Jr., 2005: **Parameters for Designing Back-Up Equipment for Solar Energy Systems**. Proceedings of the International Solar Energy Society 2005 Solar World Congress, Orlando, Florida

Zhang, T., Stackhouse, Jr., P.W., Gupta, S.K, Cox, S.J., Mokovitz, J.C., and Hinkelman, L.M., 2013. The validation of the GEWEX SRB surface shortwave flux data products using BSRN measurements: A systematic quality control, production and application approach. *J Quant Spectrosc Radiat Transf*, 122: 127-140, doi: http://dx.doi.org/10.1016/j.jqsrt.2012.10.004

Zhang, T., Stackhouse, Jr., P.W., Chandler, W.S., and Westberg, D.J., 2014. Application of a global-to-beam irradiance model to the NASA GEWEX SRB dataset: An extension of the NASA Surface meteorology and Solar Energy datasets. *Sol Energy*, 110: 117-131, doi: http://dx.doi.org/10.1016/j.solener.2014.09.006

(Return to Content)

Appendix A
Validation Methodology

The validation of the SSE parameters available is based upon comparisons of the SSE primary parameters parameter to surface observations of the corresponding parameters and where possible comparisons of the SSE parameters calculated using the primary data to the corresponding parameters calculated using surface observations of the corresponding primary parameters. Examples of primary parameters comparisons include the SSE solar and temperature values compared to surface observations; while comparisons of relative humidity and heating-degree- days typify comparisons of calculated parameters using the SSE primary data and the corresponding ground based observational data.

Statistics associated with the SSE vs. surface based values are reported to provide users with information necessary to assess the applicability of the SSE data to their particular project. Scatter plots of the SSE parameter vs. surface based values along with the correlation and accuracy parameters for each scatter plots are typically provided. The statistical parameters associated with a linear least squares fit to the respective scatter plots that are reported include: Pearson's correlation coefficient; the Bias between the mean of the respective SSE parameter and the surface observations; the root mean square error (RMSE) calculated as the root mean square difference between the respective SSE and observational values. Additional parameters typically provided are the variance in the SSE and observational data and the number of SSE:observational data pairs.

The following are the expressions used to calculate the statistical parameters:

The Pearson's correlation coefficient is calculated using expressions taken from (REF)

$$r = r_{xy} = \frac{\sum x_i y_i - n\bar{x}\bar{y}}{(n-1)s_x s_y} \quad (1)$$

where:

n = number of data samples

x_i and y_i represent the surface and SSE data respectively

$$\bar{x} = \frac{1}{n}\sum_{i=1}^{n} x_i$$

is the sample mean and analogously for $\bar{y}$

$$s_x = \sqrt{\frac{1}{n-1}\sum_{i=1}^{n}(x_i - \bar{x})^2}$$

is the standard deviation of sample x_i and similarly for y_i

The expression for the mean Bias between SSE *Parm* values and observations of *Parm* at a single surface site, j, is given as:

(1) $(\text{Bias})^j = \{\sum_i\{[(Parm_i^j)_{SSE} - (Parm_i^j)_{Sur}]\}\}/n$

Where
i = day within given time period
j = site number
n = number of data pairs within given time period
$\sum_i$ = sum over all data pairs at site j

The expression for the mean Bias for multiple surface sites is given as:

(2) $\text{Bias} = \{\sum_i(\text{Bias})^j\}/N$

Where the sum $\sum_i$ is over all sites
N = total number of sites

The expression for the RMSE between for SSE parameter, *Parm*, and surface observation of *Parm* at a single site j is given as

(1) $(\text{RMSE})^j = \{\{\sum_i[(Parm_i^j)_{SSE} - (Parm_i^j)\text{Sur }]^2\}/n\}\}^{1/2}$,

And the RMSE for multiple sites'

(3) $\text{RMSE} = \{\sum_i(\text{RMSE})^j\}/N$

Standard Deviation:

$$\sigma = \sqrt{\frac{1}{N}\sum_{i=1}^{N}(x_i - \mu)^2}$$

Where
u = mean of sample
x_i = individual values of SSE or observational values

(Return to Content)

Appendix B
Averaging Methodology

Methodology for calculating monthly, annual & climatologically averaged parameters: In general, daily averages were calculated for local solar time and stored using 3-hourly data from the Global Modeling and Assimilation Office (*GMAO*) data archive for the meteorological parameters and from the NASA/GEWEX Surface Radiation Budget Release-3.0 data sets for the solar parameters. Monthly averages by year were calculated from the dailies; annual averages, by year, were calculated from the monthly averages for the given year (i.e. the sum of the monthly averages divided by the number of months in the year, typically 12); climatologically (22-year) averages for a given month (e.g. multi-year monthly averages) were calculated as a sum of the monthly averages divided by the number of months (i.e. typically 22); climatologically annual averages were calculated as a sum of the climatologically averaged monthly averages divided by the number of months (typically 12).

The **daily average** of parameter *Parm* for day i, in month j, and year k is given by:

$$< Parm >_{ijk} = \left(\sum_{h=1}^{N} < Parm >_{h} \right) \Big/ N$$

Where

$$< Parm >_{h}$$

Is the average values of *Parm* over the 3-hour period h and N =number of 3-hourly values for the given day.

The **monthly average by year** of parameter *Parm* for month j in year k is given by:

$$< Parm >_{jk} = \left(\sum_{i=1}^{d} < Parm >_{ijk} \right) \Big/ d$$

Where

$$< Parm >_{ijk}$$

Is the daily average of parameter *Parm* for day i, in month j and year k and d = number of days in month j.

The **annual average** of Parameter *Parm* for year k is given by

$$< Parm >_{k} = \left(\sum_{j=1}^{m} < Parm >_{jk} \right) \Big/ m$$

Where

$$< Parm >_{jk}$$

Is the monthly average of parameter *Parm*, for month j and in year k and m = number monthly averages in year k.

The **climatologically monthly average** (i.e. multi-year monthly average) of parameter *Parm* for month j over n years is given by:

$$< Parm >_j = \left(\sum_{k=1}^{n} < Parm >_{jk} \right) / n$$

Where

$$< Parm >_{jk}$$

Is the monthly average of parameter *Parm* for month j, in year k and n = number of years in climate time period.

(Return to Content)

APPENDIX C: Solar Geometry

The solar geometry parameters useful for designing and application of solar panels are available for each User defined Latitude/Longitude. These parameters and equations used to calculate each parameter are given below.

C-1. Monthly Averaged Solar Noon (GMT time)

SN = 60 * hr + mn + 4 * (lon – merid) + 60*lon/15.0
SN= Solar Noon
lon = local longitude (user input); positive = East; negative West
merid = meridian through local time zone; positive = East; negative West
hr = hour
mn = minute

Return to **Solar Geometry** Section

C-2. Monthly Averaged Daylight Hours (hours)

From John A. Duffie and William A. Beckman, Solar Engineering of Thermal Process 2nd edition Wiley-Interscienc3 Publication

daylight[mo] = (sMAM - rMAM) / 60.0

Where:

daylight[mo] – daylight hours for given month

sMAM = int(12.0 * 60.0 + RS -(4.0 * (lon - merid)) - eotA);

rMAM = int(12.0 * 60.0 - RS - (4.0 * (lon - merid)) - eotA);

eotA = (L - C - alpha) / 15.0 * 60.0

alpha = L - 2.466*sin(2.0*L) + 0.053*sin(4.0*L)

L = (280.460 + (36000.770 * t) + C)
– int((280.460 + (36000.770 * t) + C) / 360.0) * 360.0

C = (1.915 * sin(G))+(0.020 * sin(2.0*G))

G = (357.528 + 35999.05 * t)
- int((357.528 + 35999.05 * t) / 360.0) * 360.0

t = ((MAM / 60.0 / 24.0) + dy + int(30.6 * cM + 0.5)
+ int(365.25 * (cY - 1976.0)) - 8707.5) / 36525.0

$RS = -1*(\sin(\Phi)*\sin(\xi) - \sin((-0.8333-0.0347*(El)^{1/2}))/\cos(\Phi)/\cos(\xi)$

Where:

RS = Sunrise-to-Sunset Local Solar time (Minutes)

If $|RS| \leq 1.0$ RS = acos(RS)*4
If $|RS| > 1.0$ RS = 0.0

Where
. δ = Declination angle for the monthly averaged day
. Φ = Latitude
. El = Elevation
. dy = monthly average day
. cy = calendar year
. merid = solar time based upon 15^0 of longitude per hour

Return to **Solar Geometry** Section

C-3. Monthly Averaged Of Hourly Cosine Solar Zenith Angles (dimensionless)

Average $\cos(\Theta_Z) = \{f \cos^{-1}(-f/g) + g[1 - (f/g)^2]^{½}\} / \cos^{-1}(-f/g)$
where:
Θ_Z = angle between the sun and directly overhead during daylight hours
f = sin(latitude) * sin(solar declination)
g = cos(latitude) * cos(solar declination)

Solar declination for each month is based upon the monthly average day (see **Table 7.1.1.)**

Gupta et al., 2001, *The Langley Parameterized Shortwave Algorithm (LPSA) for Surface Radiation Budget Studies*

Return to **Solar Geometry** Section

C-4. Monthly Averaged Cosine Solar Zenith Angle At Mid-Time Between Sunrise And Solar Noon (dimensionless)

$\cos(\Theta_{ZMT}) = f + g[(g - f) / 2g]^{½}$
where:
Θ_{ZMT} = Zenith angle at mid-time between sunrise and solar noon
f = sin(latitude) * sin(solar declination)

g = cos(latitude) * cos(solar declination)

Solar declination for each month is based upon the monthly average day (see Table 7.1.1**.)**

Gupta et al., 2001, *The Langley Parameterized Shortwave Algorithm (LPSA) for Surface Radiation Budget Studies*

Return to **Solar Geometry** Section

C-5. Monthly Averaged Declination (degrees)

$\delta = 23.45*\sin\{(360/365)*(284+JD + Hr/24)\}$

Where
δ = Declination angle
JD = Julian day
Hr = hour

Reference: P. I. Cooper, The Absorprion of solar radiation in solar stills. Solar Energy 12, 3 (1969)

Return to **Solar Geometry** Section

C-6. Monthly Averaged Sunset Hour Angle (degrees)

$\text{Cos}(\omega_s) = -\tan(\Phi)\tan(\xi)$

Where all angles for each month are based upon the monthly average day (see Table 7.1.1**.)**
ω_s = Sunset Hour angle
δ = Declination angle
Φ = Latitude

If $\text{Cos}(\omega_s) < -1.0$ set $\text{Cos}(\omega_s) = -1$
If $\text{Cos}(\omega_s) > +1.0$ set $\text{Cos}(\omega_s) = +1$
$\omega_s = \text{acos}\{\tan(\Phi)\tan(\xi)\}$

From John A. Duffie and William A. Beckman, Solar Engineering of Thermal Process 2nd edition Wiley-Interscienc3 Publication

Return to **Solar Geometry** Section

C-7. Monthly Averaged Maximum Solar Angle Relative To The Horizon (degrees)

$\Theta_z = \text{acos}\{\sin(\xi)*\sin(\Phi)+\cos(\xi)*\cos(\Phi)*\cos(\omega)\}$

Where all angles for each month are based upon the monthly average day (see Table 7.1.1**.)**
Θ_z = Zenith angle
δ = Declination angle
Φ = Latitude
ω = Hour angle = acos(cot(Φ)tan(ξ)

Max(Θ_z) = 90.0 – Θ_z

J. E. Braun & J. C. Mitchell Solar Geometry for Fixed and Tracking Surfaces, Solar Energy 31, no. 5, pp 339-444 (1983)
Return to **Solar Geometry** Section

C-8. Monthly Averaged Hourly Solar Angles Relative To The Horizon (degrees)

ha = ((MAM - 12.0 * 60.0) / 4.0)

Where all angles for each month are based upon the monthly average day (see Table 7.1.1**.)**

ha = Hour Angle

MAM = Solar Minutes After Midnight

MAM = (iMAM + (4.0 * (lon - meridian) + eotA)) + 24.0 * 60.0

iMAM = 60 * hr + mn;

eotA = (L - C - alpha) / 15.0 * 60.0

alpha = L - 2.466*sin(2.0*L) + 0.053*sin(4.0*L)

L = (280.460 + (36000.770 * t) + C)
– int((280.460 + (36000.770 * t) + C) / 360.0) * 360.0

G = (357.528 + 35999.05 * t)
- int((357.528 + 35999.05 * t) / 360.0) * 360.0

C = (1.915 * sin(G))+(0.020 * sin(2.0*G))

t = ((MAM / 60.0 / 24.0) + dy + int(30.6 * cM + 0.5)
+ int(365.25 * (cY - 1976.0)) - 8707.5) / 36525.0

Return to **Solar Geometry** Section

C-9. Monthly Averaged Hourly Solar Azimuth Angles (degrees)

#azimuthAngle = aziA in Degrees

aziA= RadToDeg * acos(((sin(altA * DegToRad) *
sin(lat * DegToRad)) - sin(decl * DegToRad)) /
(cos(altA * DegToRad) * cos(lat * DegToRad)))

Where all angles for each month are based upon the monthly average day (see Table 7.1.1**.)**
Φ = Latitude in radians
δ = Declination angle in radians
ha = hour angle in radians
altA = altitude angle in

altA = (PI/2.0 - acos((cos(Φ) * cos(ξ) * cos(hA * DegToRad))
+ (sin(Φ) * sin(ξ))))
Return to **Solar Geometry** Section

(Return to Content)

Appendix D: Downscaling Assimilation Modeled Temperatures

Introduction: In section VII temperature estimates from the GEOS-4 assimilation model were found to exhibit a globally and yearly (1983 – 2006) averaged bias for Tmax of -1.82° C , for Tmin about +0.27°, for Tave about - 0.55° C relative to ground site observations. In this Appendix factors contributions to these biases are noted with the main focus being the description of a methodology that can reduce the biases for local ground site.

The spatial resolution of the GEOS-4 assimilation model's output is initially on a global 1^o by 1.25^o grid and then re-gridded to a spatial 1^o by 1^o grid to be spatially compatible with the solar Irradiance values available through the POWER archive. The elevation of original and re-gridded cell represents the average elevation of the earth's surface enclosed by the dimensions of the grid cell. Figure A.1 illustrates the spatial features associated with a reanalysis cell and a local ground site. In mountainous regions, in particular, the elevation of the grid cell can be substantially different from that of the underlying ground site.

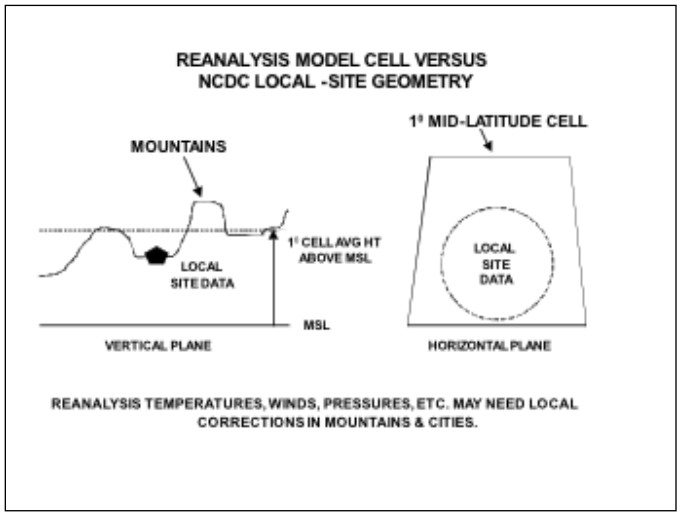

Figure A.1***:*** *Relative height and horizontal features associated with a nominal 1-degree cell and a local ground site in the mountains.*

The inverses dependence of the air temperature on elevation is well known and suggests that the elevation differences between the re-analysis grid cell and the actual ground site may be a factor contribution to the biases between the modeled and observed temperatures. In figure A-2, the yearly averaged differences between ground site measurements and reanalysis modeled values (i.e. bias) are plotted against the difference in the elevation of the ground site and the reanalysis grid for the ensemble of years 1983 – 2006. The stations have been grouped into 50m elevation difference bins (e.g. 0 to 50m; >50m to 100m; >100m to 150m; etc.) and plotted against the mean yearly bias for the respective elevation bin.

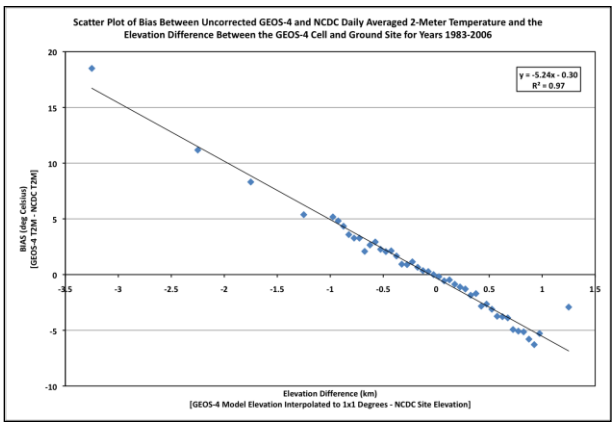

(a)

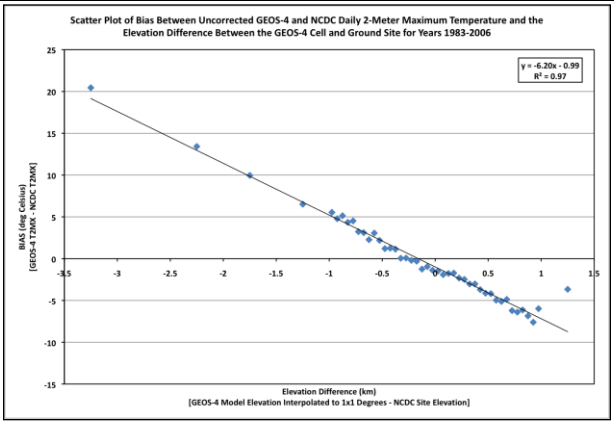

(b)

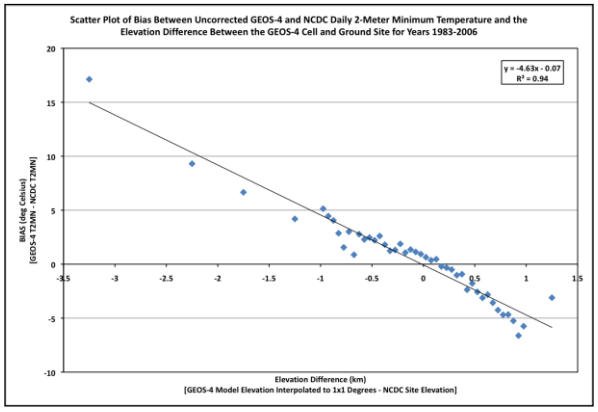

(c)

Figure A-2. Scatter plots showing the dependence of the bias between the GEOS-4 Tave (a), Tmin (b), and Tmax (c) temperatures and values from the NCEI archive on the elevation difference between the GEOS-4 cell and the ground station elevation for the years 1983 -2006. The elevation difference between stations are grouped into elevation difference bins (e.g. 0 to 50m; >50m to 100m; >100m to 150m; etc.) and plotted against the mean bias for the respective elevation bin.

The solid line is the linear least squares fit to the scatter plot and the parameters for the fit are given in the upper right hand portion of each plot. Table A-1 gives the parameters associated with linear regression fits to similar scatter plots for individual years and is included here to illustrate the year-to-year consistency in these parameters. The linear dependence of the bias between the GEOS-4 and NCEI temperature values on the elevation difference between the GEOS-4 cell and ground elevation is clearly evident in Figure A-2 and Table A-1. The mean of the slope, intercept, and R^2 for the individual years is given in the row labeled "Average". The bottom row of Table A-1 lists the fit parameters of Figure A-2.

Table A.1. Linear regression parameters associated with scatter plots of GEOS-4 yearly mean bias relative to ground site observatioions for individual years from 1983 - 2006. The bottom row gives the parametes for the scatter plots of Figure A.2.

Year	Tmax			Tmin			Tave		
	Slope (C/km)	Intercept (C)	R^2	Slope (C/km)	Intercept (C)	R^2	Slope (C/km)	Intercept (C)	R^2
1983	-6.2	-0.5	0.74	-4.4	0.4	0.87	-5.2	0.1	0.83
1984	-6.2	-0.6	0.72	-4.3	0.3	0.75	-5.2	0.0	0.79
1985	-6.8	-0.9	0.94	-4.7	0.1	0.77	-5.9	-0.1	0.95
1986	-6.6	-0.7	0.88	-4.3	0.3	0.82	-5.5	0.1	0.91
1987	-6.3	-1.0	0.92	-4.9	0.4	0.83	-5.5	0.0	0.95
1988	-6.2	-0.7	0.76	-4.0	0.5	0.68	-5.0	0.2	0.75
1989	-6.0	-1.0	0.77	-3.4	0.1	0.55	-4.5	-0.2	0.72
1990	-6.6	-0.8	0.9	-4.4	0.2	0.83	-5.4	0.1	0.88
1991	-6.1	-0.8	0.9	-4.4	0.3	0.88	-5.2	0.1	0.9
1992	-6.2	-0.8	0.93	-4.6	0.4	0.88	-5.2	0.0	0.93
1993	-6.1	-0.9	0.92	-5.0	0.2	0.93	-5.4	0.0	0.95
1994	-6.2	-1.0	0.92	-5.4	-0.1	0.92	-5.6	-0.2	0.95
1995	-5.9	-1.3	0.91	-5.4	0.6	0.94	-5.5	-0.1	0.95
1996	-5.3	-0.6	0.79	-4.8	0.7	0.89	-4.9	0.3	0.86
1997	-6.2	-0.8	0.94	-5.2	0.2	0.95	-5.5	-0.1	0.96
1998	-6.0	-0.9	0.9	-4.9	0.3	0.93	-5.2	-0.1	0.94
1999	-6.2	-0.9	0.94	-4.9	0.5	0.95	-5.3	0.0	0.96
2000	-6.2	-1.1	0.97	-5.0	-0.1	0.93	-5.4	-0.4	0.97
2001	-5.7	-1.4	0.9	-5.0	0.0	0.85	-5.3	-0.5	0.93
2002	-6.2	-1.1	0.97	-4.6	-0.1	0.92	-5.2	-0.4	0.97
2003	-6.1	-1.0	0.97	-4.4	-0.2	0.91	-5.1	-0.4	0.97
2004	-6.3	-0.9	0.98	-4.6	-0.2	0.94	-5.3	-0.4	0.98
2005	-6.1	-1.3	0.97	-4.6	-0.1	0.93	-5.2	-0.5	0.97
2006	-5.7	-1.3	0.95	-4.6	-0.4	0.92	-5.0	-0.6	0.96
Average	-6.1	-0.9	0.90	-4.6	0.2	0.87	-5.3	-0.1	0.91
STDEV	0.3	0.2	0.08	0.4	0.3	0.10	0.3	0.2	0.07
All Years Regression Analysis	-6.2	-1.0	0.97	-4.6	-0.1	0.94	-5.2	-0.3	0.97

As already noted, the inverses dependence of the air temperature on elevation is well known with -6.5^{o}C/km typically accepted as a nominal global environmentally averaged lapse rate value (Barry and Chorely 1987). Moreover, numerous studies have been published (Blandford et al., 2008; Lookingbill et al., 2003; Harlow et al., 2004) that highlight the need to use seasonal and regionally dependent lapse rates for the daily Tmin and Tmax values to adjustment ground site observations to un-sampled sites at different elevations. In the remaining sections an approach to statistically calibrate the assimilation model and downscale the reanalysis temperatures to a specific site within the reanalysis grid box is described.

(Return to Content)

A-1. Downscaling Methodology : Figure A-2 illustrates the linear dependence of the bias between the GEOS-4 temperatures and elevation differences between reanalysis grid cell and the ground site elevation. In this section a mathematical procedure is developed for statistically calibrating the GEOS-4 model relative to ground site observations resulting parameters that allow downscaled estimates of the reanalysis temperatures at localized ground sites site values. In subsequent sections the validity of the downscaling approach will demonstrated.
The downscaling discussed in this and subsequent sections is only available through the POWER/SSE archive with application to the monthly mean temperatures over the time period July 1983 – June 2005.

If we assume that the reanalysis modeled temperatures estimates can in fact be downscaled based upon a lapse rate correction, then we can express the downscaled temperatures at a local ground site as

Eq. A-1. $$(T^{grd})_{RA} = (T^{nat})_{RA} + \lambda*(H_{grd} - H_{RA}) + \beta$$

Where $(T^{grd})_{RA}$ is the downscaled reanalysis temperature, $(T^{nat})_{RA}$ is the native reanalysis value averaged over the reanalysis grid cell, λ is the seasonal/regional lapse rate (C/km) appropriate for the given ground site, H_{grd} and H_{RA} are the elevation for ground site and reanalysis grid cell respectively, and β is included to account for possible biases between the reanalysis model estimates and ground observations. Assuming that Eq. A-1 provides an accurate estimate of the air temperature we have

Eq. A-2. $$(T^{grd}) = (T^{grd})_{RA},$$

where (T^{grd}) is the air temperature at the desired ground site.

Equation Eq. A-1 and Eq. A-2 can be combined to yield

Eq. A-3. $$(T^{grd}) = (T^{nat})_{RA} + \lambda*(H_{grd} - H_{RA}) + \beta$$

or

Eq. A-4. $$\Delta T = \lambda*\Delta H + \beta$$

where ΔT is the differences between the air temperature at desired ground site and reanalysis cell temperature or Bias, and ΔH is the difference between the elevation of the ground site and the model cell. Equation Eq. A-4 gives a linear relation between ΔT and ΔH with the slope given by λ, the lapse rate, and an intercept value given by β. A linear least squares fit to a scatter plot of ΔT vs ΔH (i.e. Figure A-2) yields λ, the lapse rate, and β, the model bias. These parameters can then be used to downscale the reanalysis temperature values to any ground site within a region that the λ and β values are valid. Note that this methodology lends itself to generating λ and β

values averaged over any arbitrary time period and/or investigating other environmental factors such as the influence of the vegetation type on the downscaling methodology.

The scatter plots shown in Figure A-2 are constructed using the yearly mean bias between GEOS-4 and NCEI temperatures (i.e. ΔT) vs the difference in the elevation between the GEOS-4 grid cell and the ground site (i.e. ΔH). Consequently, from Eq. A-4 the slope and intercept associated with the linear fit to the scatter plot give a set of globally averaged λ and β parameters for downscaling the reanalysis temperatures Tave, Tmin, and Tmax to any geographical site. Table A-2 summarizes the values for λ (e.g. lapse rate) and β (e.g. offset) based upon the use of the NCEI GSOD meteorological data as the "calibration" source. The values given in Table A.2 are based upon the globally distributed ground sites in the NCEI GSOD data base, and are based upon yearly mean ground and GEOS-4 data.

Table A-2. Globally and yearly and averaged lapse rate and offset values for adjusting GEOS-4 temperatures to local ground site values (based upon 1983 – 2006 NCEI and GEOS-4 global data).

	Lapse Rate (^{o}C/km)	Off Set (^{o}C)
Tmax	-6.20	-0.99
Tmin	-4.63	-0.07
Tave	-5.24	-0.30

Figure A-3 illustrates that bias between the ground observations and the GEOS-4 values after applying the lapse rate correction and offset values given in Table A-2 is independent of the elevation difference between the ground site and the GEOS-4 1-degree cell and that the average bias is also near zero.

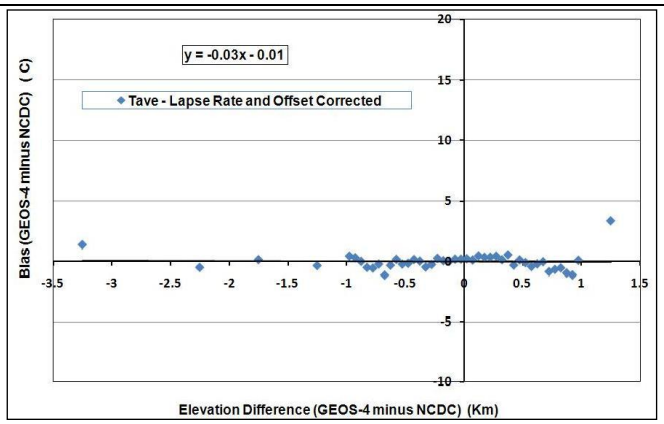

(a)

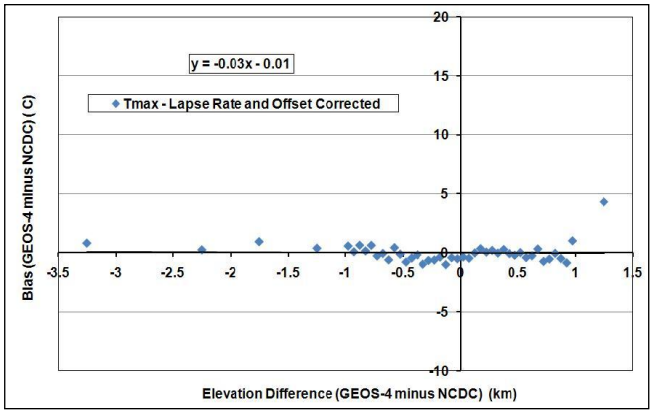

(b)

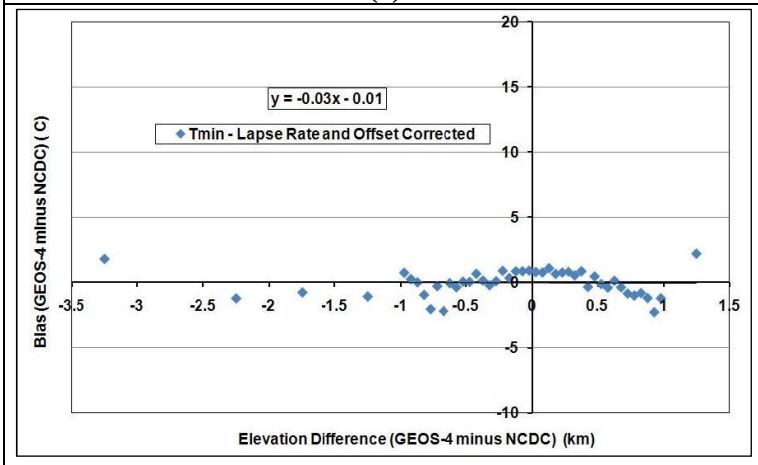

(c)

Figure A-3. Scatter plots showing the dependence of the bias between the GEOS-4 Tave (a), Tmin (b), and Tmax (c) temperatures and values from the NCEI archive on the elevation difference between the GEOS-4 cell and the ground station elevation for the years 1983 -2006 after adjusting the GEOS-4 values using Eq. VII – 3. The elevation difference between stations are grouped into elevation difference bins (e.g. 0 to 50m; >50m to 100m; >100m to 150m; etc.) and plotted against the mean bias for the respective elevation bin.

(Return to Content)

Global Downscaling: Table A-3 gives the yearly mean global MBE and RMSE of the native (i.e. un-corrected) and downscaled GEOS-4 temperature values relative to NCEI values for the year 2007. The 2007 GEOS-4 values were downscaled via Eq. A-3 using the lapse rate and offset parameters given in Table A-2. Since the λ and β parameters for downscaling were developed

Table A-3. Globally and yearly averaged Mean Bias Error (MBE) and Root Mean Square Error (RMSE) for 2007 un-corrected and downscaled GEOS-4 temperatures relative to NCEI temperatures. The downscaled GEOS-4 values are based upon the downscaling parameters given in Table A-2 .

		Un-corrected GEOS-4	Downscaled GEOS-4
Tmax	**MBE**	-1.58	-0.10
	RMSE	3.79	3.17
Tmin	**MBE**	0.27	0.71
	RMSE	3.57	3.42
Tave	**MBE**	-0.50	0.22
	RMSE	2.82	2.47

using NCEI data over the years 1983 – 2006, the use of data from 2007 serves as an independent data set for this test.

Note that the lapse rates and offset values given in Table A-2 are yearly averaged values based upon globally distributed ground sites in the NCEI data base. Results from a number of studies have indicated that tropospheric lapse rates can be seasonally and regionally dependent. Table A-4 gives the globally and monthly averaged lapse rate and offset downscaling parameters for GEOS-4 temperatures. These parameters were developed from eq. Eq. A-4 using the monthly averaged temperature data over the years 1983 – 2006 in global distribution of GEOS-4 and NCEI. Tables A-5 and A-6 give respectively the globally and monthly averaged MBE and RMSE of the 2007 GEOS-4 temperatures relative to NCEI ground site values for the unadjusted and downscaled respectively.

Table A-4. Globally and monthly averaged lapse rates and offset values for adjusting GEOS-4 temperatures to local ground site values. Based upon 1983 – 2006 NCEI and GEOS-4 global data.

	JAN	FEB	MAR	APR	MAY	JUN	JUL	AUG	SEP	OCT	NOV	DEC	YR
Tmx λ	-5.12	-5.97	-6.73	-7.2	-7.14	-6.78	-6.52	-6.44	-6.31	-5.91	-5.44	-4.85	-6.22
Tmx β	-1.61	-1.57	-1.4	-1.01	-0.56	-0.29	-0.24	-0.46	-0.67	-1.08	-1.44	-1.55	-0.99
Tmn λ	-4.34	-4.89	-5.17	-5.16	-4.93	-4.67	-4.46	-4.33	-4.28	-4.31	-4.6	-4.44	-4.63
Tmn β	-0.96	-0.95	-0.69	-0.14	0.22	0.34	0.43	0.5	0.58	0.42	-0.06	-0.61	-0.07
Tm λ	-4.49	-5.19	-5.73	-6.06	-5.91	-5.59	-5.35	-5.27	-5.14	-4.9	-4.8	-4.45	-5.24
Tm β	-1.16	-1.09	-0.9	-0.34	0.17	0.42	0.51	0.35	0.13	-0.18	-0.61	-0.97	-0.3

Table A-5. Globally and monthly averaged MBE and RMSE values associated with unadjusted 2007 GEOS-4 temperatures relative to 2007 NCEI GSOD temperatures.

	JAN	FEB	MAR	APR	MAY	JUN	JUL	AUG	SEP	OCT	NOV	DEC	YR
Tmax MBE	-2.00	-2.11	-2.00	-1.64	-1.13	-1.15	-0.84	-1.27	-1.49	-1.85	-1.73	-1.90	-1.89
Tmax RMSE	4.04	4.00	4.01	3.75	3.73	3.64	3.57	3.64	3.66	3.72	3.71	4.02	3.79
Tmin MBE	-0.24	-0.49	-0.23	0.19	0.56	0.49	0.66	0.61	0.81	0.76	0.50	-0.41	0.27
Tmin RMSE	4.13	4.02	3.70	3.32	3.25	3.09	3.10	3.13	3.30	3.50	3.84	4.26	3.55
Tave MBE	-1.0	-1.15	-0.88	-0.54	-0.03	-0.06	-0.13	-0.18	-0.15	-0.43	-0.59	-1.08	-0.50
Tave RMSE	3.20	3.18	2.92	2.62	2.66	2.54	2.55	2.50	2.51	2.56	2.91	3.41	2.80

Table A-6. Globally averaged monthly MBE and RMSE associated with downscaled 2007 temperatures relative to 2007 NCEI GSOD temperatures. The GEOS-4 temperatures were downscaled using the globally and monthly averaged λ and β values given in Table A-4.

	JAN	FEB	MAR	APR	MAY	JUN	JUL	AUG	SEP	OCT	NOV	DEC	YR
Tmax MBE	0.04	-0.07	-0.04	-0.06	0.00	-0.32	-0.08	-0.30	-0.32	-0.29	0.14	0.04	-0.10
Tmax RMSE	3.35	3.11	3.17	2.97	3.18	3.16	3.18	3.13	3.02	2.98	3.06	3.40	3.14
Tmin MBE	1.06	0.85	0.87	0.74	0.74	0.52	0.59	0.45	0.57	0.69	0.92	0.56	0.71
Tmin RMSE	4.11	3.87	3.54	3.13	2.99	2.83	2.86	2.87	3.01	3.26	3.71	4.12	3.36
Tave MBE	0.52	0.33	0.48	0.28	0.27	-0.04	0.04	-0.11	0.13	0.14	0.41	0.25	0.22
Tave RMSE	2.94	2.69	2.44	2.11	2.22	2.18	2.24	2.16	2.12	2.20	2.61	3.06	2.41

(Return to Content)

Regional Downscaling: Eq. A-4 can also be used to develop regional specific λ and β values which, for some applications, may be more appropriate than the yearly (Table A-2) or monthly and globally averaged (Table A-4) values. As an example, Table A-7 gives the regionally and monthly averaged λ and β values for Tmax, Tmin, and Tave along with the regionally yearly averaged values for the Pacific Northwest region (40 - 50N, 125 – 110W). These values were developed via Eq. 4 for the US Pacific Northwest using GEOS-4 and NCEI GSOD temperatures over the years from 1983 through 2006.

Table A-7. Regional and monthly averaged lapse rate and offset values for adjusting GEOS-4 temperatures to local ground site values Based upon 1983 – 2006 NCEI and GEOS-4 temperatures in the US Pacific Northwest region.

	JAN	FEB	MAR	APR	MAY	JUN	JUL	AUG	SEP	OCT	NOV	DEC	YR
Tmx λ	-5.13	-6.22	-7.54	-7.88	-7.09	-6.61	-6.29	-5.87	-6.09	-5.83	-5.56	-4.69	-6.23
Tmx β	-1.47	-1.69	-1.63	-1.55	-1.23	-1.12	-1.03	-1.64	-1.82	-2.15	-1.74	-1.09	-1.51
Tmn λ	-5.55	-6.46	-6.68	-6.06	-5.53	-5.64	-5.25	-4.77	-4.7	-4.64	-5.54	-5.37	-5.51
Tmn β	-0.9	-0.69	-0.12	0.31	0.48	0.78	1.36	1.43	1.31	0.81	0.31	-0.68	0.37
Tm λ	-5.35	-6.38	-7.11	-7.26	-6.55	-6.27	-5.87	-5.54	-5.58	-5.39	-5.55	-5.02	-5.98
Tm β	-0.81	-0.7	-0.48	-0.06	0.4	0.7	0.97	0.58	0.2	-0.19	-0.32	-0.61	-0.02

The MBE and RMSE of the unadjusted 2007 GEOS-4 temperatures in the US Pacific Region relative to the ground observations are given in Table A-8, and for comparison the MBE and

RMSE associated with the downscaled 2007 GEOS-4 temperatures are given in Table A-9. The downscaled temperatures are based upon Eq. 3 using the regional λ and β values given in Table 7.

Table A-8. Regional monthly MBE and RMSE values associated with unadjusted 2007 GEOS-4 temperatures in the US Pacific region relative to 2007 NCEI GSOD temperatures

	JAN	FEB	MAR	APR	MAY	JUN	JUL	AUG	SEP	OCT	NOV	DEC	YR
Tmax MBE	-3.05	-3.41	-4.47	-3.96	-3.10	-3.47	-2.74	-3.23	-3.58	-3.77	-3.25	-3.18	-3.43
Tmax RMSE	5.06	5.11	5.78	5.34	5.06	5.18	4.85	5.28	5.63	5.36	4.99	4.76	5.20
Tmin MBE	-2.59	-2.90	-2.85	-2.30	-1.51	-1.50	-0.34	-0.12	-0.39	-1.19	-1.40	-2.94	-1.67
Tmin RMSE	5.58	5.32	5.03	4.45	4.18	4.36	4.25	4.22	4.33	3.95	4.71	5.53	4.66
Tave MBE	-2.40	-2.56	-3.12	-2.59	-1.52	-1.65	-0.83	-1.15	-1.54	-1.99	-2.11	-2.79	-2.02
Tave RMSE	4.36	4.12	4.33	3.92	3.33	3.38	3.16	3.21	3.41	3.48	3.92	4.52	3.76

Table A-9. Regional monthly MBE and RMSE values associated with downscaled 2007 GEOS-4 temperatures in the US Pacific region relative to 2007 NCEI GSOD temperatures. The GEOS-4 temperatures were downscaled using the regionally and monthly averaged λ and β values for the US pacific Region given in Table A-7.

	JAN	FEB	MAR	APR	MAY	JUN	JUL	AUG	SEP	OCT	NOV	DEC	YR
Tmax MBE	0.28	0.54	-0.11	0.45	0.70	0.05	0.58	0.54	0.45	0.50	0.51	-0.39	0.34
Tmax RMSE	4.00	3.63	3.45	3.11	3.77	3.55	3.90	4.05	4.21	3.70	3.71	3.30	3.70
Tmin MBE	0.32	0.14	-0.32	-0.41	0.01	-0.23	0.20	0.18	0.00	-0.31	0.30	-0.32	-0.04
Tmin RMSE	4.58	3.96	3.62	3.25	3.38	3.49	3.70	3.71	3.88	3.41	4.05	4.31	3.78
Tave MBE	0.35	0.46	-0.07	0.10	0.46	-0.08	0.33	0.28	0.28	0.15	0.22	-0.36	0.18
Tave RMSE	3.41	2.81	2.42	2.09	2.36	2.32	2.58	2.47	2.49	2.45	2.91	3.25	2.63

As an additional point of comparison Table A-10 gives the MBE and RMSE values associated with downscaled 2007 GEOS-4 temperatures in the US Pacific Northwest relative to 2007 NCEI

GSOD temperatures where the globally and monthly averaged (Table 4) downscaling parameters (i.e. λ and β) have been used.

Table A-10. MBE and RMSE associated with downscaled 2007 temperatures relative to 2007 NCEI GSOD temperatures in the US Pacific Northwest region (40 – 50N, 125 – 110W). The GEOS-4 temperatures were downscaled using the globally and monthly averaged λ and β values given in Table A.6

	JAN	FEB	MAR	APR	MAY	JUN	JUL	AUG	SEP	OCT	NOV	DEC	YR
Tmax MBE	0.42	0.33	-0.63	-0.33	0.05	-0.72	-0.13	-0.43	-0.63	-0.54	0.16	0.13	-0.19
Tmax RMSE	4.02	3.60	3.48	3.08	3.71	3.62	3.86	4.05	4.24	3.71	3.67	3.28	3.69
Tmin MBE	-0.06	-0.17	-0.29	-0.29	0.05	-0.15	0.85	0.95	0.58	-0.04	0.33	-0.72	0.09
Tmin RMSE	4.61	4.02	3.67	3.28	3.41	3.55	3.85	3.85	3.95	3.41	4.10	4.40	3.84
Tave MBE	0.39	0.42	-0.15	-0.05	0.45	-0.05	0.60	0.41	0.20	-0.03	0.24	-0.20	0.18
Tave RMSE	3.42	2.82	2.44	2.13	2.37	2.34	2.64	2.50	2.50	2.45	2.93	3.25	2.65

The monthly time series (Figure A-4) of MBE and RMSE values for GEOS-4 2007 temperatures relative to NCEI ground site values provide a summary for the un-scaled and downscaled temperatures in the US Pacific Northwest region. The 2007 downscaled GEOS-4 temperatures are based upon the monthly averaged λ and β values developed from 1983 – 2006 GEOS-4 and NCEI data in this region. The MBE and RMSE monthly time series values are plotted for the uncorrected GEOS-4 and GEOS-4 downscaled using (1) yearly and global mean lapse rate and offset values, (2) monthly mean global lapse rate and offset values, (3) yearly mean regional lapse rate and offset values, and (4) monthly mean regional lapse rate and offset values.

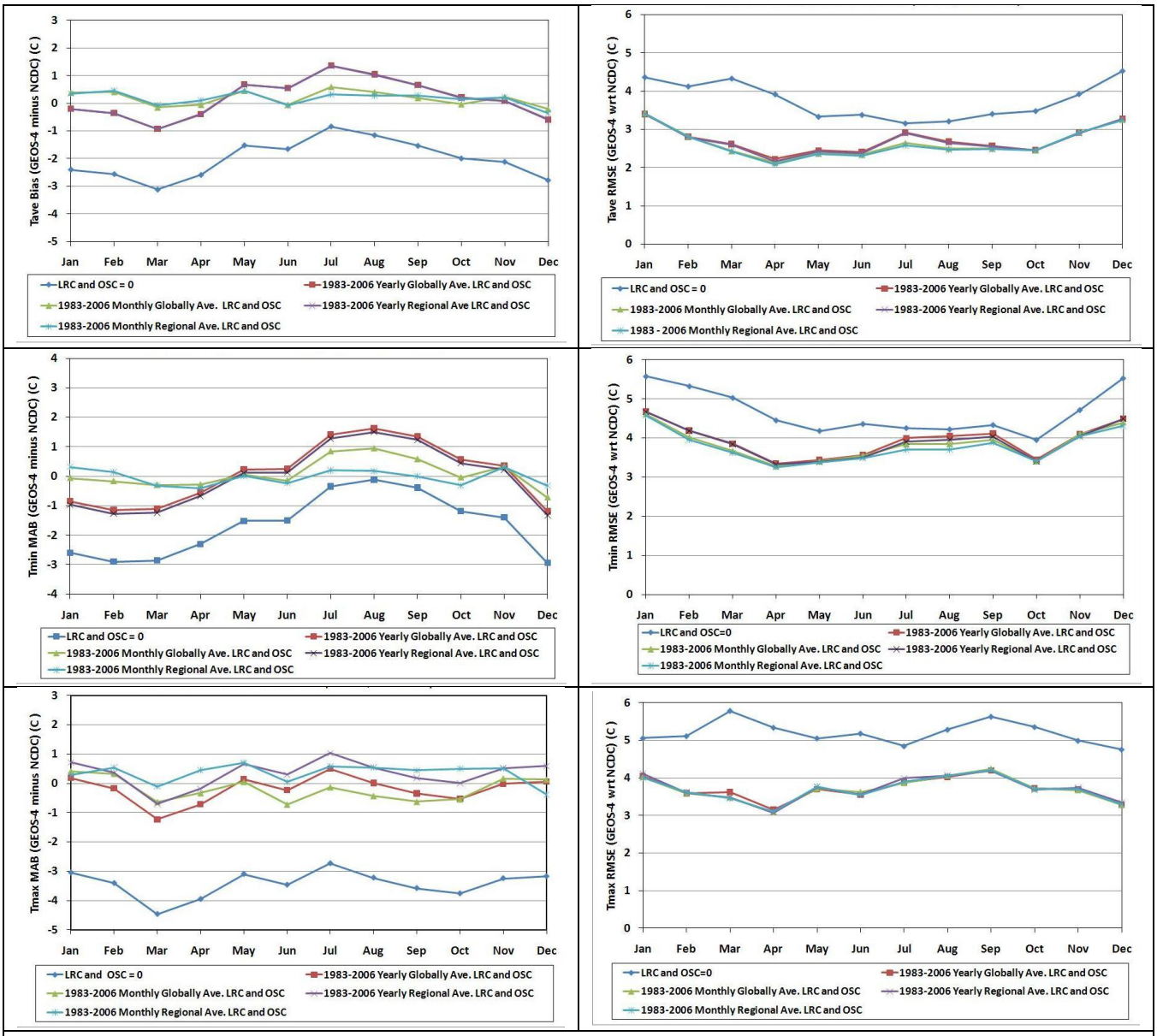

Figure A-4. Monthly time series of the MBE (left column) and RMSE (right column) between 2007 un-scaled and downscaled GEOS-4 and NCEI ground sites observations in the Pacific Northwest region (40 - 50N, 125 – 110W). The MBE and RMSE monthly time series values are plotted for the (1) uncorrected GEOS-4 (i.e. LRC and OSC = 0) and GEOS-4 corrected using (2) yearly and global mean lapse rate and offset values, (3) monthly mean global lapse rate and offset values, (4) yearly mean regional lapse rate and offset values, and (5) monthly mean regional lapse rate and offset values. The downscaling parameters are based upon GEOS-4 and NCEI station temperatures over the years 1983 – 2006.

For each set of downscaling parameters (i.e. lapse rate and offset) there is a substantial reduction in the RMSE relative to the un-adjusted GEOS-4 values; however, there is little difference in the RMSE values relative to the temporal averaging period (i.e. yearly vs. monthly average) or geographical region (global vs. regional) used to generate the downscaling parameters. The MBE is, however somewhat more dependent on the set of downscaling parameters, with the monthly mean regional values yielding the lowest MBE error particularly in the MBE for Tmin.

The regional downscaling discussed above is not available through the POWER/SSE archive, and is discussed here only to give users guidance in its application.

(Return to Content)

Heating/Cooling Degree Days: Tables A-11 and A-12 give the year-by-year statistics associated with comparing the heating degree days (HDD) and the cooling degree days (CDD) based upon the uncorrected GEOS-4 assimilation model temperatures and the downscaled or adjusted temperatures with observational data. In each table the bottom row gives the mean over the years. The GEOS-4 values used in Table A-12 were downscaled using the globally averaged λ and β values given in Table A-3. Note that the use of the downscaled GEOS-4 temperatures result in a significant improvement in the agreements between the GEOS-4 and NCEI based HDD and CDD, particularly in the bias values.

Table A.11

Yearly Mean Heating Degree Days (HDD)															
Year	Uncorrected GEOS-4 Temperatures vs ground site observations reported in NCDC GSOD files							Corrected (i.e. downscaled) GEOS-4 Temperatures vs ground site observations reported in NCDC GSOD files							No. Stations
	Bias (HDD)	Bias (%)	RMSE (HDD)	RMSE (%)	Slope	Intercept (HDD)	Rsqd	Bias (HDD)	Bias (%)	RMSE (HDD)	RMSE (%)	Slope	Intercept (HDD)	Rsqd	
1983	16.30	6.44	68.59	27.11	1.03	9.85	0.95	0.48	0.19	57.56	22.75	1.01	-1.06	0.96	1101
1984	16.37	6.34	64.45	24.97	1.03	8.46	0.95	0.06	0.02	52.69	20.41	1.01	-1.96	0.96	1127
1985	16.13	6.01	64.31	23.97	1.03	9.19	0.96	-0.68	-0.25	54.86	20.45	1.00	-1.97	0.96	1102
1986	14.07	5.55	85.41	33.72	0.98	18.25	0.91	-2.55	-1.01	78.34	30.93	0.96	6.42	0.92	1162
1987	14.92	5.91	69.30	27.42	1.02	10.71	0.94	-0.79	-0.31	60.04	23.76	1.00	-0.16	0.95	1140
1988	15.20	6.20	65.39	26.68	1.03	6.79	0.95	-0.35	-0.14	55.38	22.59	1.01	-3.68	0.96	1155
1989	14.71	5.85	66.75	26.54	1.03	7.55	0.95	-0.58	-0.23	57.80	22.98	1.01	-3.33	0.96	1194
1990	16.84	7.09	66.45	27.97	1.04	7.67	0.95	2.04	0.86	53.42	22.49	1.02	-2.71	0.96	1258
1991	14.69	6.03	78.74	32.33	1.01	11.89	0.92	0.00	0.00	67.86	27.86	0.99	1.30	0.94	1223
1992	12.94	5.19	79.58	31.91	1.00	12.11	0.92	-2.55	-1.02	69.80	27.99	0.99	0.69	0.93	1373
1993	17.79	6.94	71.34	27.83	1.03	10.14	0.94	0.92	0.36	61.86	24.13	1.01	-1.93	0.95	1477
1994	22.88	9.24	72.22	29.17	1.05	11.59	0.95	4.72	1.91	59.03	23.84	1.03	-1.85	0.96	1508
1995	17.54	7.10	70.60	28.60	1.03	9.83	0.95	0.92	0.37	59.47	24.09	1.01	-2.25	0.96	1311
1996	10.15	4.64	99.68	45.60	0.93	25.32	0.84	-5.88	-2.69	93.53	42.78	0.91	13.74	0.85	1216
1997	19.61	8.56	62.21	27.16	1.05	7.08	0.95	2.86	1.25	47.93	20.92	1.03	-4.71	0.97	1497
1998	24.65	11.56	68.35	32.06	1.09	5.74	0.94	7.41	3.48	53.79	25.23	1.06	-5.63	0.96	1487
1999	18.58	8.53	61.38	28.18	1.06	6.22	0.95	2.32	1.06	47.22	21.68	1.03	-4.64	0.97	1832
2000	17.61	7.32	66.54	27.67	1.05	6.15	0.95	0.45	0.19	51.64	21.48	1.03	-6.58	0.96	2324
2001	24.33	9.94	64.77	26.46	1.06	8.60	0.96	6.89	2.82	49.99	20.42	1.04	-3.02	0.97	1799
2002	16.62	6.92	67.75	28.22	1.03	9.73	0.94	0.25	0.11	55.07	22.94	1.01	-2.59	0.95	2382
2003	14.75	6.24	66.15	27.96	1.04	6.33	0.94	-0.66	-0.28	53.93	22.80	1.02	-5.05	0.96	2676
2004	16.52	6.87	90.29	37.56	1.00	17.33	0.90	-0.27	-0.11	81.18	33.77	0.98	4.36	0.91	2704
2005	20.40	8.32	66.41	27.07	1.05	7.56	0.95	3.43	1.40	53.04	21.62	1.03	-4.88	0.96	3020
2006	16.56	6.76	126.66	51.69	0.91	39.49	0.81	0.25	0.10	120.46	49.15	0.89	27.04	0.82	3077
Mean of individual years	**17.09**	**7.07**	**73.47**	**30.33**	**1.02**	**11.40**	**0.93**	**0.78**	**0.34**	**62.33**	**25.71**	**1.00**	**-0.19**	**0.94**	

Table A.12

Yearly Mean Cooling Degree Days (CDD)															
Year	Uncorrected GEOS-4 Temperatures vs ground site observations reported in NCDC GSOD files							Corrected (i.e. downscaled) GEOS-4 Temperatures vs ground site observations reported in NCDC GSOD files							No. Stations
	Bias (CDD)	Bias (%)	RMSE (CDD)	RMSE (%)	Slope	Intercept (CDD)	Rsqd	Bias (CDD)	Bias (%)	RMSE (CDD)	RMSE (%)	Slope	Intercept (CDD)	Rsqd	
1983	-4.78	-8.93	28.53	53.34	0.86	2.68	0.92	2.29	4.28	28.59	53.45	0.94	5.27	0.91	1101
1984	-4.25	-8.35	27.01	53.07	0.86	2.86	0.92	2.27	4.46	27.52	54.05	0.94	5.21	0.91	1127
1985	-5.96	-11.21	27.82	52.33	0.85	1.80	0.92	0.94	1.77	26.66	50.18	0.94	4.35	0.92	1102
1986	-6.60	-12.50	27.73	52.56	0.84	1.91	0.93	0.38	0.72	25.87	49.01	0.92	4.61	0.93	1162
1987	-6.21	-12.01	27.17	52.52	0.85	1.76	0.93	0.42	0.81	25.74	49.74	0.93	4.11	0.93	1140
1988	-5.53	-10.10	27.39	50.05	0.86	2.22	0.93	1.14	2.08	26.62	48.64	0.94	4.62	0.93	1155
1989	-6.29	-11.91	29.02	54.96	0.84	2.35	0.91	0.37	0.70	27.79	52.63	0.91	4.93	0.91	1194
1990	-6.63	-11.92	28.70	51.60	0.83	2.66	0.93	0.16	0.29	26.45	47.55	0.91	5.09	0.93	1258
1991	-6.93	-11.60	30.28	50.71	0.84	2.59	0.92	0.74	1.24	28.36	47.49	0.93	4.84	0.92	1223
1992	-4.94	-10.62	25.52	54.79	0.86	1.80	0.92	1.83	3.93	23.87	51.24	0.95	4.13	0.93	1373
1993	-5.32	-9.97	26.29	49.30	0.88	1.10	0.93	1.84	3.46	25.96	48.68	0.96	4.07	0.93	1477
1994	-6.12	-10.75	27.96	49.09	0.87	1.36	0.93	1.97	3.46	28.10	49.32	0.96	4.41	0.92	1508
1995	-5.38	-9.13	28.04	47.55	0.87	2.28	0.93	2.27	3.85	27.28	46.27	0.95	5.31	0.93	1311
1996	-6.66	-10.70	30.31	48.68	0.86	2.09	0.92	2.73	4.38	30.52	49.01	0.95	6.07	0.91	1216
1997	-6.39	-11.33	28.24	50.06	0.85	2.02	0.92	1.97	3.48	26.52	47.00	0.94	5.17	0.92	1497
1998	-5.19	-8.91	27.48	47.17	0.87	2.30	0.93	3.34	5.74	27.21	46.70	0.96	5.56	0.93	1487
1999	-3.92	-6.53	28.87	48.11	0.88	3.01	0.92	4.49	7.48	29.46	49.07	0.97	6.49	0.92	1832
2000	-3.23	-6.06	27.74	52.00	0.88	3.06	0.92	4.51	8.45	28.40	53.22	0.97	6.33	0.92	2324
2001	-7.08	-12.74	30.00	53.97	0.84	1.75	0.92	0.51	0.91	29.40	52.89	0.92	4.70	0.91	1799
2002	-7.95	-13.80	29.96	52.00	0.83	1.58	0.92	-0.24	-0.42	28.45	49.35	0.92	4.65	0.92	2382
2003	-5.84	-9.97	30.91	52.77	0.85	3.23	0.91	2.55	4.35	29.83	50.90	0.94	6.34	0.91	2676
2004	-6.14	-11.66	27.97	53.10	0.84	2.19	0.92	1.82	3.45	26.77	50.80	0.93	5.33	0.92	2704
2005	-5.80	-9.96	29.13	49.99	0.86	2.39	0.93	1.85	3.17	28.47	48.84	0.94	5.40	0.92	3020
2006	-4.88	-8.89	29.25	53.28	0.87	2.44	0.92	2.63	4.79	28.94	52.70	0.95	5.37	0.91	3077
Mean of individual years	-5.75	-10.40	28.39	51.37	0.86	2.23	0.92	1.78	3.20	27.61	49.95	0.94	5.10	0.92	

(Return to Content)